

Regulation of apical vesicle formation from the trans-Golgi network.

by

Mark A. Ellis

B.S. Biotechnology, Rutgers University, 1999

Submitted to the Graduate Faculty of

School of Medicine in partial fulfillment

of the requirements for the degree of

Doctor of Philosophy in Cell Biology and Molecular Physiology

University of Pittsburgh

2006

UNIVERSITY OF PITTSBURGH
FACULTY OF MEDICINE

This dissertation was presented

by

Mark A. Ellis

It was defended on

January 23, 2006

and approved by

Jeffery Brodsky, PhD, Associate Professor

Rebecca Hughey, PhD, Associate Professor

Linton Traub, PhD, Associate Professor

Meir Aridor, PhD, Assistant Professor

Gerard Apodaca, PhD, Associate Professor

Ora A. Weisz, PhD, Associate Professor
Dissertation Director

[Optional: Insert Copyright notice]

Regulation of apical vesicle formation from the trans-Golgi network.

Mark A. Ellis, PhD

University of Pittsburgh, 2006

Polarized epithelial cells efficiently sort newly-synthesized apical and basolateral proteins into distinct transport carriers that emerge from the trans-Golgi network (TGN), and this sorting may be recapitulated in nonpolarized cells. While the targeting signals of basolaterally-destined proteins are generally cytoplasmically-disposed, apical sorting signals are not typically accessible to the cytosol, and the transport machinery required for segregation and export of apical cargo remain largely unknown. We are interested in identifying the molecular requirements for TGN export of the apical marker influenza hemagglutinin (HA). To identify cytosolic proteins responsible for HA export from the TGN, we developed an *in vitro* assay to measure this process. We found that HA export does not require the brefeldin A-sensitive GTPase ARF1, but does depend on the GTPase dynamin 2. Furthermore, using biochemical fractionation, we identified the adaptor protein 14-3-3 epsilon as an effector of HA export from the TGN. This work 1) establishes a method to accurately observe anterograde TGN export of an apical cargo, 2) characterizes a requirement for GTP in vesicle formation, and 3) identifies a novel component in trafficking from the TGN. We expand these studies by comparing HA export to the release of basolateral cargo, showing that nonpolarized cells are capable of differentially sorting distinct classes of cargo into discrete vesicles derived from the TGN. Together, these data further our understanding of the regulatory mechanisms underlying apical transmembrane protein export from the TGN.

TABLE OF CONTENTS

1. Biosynthetic Sorting at the trans-Golgi network in Mammalian Cells.	1
Introduction	1
Polarized cells and membrane domains	2
<i>Epithelial polarity and membrane trafficking:</i>	3
Cytoskeletal contributions to polarity:	3
Trafficking pathways in epithelia:	4
<i>Protein sorting in the trans-Golgi network.</i>	7
<i>Packaging cargo into transport intermediates.</i>	8
Export from the TGN:	10
<i>Proteins involved in TGN export:</i>	10
Coats and adapters:	13
GTP binding proteins/GTPases	14
Lipid metabolism and TGN export:	16
Requirements for the fission of transport carriers from the TGN:	19
Regulation of TGN export by kinases and phosphatases:	20
Other regulators of export:	22
Morphology of TGN derived carriers:	23
Trafficking Routes and Pathways to the Plasma Membrane	25
<i>An indirect biosynthetic pathway to the cell surface:</i>	27
Aims of My Project	29
Specific aim 1: To develop an assay that measures apical carrier formation from the TGN.	29
Specific aim 2: To characterize the selective requirements for TGN export of HA compared with a basolateral marker.	30
Specific aim 3: To identify novel proteins that regulate HA export from the TGN.	30
2. In vitro assays differentially recapitulate protein export from the trans-Golgi network.	32
3. ARF1-Independent Protein Sorting and Export from the trans-Golgi Network.	39
INTRODUCTION	39
RESULTS	41
<i>Reconstitution of HA release from perforated cells-</i>	41
<i>Nucleotide dependence of HA release-</i>	46
<i>HA release is sensitive to in vivo perturbants of biosynthetic traffic-</i>	48
<i>ARF-independent release of HA-</i>	50
DISCUSSION	55
<i>Morphology of TGN-derived transport carriers.</i>	57
<i>HA export from the TGN is ARF1-independent.</i>	59
4. Identification of cytosolic proteins important for HA release from the trans-Golgi network.	61
<i>HA release from the TGN is dependent on exogenous cytosol:</i>	63

<i>HA release activity is enriched by ion-exchange fractionation:</i>	65
Effect of dynamin 2 K44A expression on HA and G surface delivery:	69
<i>Effect of dynamin 2 K44A expression on HA and VSV G export from the TGN:</i>	73
<i>Further isolation of HA release activity from rat brain cytosol</i>	74
<i>Proteins identified in the fraction enriched for HA release activity:</i>	75
Discussion:	79
<i>Dynamin 2</i>	79
<i>Diacylglycerol kinase</i>	80
<i>Secernin 1</i>	80
<i>14-3-3 epsilon/zeta</i>	81
5. Conclusion and Future Directions	83
<i>Applications for the scraped cell assay:</i>	85
<i>How does brefeldin A affect HA surface delivery?</i>	85
<i>Does dynamin 2 regulate HA containing vesicle fission from the TGN?</i>	86
<i>Isolation of cytosolic proteins involved in HA export from the TGN: the fun has just begun!</i>	86
6. Reference list:	88
Appendix A- Materials and Methods:	100
Section 1: Characterization of HA export from the TGN	100
<i>Antibodies-</i>	100
<i>Cell culture and virus infection-</i>	100
<i>Cytosol preparation-</i>	100
<i>Enriched Golgi assay-</i>	101
<i>Protein staging in the TGN of HeLa cells-</i>	101
<i>Surface delivery assay-</i>	102
<i>Reconstitution of vesicle release from perforated cells-</i>	102
<i>Protease protection assay-</i>	102
<i>β-COP and ARF1 recruitment to permeabilized cells-</i>	103
<i>Western blotting & Far-Western blotting-</i>	103
<i>Electron microscopy-</i>	103
<i>Immunogold electron microscopy-</i>	103
<i>Indirect Immunofluorescence-</i>	103
Section 2: Biochemical fractionation of HA release activity from cytosol	104
<i>Release Assay-</i>	104
<i>Ammonium sulfate precipitation-</i>	104
<i>Anion exchange chromatography-</i>	104
<i>Gel Filtration Chromatography-</i>	105
<i>Tryptic digest of isolated bands-</i>	105
<i>Peptide Mass Fingerprinting-</i>	105

LIST OF FIGURES & TABLES

Figure 1. 1 : Organization of the cytoskeleton in polarized cell types.	3
Table 1.1 : Molecules involved in export from the TGN.....	12
Figure 1.2: Potential mechanisms for apical and basolateral export from the TGN.	23
Figure 2.1: Schematic description of in vitro cell-based and cell-free assays.	34
Figure 2.2. Comparison of GTP and pH requirements in cell-based versus cell-free assays.	36
Figure 3.1. ATP- and cytosol-dependent release of TGN-staged HA from perforated cells.....	42
Figure 3. 2. Kinetics and cytosol dose-dependence of HA release.	43
Figure 3. 3. Released HA is recovered in membrane-bound vesicles.	45
Figure 3. 4. Effect of GTP γ S and GMP-PNP on release of HA and TGN46 from the TGN.....	47
Figure 3. 5. Disruption of TGN luminal pH inhibits HA but not TGN46 release from perforated cells.....	49
Figure 3. 6. HA release from the TGN is ARF-independent.	53
Figure 3. 7. ARF-independent HA release from the TGN is inhibited by GTP γ S and by expression of influenza M2.	54
Figure 4. 1: 500mM KCl buffer increases cytosol dependent release of HA staged in the TGN.....	62
Figure 4. 2: Schematic describing the enrichment of HA release activity from rat brains.	64
Table 2: Enrichment of HA release activity using standard chromatographic techniques.	65
Figure 4.3: Dynamin 2 is enriched in the 400mM fraction compared to an equal concentration of cytosol.	66
Figure 4. 4: Dynamin 2 localization in HeLa cells.	68
Figure 4. 5: Dynamin 2 K44A expression inhibits HA trafficking through the biosynthetic pathway.....	71
Figure 4. 6: Dynamin 2 K44A expression inhibits VSV G trafficking only at late time points. .	73
Figure 4. 7: Dynamin 2 K44A differentially regulates HA and VSV G export from the TGN...	74
Figure 4. 8: Fractionation of rat brain cytosol for enrichment of HA release activity.	75
Table 2: Proteins identified by mass spec analysis.....	77
Figure 4. 9: Proteins identified by peptide mass fingerprinting.	78
Figure 5.1. Model describing HA export from the TGN.	84
Table 3: Rat Brain Cytosol preparation	101

1. Biosynthetic Sorting at the *trans*-Golgi network in Mammalian Cells.

Introduction

The identity of cellular organelles and compartments is determined by their unique steady state protein and lipid composition which is maintained despite continuous addition and removal of membrane as itinerant molecules traffic through these compartments. In the case of the plasma membrane, new membrane is added upon the exocytic fusion of intracellular vesicles whereas membranes are retrieved via several internalization pathways collectively referred to here as endocytosis ([1, 2]). In polarized epithelial cells such as renal, intestinal, or hepatic cells, the subdivision of proteins and lipids is more pronounced in that the cell surface itself is divided into distinct domains. In these cells, the apical surface faces tubular lumens that are in continuity with the external environment of the organism, whereas the basolateral surface maintains contact with adjacent cells and the substratum. The protein and lipid compositions of these surfaces are specified for the particular functions of each domain, which include barrier protection, absorption or secretion of nutrients, signaling, and ion transport. In recent years, polarized sorting, or the segregation of discrete protein populations, has been recapitulated in many different cell types including nonpolarized cells (reviewed in [3]).

The mechanisms that regulate polarized secretion in animal cells remain largely unknown. In this chapter, I will review the morphology of polarized epithelial cells and the trafficking signals that are known to direct proteins to the apical or basolateral domain, and describe our current understanding of how apical and basolateral proteins are sorted from one

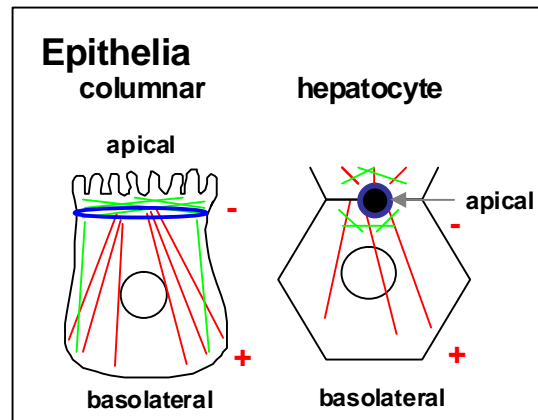
another in the TGN and packaged into distinct transport carriers. This review will establish the background and relevance for the work I describe in the following chapters.

Polarized cells and membrane domains

Cellular polarity refers to the distinct organization of the plasma membrane of a cell into domains with discrete lipid and protein compositions. Polarity is best described in cells that possess an obvious polarized distribution of markers, such as neurons or polarized epithelia. These cell types have exquisitely organized plasma membrane domains required for their particular physiological function. Figure 1 describes the polarized organization of the cell types discussed in this section. Because cytoskeletal organization plays a key role in the maintenance of polarized membrane domains, the orientation of actin and microtubules is shown for each cell type.

Figure 1. 1 : Organization of the cytoskeleton in polarized cell types.

Cell types discussed in the text are drawn indicating polarized domains of the plasma membrane. Microtubules are drawn in red, actin in green, and tight junctions in blue. + and – represent microtubule directionality.



Epithelial polarity and membrane trafficking:

Cytoskeletal contributions to polarity:

Epithelial cells line the organs of the body, separating the blood supply from external and endocrine environments. The surface of these cells is polarized to generate a tight barrier to prevent the unregulated diffusion of proteins and solutes between the lumen (the external environment) and the blood (reviewed in [4]). Tight junctions composed of the claudin protein family form a belt-like barrier between the apical (lumen-facing) and basolateral (exposed to adjacent cells and the underlying connective tissue) domains of the plasma membrane (reviewed in [5]). Microtubule organization is primarily responsible for the polarity of epithelial cells (kidney and hepatocyte) and the organization of microtubules through partitioning (Par) proteins determines the ultimate organization of the epithelia to either a kidney-like simple cuboidal phenotype [6], or a hepatocyte-like morphology [7]. Kidney cells are polarized in a cuboidal phenotype with a single apical domain. The apical domain is largely composed of glycolipid-enriched membrane lipid domains (lipid rafts), that are thought to directly influence the protein composition of these domains [8]. In contrast to cuboidal epithelia, hepatocytes maintain a

radically different alignment of their polarized domains. In these cells, the apical domains of two or more adjacent cells together form the bile canaliculus, a narrow tube that winds around the hepatocytes (reviewed in [9] see fig 1).

A subset of apical proteins require microtubule integrity for efficient surface delivery, suggesting that microtubules may also play a critical role in the transport of post-Golgi vesicles to the plasma membrane [10]. Interestingly, two kinases implicated in polarized organization of many different cell types, PAR-1 and PAK5, positively regulate the polymerization of actin and microtubules respectively [11]. Therefore, an interdependence of actin and microtubule organization may govern the establishment of polarity.

Trafficking pathways in epithelia:

As mentioned earlier, the apical membrane of cuboidal epithelial cells (such as the common model kidney epithelial cell line Madin-Darby Canine Kidney cells [MDCK]) is enriched in glycolipids that coalesce to form microdomains or rafts. It has been proposed that lipid rafts may serve as a platform for accumulation of cargo as well as an indirect trafficking signal [12]. Sorting to both the apical and basolateral surface is signal driven, and cargo lacking a signal is secreted in a non-polarized fashion [13]. The bulk of polarized sorting of proteins in MDCK cells occurs in both the TGN and endosomes [1, 14] (see later section of this chapter). Basolateral cargo secretion is regulated by the interaction of cytoplasmically-disposed sorting signals with sorting receptors (discussed in detail later) (reviewed in [15]). Apical cargo is sorted via mechanisms dependent on either cytoplasmic, glycan-mediated, or lipid-interacting sorting signals (reviewed in [8]). Apical and basolateral cargo are sorted in discrete tubular and vesicular carriers that bud from the TGN and are ultimately delivered to the plasma membrane.

Several recent studies have suggested that at least a subset of biosynthetic cargo transits recycling endosomes *en route* to the cell surface [16, 17]. The implications of this pathway to biosynthetic sorting will be discussed below.

Interestingly, a thyroid derived epithelial cell line (Fischer rat thyroid [FRT] cells) with a similar phenotype compared to MDCK cells has significant differences in polarity of some proteins. Newly-synthesized polymeric immunoglobulin receptor, which is normally delivered to the basolateral surface in MDCK cells [18], is delivered to both plasma membrane domains in FRT cells [19]. Moreover, whereas glycosylphosphatidylinositol (GPI)-anchored proteins are normally found on the apical surface of MDCK cells [20], most endogenous GPI-anchored proteins are found basolaterally in FRT cells. GPI-linkage appears to serve as a dominant basolateral targeting signal in this cell type, at least in the context of the normally apical decay accelerating factor (DAF) [21], though this is not the case for alkaline phosphatase [22]. This may be due to differences in additional sorting signals [22] which will be discussed later. There is no apparent difference between the GPI-lipids synthesized by the two different cell types, in that both partition into lipid rafts *in vitro* and *in vivo* [23]. More recently, the same research group has found that apical GPI-anchored proteins oligomerize in the Golgi complex and propose that oligomerization regulates association of these proteins with lipid rafts, thus generating an apical sorting signal [12]. It is unclear how or if oligomerization is affected in FRT cells.

Trafficking of apical cargo in hepatocytes occurs somewhat differently than in columnar epithelia. Biosynthetic delivery of most apical proteins in hepatocytes (with the exception of some polytopic membrane proteins [24]) occurs via transient passage through the basolateral surface [24]. The apical proteins are then internalized from the basolateral surface, delivered to a

sub-apical compartment, and then directed (transcytosed) to the apical domain [25, 26]. Though trafficking of many proteins to the apical membrane in columnar-type epithelia can occur through a direct (vectorial) pathway [27], a transcytotic route has also been described. Polarized intestinal epithelial cells utilize the direct and transcytotic delivery pathways to different extents in the biosynthetic delivery of various newly synthesized apical proteins ([17, 28, 29]), and transcytotic delivery of the apical hydrolase dipeptidylpeptidase IV has been demonstrated in MDCK cells [30]. Postendocytic transcytosis has also been demonstrated in these cell types [31, 32].

Protein sorting:

Protein sorting in the ER and the Golgi complex:

Newly synthesized transmembrane and secretory proteins are translocated across the membrane of the endoplasmic reticulum (ER) during translation [46]. Coatamer II (COPII), along with the small GTPase Sar1, drives the formation of exocytic vesicles at specific ER export sites [50]. ER derived carriers coalesce or fuse to form the ER-Golgi intermediate compartment (ERGIC) where ER-resident proteins are retrieved in COPI vesicles (retrograde traffic) [51], while secretory (anterograde) cargo reaches the *cis*-face of the Golgi complex. Sorting receptors, including the p24 family of transmembrane proteins and the mannose-binding lectins (ERGIC53 [52] and VIP36 [53]) are believed to bridge the interaction between some secretory cargo and the COPII export machinery [54].

Three models have been proposed to describe the progression of cargo from the *cis*-face of the Golgi to the TGN (reviewed in [55]). These models differ primarily in the membrane dynamics regulating trafficking of cargo through the Golgi: either through vesicles, maturation

of cisternae, or temporary intercisternal connections. Regardless of the mechanism that directs intra-Golgi trafficking, cargo proteins progress from the *cis*- towards the *trans*-Golgi cisternae, and are ultimately delivered to the TGN, a tubular-vesicular compartment that defines the *trans*-face of the Golgi.

Protein sorting in the trans-Golgi network.

Vesicles and tubules are generated from the TGN through the coordinate action of cargo sorting and cargo packaging. Cargo molecules are sorted based on discrete sorting information associated with the primary, secondary, or tertiary structure of the protein.

Basolateral sorting motifs are found within cytoplasmically-disposed portions of proteins and are composed of amino acid primary sequences such as NPxY or Yxx? (? representing any bulky hydrophobic amino acid). These motifs likely interact with cytosolic proteins for packaging into transport carriers [14]. Basolateral sorting has been more extensively studied than apical sorting due to the discrete signals. However, it is still not clear how basolateral proteins are trafficked from the TGN to the cell surface. Recent studies suggest that basolateral proteins may traverse recycling endosomes *en route* to the cell surface (see later section on indirect trafficking), and it is possible that polarized trafficking signals are interpreted at this site instead of or in addition to functioning at the TGN.

In contrast, apical targeting motifs are far more diverse and can be localized to domains that are exposed to the lumen, membrane, or cytosol. Furthermore, apical sorting signals are generally not discrete amino acid sequences, but rather post-translation modifications (such as glycans or GPI-linkage) or transmembrane domain properties attributed to lipid raft association [14]. Both N- and O-linked glycans have been described as sorting motifs for a number of

proteins (reviewed in [61, 62]), though it is not clear if this sorting occurs at the TGN or in endosomes [63]. Glycan-based sorting (eg., the p75 neurotrophin receptor and endolyn) could be mediated by association of glycosylated proteins with a sorting receptor, similar to the lectins (glycan binding proteins) that are thought to mediate this process in ER-export. Alternatively, glycans may cause proteins to aggregate into pre-export complexes, as occurs during TGN export of prohormones such as pro-insulin (reviewed in [64]). One apical protein, influenza hemagglutinin (HA), is thought to acquire apical targeting information through association with detergent-resistant membranes termed lipid rafts. Although lipid rafts have been implicated in apical sorting of GPI-anchored proteins also, lipid raft association can be uncoupled from apical delivery of influenza hemagglutinin [65] and GPI-anchoring does not always impart apical targeting (see previous section on FRT cells). Analysis of polytopic apical transmembrane proteins, which generally possess cytoplasmic sorting signals, has not generated a consensus sequence for apical targeting, as described for basolateral targeting, but rather suggests a structural requirement [66, 67].

Packaging cargo into transport intermediates.

During export from the TGN, proteins are packaged into vesicular and tubular cargo carriers. A number of proteins have been implicated in the formation of such vesicles, which will be further discussed in the next section. Vesicle formation is an energy- and protein-driven process [15]. The development of *in vitro* methods to generate vesicles from intact organelles has greatly enhanced the understanding of vesicle biogenesis. As an example, consider the generation of clathrin-coated endocytic vesicles (reviewed in [68, 69]). In this context, cargo is recognized by an adaptor protein or adaptor complex which links the cargo to a coat, clathrin.

The recruitment of clathrin and accessory proteins into a lattice, coupled to lipid modifications in the membrane, promotes the formation of a curved membrane. At a later time, the GTPase dynamin is recruited through the generation of phosphatidylinositol-4,5-bisphosphate in the inner leaflet of the lipid bilayer [70]. GTP hydrolysis results in a conformational change in dynamin, providing the force required for separating the vesicle from the source membrane [71]. From this example, one can predict that the formation of a vesicle requires a mechanism for curvature of the membrane followed by a force generating reaction to overcome the unfavorable energy required for fission from the membrane.

An alternative to trafficking through a vesicular intermediate would be a tubular carrier, which may be formed somewhat differently. A few proteins have been implicated in the fission of tubular carriers, including protein kinase D [72] and dynamin II [73]. As molecular motors are being linked to protein trafficking from the TGN, [74, 75] a model is proposed [76] in which the generation of tubules may not require a coat at all. If a microtubule based motor recognizes cargo and begins to migrate from the TGN carrying that cargo, the force will generate the membrane deformation required. Following this process, either dynamin 2 can promote membrane fission [77], or protein kinase D can drive the generation of diacylglycerol in the membrane, creating an unstable neck to the tubule [78]. In support of this model, expression of a mutant dynamin 2 [74] or of a mutant protein kinase D [79] results in tubules emanating from the TGN. Recently, a kinesin KIFC3 was found associated with putative TGN-derived vesicles containing cargo, which indicates a potential mechanism for microtubule-based membrane fission [75]. Therefore, membrane deformation could be regulated either by a coat-mediated process, a mechanical process, or by generation of a discrete lipid environment. It is unclear at

present whether specific types of cargo are preferentially associated with tubules as opposed to vesicles.

Export from the TGN:

A number of studies have focused on identifying key factors involved in polarized protein exit from the TGN. In general, these studies have taken advantage of the ability to stage mature, newly-synthesized proteins in the TGN by a 20°C temp block [80]. Upon warming the cells to 37°C, the cargo proteins are rapidly exported in transport carriers. Perturbation of cargo export *in vivo* by small interfering RNA or expression of dominant-negative mutants of trafficking effectors will result in an inhibition of surface delivery. Alternatively, antibodies or inhibitors can be added *in vitro* to perforated cells and the effects on cargo release from the TGN assayed. Such studies have yielded a laundry list of proteins that are thought to be involved in polarized membrane traffic; however how they function together to enable efficient sorting and packaging of apical and basolateral cargo remains largely unknown. To characterize the regulation of apical cargo export, I sought to develop an *in vitro* assay to measure TGN export (chapter 2), that could be used to analyze the requirements and fidelity of apical protein export (chapter 3), and to identify novel components involved in this process (chapter 4). The following section describes the known components and proposed mechanisms underlying apical and basolateral cargo export from the TGN, and thus will provide the basis for the work described in the subsequent chapters.

Proteins involved in TGN export:

Numerous proteins have been implicated in cargo sorting at the TGN in non-polarized cells. Yoshimori et al. showed initially that baby hamster kidney (BHK) and Chinese hamster ovary (CHO) cells are capable of differentially regulating the surface delivery of an apical versus a basolateral marker [45]. Furthermore, this sorting is mediated by the same signal in polarized and non-polarized cells [81], suggesting the pathways share common sorting components. Though differences exist between polarized and non-polarized cells, the sorting of different cargoes from each other in the TGN is conserved or redundant.

Table 1.1 : Molecules involved in export from the TGN.

<u>Classification</u>	<u>Protein</u>	<u>Cargo type</u>	<u>Associated with...</u>	<u>Reference</u>
GTPases	Rab6	Apical	Golgi resident protein distribution	[82, 83]
	ARF1	Apical	PI4K, FAPP	[84, 85]
	G(s)	Apical	?	[86]
	Rab8	Basolateral	AP-1b	[87]
	Rab11	Basolateral	PI4K	[88, 89]
	ARFRP-1	Basolateral	?	[90]
	Cdc42	Basolateral	AP-1b, actin	[91, 92]
	G(i)	Basolateral	PKD	[86, 93]
Coat/Adaptor	AP-1	Basolateral	Clathrin	[87, 94]
	AP-3	Basolateral	Clathrin	[95]
	AP-4	Basolateral	?	[96]
	FAPP1	Basolateral	PI4P	[84]
	FAPP2	Apical	PI4P	[97]
	p230/golgin	Basolateral	e-cadherin	[98]
Lipids	PI4P	Both	PI4K, FAPP	[84, 97, 99]
	PI4,5P2	Both	PI4P5K, dynamin II, actin	[74, 100]
	Cholesterol	Apical	Annexins, VIP17MAL	[101, 102]
Fission machinery	Dynamin II	Both	PI4,5P2, actin	[73, 74, 100]
	CtBP3/BARS	Basolateral	PI4,5P2	[103]
Phosphorylation			Target	
	PKD	Basolateral	PI4K, 14-3-3	[104]
	PKC	Basolateral	Cargo	[105]
	PP2A	Basolateral	Cargo	[105]

Coats and adapters:

Many adaptor and coat proteins have been implicated in the surface delivery of biosynthetic cargos. As described above, coats serve as scaffolding for vesicle formation, but may not be essential for tubule elongation. The common link between these coats is that the membrane recruitment and assembly of each is regulated by the small GTP-binding protein ARF-1 (described in detail later)

The adaptor complex (AP1-4) family plays a significant part in the surface expression of many proteins. AP-1 complexes, which in some polarized epithelial cells can be subdivided into AP-1a and AP-1b based on the incorporation of distinct medium chain subunits, are localized to the TGN and endosomes. These complexes are thought to regulate both TGN to endosome and endosome to TGN trafficking. The epithelial specific μ 1b subunit of AP-1b has been suggested to regulate surface delivery of basolateral cargo [106], though μ 1b can complement μ 1a-deficiency in non-polarized cells, suggesting a redundant function [107]. However, the association of AP1b with endosomal compartments suggests that this complex plays a role in basolateral sorting within endosomes rather than at the TGN sorting [108]. AP-2 is present only at the cell surface and is involved in clustering cargo in clathrin-coated endocytic vesicles. AP-3 has been implicated in delivery of newly synthesized lysosomal membrane proteins from the TGN to lysosomes [109] and in the generation of synaptic vesicles from endosomes [110], AP-3 has also been implicated in basolateral targeting of VSV G [95]. while AP-4 has been associated with basolateral trafficking in MDCK cells but does not interact with clathrin [96]. Although more than one AP complex was found to play a role in basolateral trafficking, it is still unclear as

to whether this role is in basolateral cargo export from the TGN or endosomes, which will be described later.

GTP binding proteins/GTPases

Efficient reconstitution of protein export from the TGN of MDCK cells *in vitro* is sensitive to non-hydrolyzable GTP analogues and requires energy [113]. Interestingly, both small GTPases and heterotrimeric G proteins have been implicated in TGN export of both apical and basolateral cargo. These findings suggest multiple stages of TGN export requiring GTP hydrolysis.

Small GTPases are imperative to vesicle formation as these proteins typically regulate the temporal aspects of protein sorting, such as coat recruitment at the appropriate location. Furthermore, GTPases can serve as molecular cues, marking the location at which a vesicle may form. GTPases are also important for the temporal regulation of coat assembly, as the intrinsic GTP hydrolysis activity of these proteins may regulate the rate of dissociation of coat proteins from newly-formed transport carriers.

The ARF-family of GTPases are an attractive target for regulating TGN export as these proteins have been localized to the TGN at steady-state. A universally important small GTPase involved in TGN export is ARF1 (ADP-ribosylation factor 1). In non-polarized cells ARF1 seems to regulate surface delivery of both HA and VSV G [114, 115] whereas only a role in VSV G transport was observed in polarized cells [116]. Interestingly, this effect may be indirect as ARF1 is not necessary for the sorting or export of HA from the TGN in HeLa cells, as I show in chapter 3 [115]. Brefeldin A, an inhibitor of guanine nucleotide exchangers of ADP-ribosylation factors (ARFs), has been shown to decrease apical surface delivery of HA in MDCK

cells, suggesting another brefeldin A sensitive GTPase responsible for apical trafficking [116]. ARF-like GTPase (Arl) is also regulated by brefeldin A and localizes to the Golgi complex [117]. Therefore, this could prove an intriguing target for future studies. Alternatively, an ARF-related protein (ARFRP-1) has recently been described and implicated in both endosome to TGN and TGN to surface trafficking [90]. This molecule may be an interesting target to identify ARF-independent export from the TGN, as the ARF1 inhibitor brefeldin A does not affect ARFRP-1.

Additional GTPases have been found to function in protein trafficking from the TGN to the cell surface and could also represent targets for nonhydrolyzable GTP-analogs. Another GTPase, *cdc42*, seems to regulate the sorting of basolateral cargo in polarized cells [91, 95], and specifically may regulate the AP-1b sorting pathway [87]. In non-polarized cells, the role of *cdc42* in TGN export has not yet been examined in depth, though *cdc42* has been implicated in ATP7A protein (Menkes-disease ATPase) export from the TGN in response to copper [118]. Rab8 has also been shown to play a role in basolateral cargo trafficking in polarized epithelia [87] and in delivery to the somatodendrites of neurons [119].

Another intriguing candidate that has been implicated in the regulation of TGN export is Rab11, a GTPase known to be associated with recycling endosomes. Overexpressed Rab11 has been localized to the TGN by some groups but not others [120, 121], and has been suggested to participate in the TGN export of some cargo [88]. However, endogenous rab11 has yet to be localized to the TGN. Rab11 is thought to be recruited to the TGN by interaction with a phosphatidylinositol 4-kinase, and disruption of this recruitment resulted in decreased basolateral surface delivery of VSV G [89]. Given the uncertainty over the localization of rab11 and recent studies demonstrating the passage of newly-synthesized proteins through recycling endosomes

(see section on indirect trafficking to the surface), it is possible that the effects of rab11-mutants on biosynthetic traffic occur at a post-TGN site.

In addition to Rab11, another rab-family GTPase, Rab6, may play a role in protein export from the TGN. Overexpression of dominant-negative rab6 was found to decrease the surface delivery of influenza HA and alkaline phosphatase in HeLa cells [82], though it has since been shown to regulate the retrograde trafficking of Golgi resident proteins in COPI-coated vesicles from the TGN [83], and therefore may be indirectly involved in export. The effect of Rab6 mutant on HA surface delivery shows that a concerted forward and reverse trafficking of Golgi and TGN components is required for efficient trafficking of biosynthetic cargo.

In addition to small GTPases, heterotrimeric G proteins have also been implicated in cargo export. Interestingly, the stimulatory G (Gs) protein was shown to play a role in apical sorting or export from the TGN, while the inhibitory G (Gi) protein was involved in basolateral trafficking [86]. Gi-dependent export has also been characterized in non-polarized cells, where recruitment of protein kinase D to the Golgi is regulated by Gi [93]. Gi has also been shown to regulate the export of prohormones from the TGN in coordination with dynamin II [122] and may serve as a cue for the formation of different classes of vesicles. These findings may indicate a relationship between stimulatory or inhibitory G proteins and their differential effects on apical versus basolateral trafficking.

Lipid metabolism and TGN export:

Lipids and lipid remodeling also play critical roles in polarized biosynthetic traffic and have been demonstrated to function in both protein sorting and in the biogenesis of vesicular and tubular transport carriers. Cholesterol depletion using methyl-beta-cyclodextrin inhibits apical

cargo export from the TGN [123], while cholesterol loading (increased amounts) causes an inhibition of basolateral cargo export [124]. This suggests that membrane lipid composition is critical to both trafficking pathways, and may allude to a competitive mechanism for the generation of apical versus basolateral transport carriers. Unfortunately most methods for affecting cholesterol levels are chronic (requiring long periods of treatment time), and the acute effect of cholesterol depletion has not been examined directly.

In recent years, an emerging role for phosphatidylinositol (PI) lipids in biosynthetic transport, and particularly in TGN export, has emerged. (reviewed in [125, 126]). PI lipids fall into classes based on the number of times and position of phosphorylation on the inositol head group, including PI-3-phosphate (PI3P), PI-4-phosphate (PI4P), and PI-4,5-bisphosphate (PI4,5P₂). Many proteins in eukaryotic cells possess discrete domains capable of interacting directly with these different isoforms of PI (reviewed in [127]). Therefore, the local synthesis of these lipids may generate a signal for association of certain proteins with the TGN and subsequent vesicle or tubule formation. In fact, PI4P can drive the recruitment of AP-1 complexes to the TGN [128] while PI4,5P₂ can recruit dynamin II to the plasma membrane during endocytosis [129].

PI lipid biosynthesis may regulate both apical and basolateral export from the TGN, though through two different lipid mechanisms. Protein kinase D (PKD) has been shown to regulate the export of basolateral markers, likely through a heterotrimeric G-protein mediated pathway [79, 93], though it may also regulate the lipid composition by positively modulating phosphatidylinositol 4-phosphate biosynthesis at the TGN [130]. Recently, Godi et al., found that overexpression of a mislocalized mutant form of FAPP1, decreased FAPP1 expression, or overexpression of the PI4P lipid binding pleckstrin homology domain inhibited both VSV G and

glycosaminoglycan surface delivery in non-polarized cells [84], while Vieira et al. found that FAPP2 was important for apical sorting [97]. Interestingly, increased PI4P generation has been shown to decrease surface delivery of HA [99], while active phosphatidylinositol4-phosphate5-kinase (PI5K) seems to increase the rate of HA surface delivery (Guerriero CJ and OA Weisz, personal communication). This further suggests, similar to the cholesterol experiments described earlier, that distinct lipid species control the trafficking of apical versus basolateral cargo from the TGN. It will be important to show that PI4K and PI5K affect export from the TGN in an *in vitro* assay, to rule out potential post-TGN trafficking effects.

Another example of proteins that bind phosphatidylinositols are the annexin family. Specifically, annexin XIII [101] and annexin II [102] have been identified as mediators of apical export from the TGN. Annexin XIII at high concentrations *in vitro* stimulates apical trafficking of HA but has an inhibitory effect on basolateral trafficking of VSV G [131]. Furthermore, annexin XIII and influenza HA trafficking to the apical surface require the kinesin KIFC3, suggesting that annexin XIII and HA share a common carrier [75]. The specific role of annexins in apical vesicle formation from the TGN has not yet been described, though it is likely to bridge phosphatidylinositols to other effectors of trafficking, as these proteins are capable of binding phosphatidylinositols.

Novel approaches to identify regulators of protein export from the TGN:

Though the previous sections outline the large number of proteins implicated in TGN export, it is clear that many steps are poorly understood, and the molecular machinery regulating TGN export is not yet fully characterized. Identifying the various effectors of trafficking will involve significant effort, and will likely require exploiting a large number of systems. Recently

a group performed a visual genetic screen in the budding yeast *Saccharomyces cerevisiae* for trafficking mutants of a raft-dependent synthetic cargo and found many effectors including sterol synthesis enzymes and actin-modifying proteins [132]. Mutants identified were categorized into a variety of classes based on localization of the cargo molecules (eg., Golgi localization versus vesicular localization). These proteins can now be tested in polarized cells to determine the effects on sorting and polarized secretion. Screens, such as the one referenced, here will provide invaluable information toward the understanding of protein sorting and export from the TGN. Small interfering (si)RNA technology (decreased expression of target protein) has recently become an attractive approach to screen the genome for proteins involved in Golgi function [133]. An siRNA-based approach has been used to screen eukaryotic kinases for effects on caveolar mediated endocytosis [134]. These methods will only identify non-essential genes, however, as siRNA decreases protein expression after chronic treatment for days. To address the contribution of both essential and non-essential genes, classical biochemistry coupled to a sensitive *in vitro* assay may provide a less biased perspective.

Requirements for the fission of transport carriers from the TGN:

Fission of transport carriers from the TGN involves protein- or lipid-mediated constriction of the vesicle that ultimately results in separation of the carrier from the TGN membrane. Fission of basolaterally-destined transport carriers has been shown to require PKD [72]. This may reflect the indirect role of PKD in regulating the synthesis of PI4P [130]. Based on our current understanding of the role of this lipid in TGN export, the prediction is that PKD-induced changes in PI4P would affect the association of specific proteins with the TGN.

Dynamin, a 100kD protein initially identified as a component of the endocytic machinery, has been also implicated in membrane fission steps along the biosynthetic pathway. Based on studies with dominant negative dynamin 2, a role for dynamin in TGN export of the basolaterally-directed proteins VSV G [73, 77] and the polymeric immunoglobulin receptor (pIgR) [100] has been suggested; however, another study found no effect of expressing dominant-negative dynamin 1 or 2 on biosynthetic delivery of newly synthesized pIgR, but did report an effect on endocytosis [135]. As dynamin has been implicated in the recycling of proteins from endosomes to the TGN, expression of dominant negative constructs may exert an indirect effect on cargo trafficking by blocking the retrieval of resident TGN proteins [136]. With respect to the possible role of dynamin in apical protein export, two groups have shown that dynamin 2 is important for the trafficking of the apical cargo p75-neurotrophin receptor from the TGN to the surface [74, 103]. However, in one of these studies, CtBP3/BARS, a protein that contains a curvature-inducing membrane association BAR domain, rather than dynamin 2 was suggested to be responsible for the fission of basolateral transport intermediates [103]. This observation suggests the intriguing possibility that distinct fission machineries control the generation of different types of transport carriers destined for delivery to opposing membrane domains.

Regulation of TGN export by kinases and phosphatases:

Phosphorylation of amino-acid residues in a protein can temporally activate or inactivate proteins involved in TGN export or even, in one described case, can generate an export signal on cargo. This process is regulated by kinases, enzymes that phosphorylate substrates, and phosphatases, proteins that remove the phosphorylation from substrates. A plethora of

pharmacological inhibitors have been described for different kinases and phosphatases expressed in eukaryotic cells (reviewed in [137, 138]). Export of pIgR from the TGN has been shown to be negatively regulated by protein kinase C, and requires protein phosphatase 2A activity [139]. This is correlated with previous findings that PP2A inhibition resulted in decreased surface delivery of VSV G [140]. Furthermore, PP2A activity positively regulates the association of AP-1 with cargo at the TGN [95]. Therefore, phosphorylation-dependent interaction with adaptor complexes may drive export of basolateral cargo. Interestingly, and notably similar to the inverse relationship of cholesterol, PI4P, and G proteins on apical versus basolateral export, HA surface delivery is positively regulated by protein kinase C (CJ Guerriero and OA Weisz, communication). Protein kinase A has also been shown to positively regulate HA export from the TGN [141]. Whether a mechanism similar to AP-1 phosphorylation-dependent interaction with cargo may operate in apical traffic remains to be determined. It is unclear how kinases and phosphatases regulate apical and basolateral trafficking, though the substrates of these enzymes could shed light on the underlying mechanism. Recently developed protein microarrays may serve as invaluable tools in identifying these substrates by providing a large-scale screen of potential targets [142]. A large number of protein domains can be rapidly expressed from bacteria and blotted onto nitrocellulose. Purified kinases can then be tested for their ability to phosphorylate substrates *in vitro* by incorporation of radioactive phosphate. This will provide a library of candidates which can then be tested *in vivo* for kinase specific phosphorylation (through siRNA) and a role in membrane trafficking.

Other regulators of export:

Organelle pH has also been implicated in the export of apical cargo from the TGN in MDCK cells [143], and may regulate the recruitment of coat proteins or sorting receptors. The TGN is acidified to ~pH 6.1 by the vacuolar ATPase proton pump, and is maintained by a combination of counterion conductance and proton leak, as well as the activity of the vacuolar ATPase [144-146]. Trafficking of apical cargo is inhibited by either overexpressing a channel that enhances proton leak [143] or blocking the vacuolar ATPase with the channel blocker bafilomycin A1 (Weisz OA, unpublished data; see chapter 2). Proton leak enhancement, by expression of the influenza M2 proton pore, was shown to specifically affect export from the TGN [143]. Furthermore, this channel can be blocked by the antiviral drug amantadine which abrogated the effect of M2 expression on apical traffic [143]. Interestingly, proton-pore expression does not affect basolateral trafficking to the plasma membrane, while bafilomycin does. This may mean that a threshold acidic pH is required for TGN export of all cargo, while apical cargo export has a more stringent acidic pH requirement.

Presently, it is unclear how pH may regulate vesicle formation from the TGN. The recruitment of COPI to endosomes, and subsequent formation of multivesicular bodies but not recycling of cargo [147], is thought to be regulated by a pH sensor [148]. Furthermore, it has been shown that ARF6 is recruited to the endosome by a subunit of the vacuolar ATPase, which has been proposed to serve as the pH sensor in COPI recruitment to endosomes [149]. Recently, the PI4P-binding protein FAPP2 has been implicated in apical sorting and has been proposed to serve as a coat for apical vesicle formation [97, 150] It will be very exciting to determine whether FAPP2 recruitment to the TGN is dependent on acidification of this compartment.

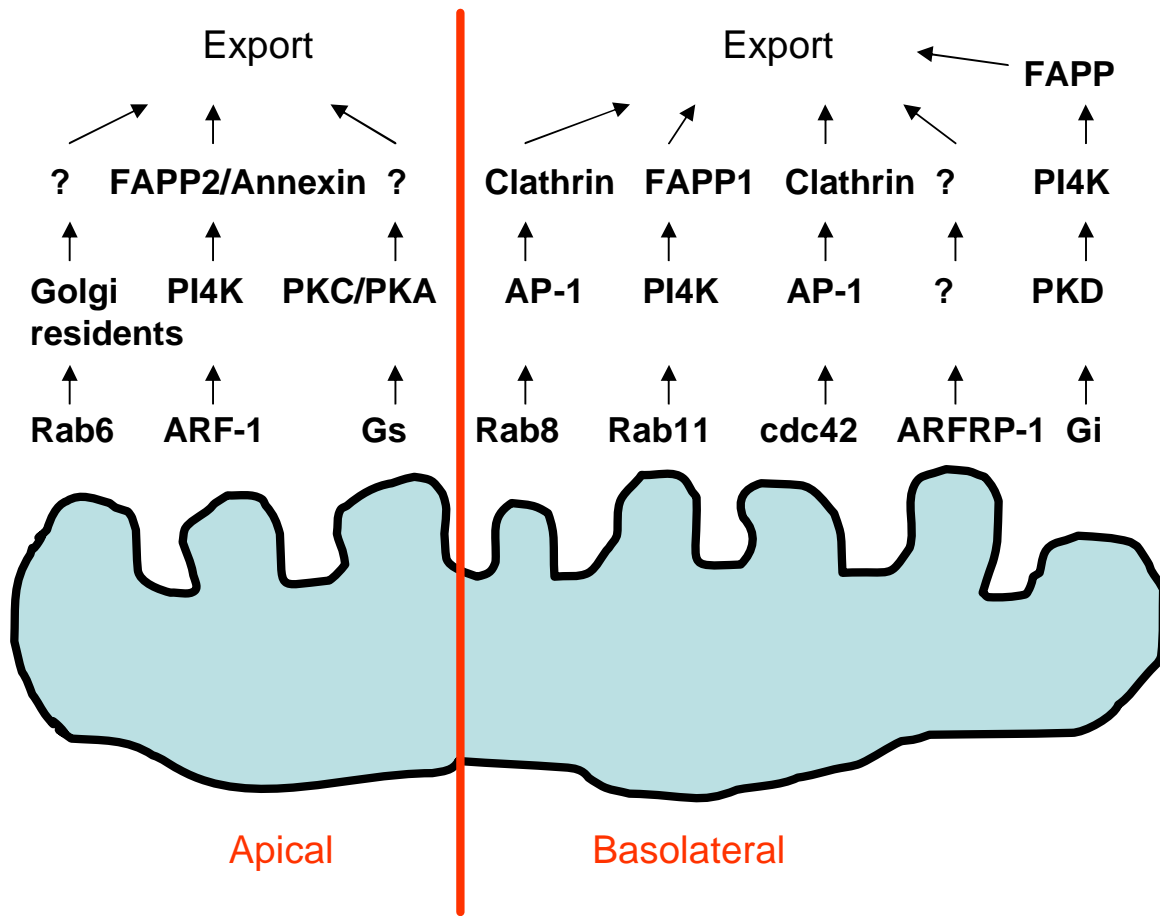


Figure 1.2: Potential mechanisms for apical and basolateral export from the TGN.

Progressive recruitment of trafficking effectors is indicated by arrows. Question marks represent steps that have not been described.

Morphology of TGN derived carriers:

Live cell microscopy, along with the advent of fluorescent-protein (FP) technology, have provided scientists with the means to study biosynthetic trafficking in living cells. TGN- staged FP labeled cargoes have been visualized exiting the TGN as well as fusing with the plasma membrane, allowing morphological examination of the transport carriers *in vivo*. The first cargo observed to exit the TGN in live cells was the basolateral marker vesicular stomatitis virus G protein (VSV G) fused to green fluorescent protein (GFP) [151]. Hirschberg et al. found that VSV G-GFP exited the TGN in large pleomorphic vesicles that did not fuse with other

compartments *en route* to the plasma membrane. Toomre et al. [152] extended these studies to observe both vesicles and long tubules containing VSV-G-GFP emanating from the TGN. The vesicles and tubules were highly dynamic, both fusing with each other and fragmenting as they traveled along microtubules. Keller et al. [16] progressed these findings to observe sorting of VSVG-YFP from glycosylated CFP linked to GPI. The researchers found that VSVG-YFP and GPI-CFP are sorted into distinct tubular and vesicular carriers that exit the TGN, and that these carriers were not found to fuse with endosomes prior to plasma membrane delivery during long movies.

Some proteins involved in TGN export could regulate vesicle/tubule formation or post-TGN trafficking steps. Kreitzer et al. observed export of an apical transmembrane protein, p75-GFP, in tubular carriers that required both dynamin 2 and a nonconventional kinesin for formation [74]. The involvement of a kinesin suggests at the least that tubule formation requires microtubule-based motors, but also supports the mechanical fission hypothesis described earlier. Dynamin and kinesin were independently involved in formation of carriers with different morphologies in this study. Musch et al. found that constitutively active mutants of a small GTPase *cdc42* stimulate apical protein (p75-GFP) export from the Golgi, while inhibiting the kinetics of basolateral protein (NCAM-GFP) export [92]. These results suggest a possible role for actin polymerization in TGN to plasma membrane delivery, though the role of actin at the TGN has not yet been described. One mechanism for actin involvement in biosynthetic trafficking may be via the generation of actin comets that function to propel transport carriers through the cytoplasm (reviewed in [153]). This method of motility has specifically been implicated in the post-Golgi trafficking of a subset of apical cargo (CJ Guerriero and OA Weisz, communication).

Trafficking Routes and Pathways to the Plasma Membrane

Although we commonly imagine multiple apical cargo to follow a single pathway, it is unclear whether all apical cargo (or basolateral cargo) share a common carrier. Based on a few examples, the simple answer is yes and no. Therefore, apical export may be further broken down into multiple trafficking pathways. This complicates our understanding of this event, however it may indicate that export is cargo-specific and that the cargo itself may direct its own export.

One of the first investigations into whether different proteins sorting into common carriers was performed by Jacob et al. [17]. This group followed TGN export of two fluorescently tagged apical proteins with different sorting motifs, lipid raft association or glycan-based sorting. These two apical proteins were found to initially segregate together from the TGN in a large vesicular compartment, which gave rise to smaller vesicles with the two cargoes segregated from each other. This work suggests that a common carrier initially exits the TGN with both apical cargoes, but then the two cargoes are segregated into smaller carriers before trafficking to the surface. The particular steps observed using biochemical assays may not accurately describe this stage in trafficking, as the large vesicular compartment may be too large to separate by a simple centrifugation step, and may require more complicated isolation on density gradients. Furthermore, it is completely unknown which effectors are responsible for large vesicle formation versus smaller vesicle formation. They also observe very different maturation kinetics of their proteins, so it is not clear whether they are really looking at TGN export.

Additional studies further support the existence of multiple trafficking pathways to the apical surface. Notably, post-TGN trafficking of one apical cargo was found to be actin-

dependent, while the other was not [154], though both required microtubules for post-TGN trafficking. This further indicates two steps of trafficking between the TGN and the plasma membrane which may represent two sorting events. Lastly, a potential motor, brush border myosin, involved in raft-dependent trafficking was identified recently [155], however it is unclear whether single-headed myosins are capable of motor activity associated with two-headed conventional myosins, and the function of this protein is not yet fully understood in this context.

If multiple trafficking pathways exist to the apical surface, would this mean that when one is perturbed, the other may serve as a default pathway? It doesn't appear to work that way. Delacour and colleagues recently showed that a glycan-dependent sorting receptor (galectin-3) was required for the proper sorting of a raft-independent apical cargo. When galectin-3 was removed from the system, the raft-independent apical cargo was mislocalized to the basolateral domain, while a raft-dependent apical cargo was trafficked normally [156]. This suggests that either the raft-independent cargo possesses a recessive basolateral motif, or that different apical cargoes are actively sorted into apical carriers, while basolateral cargoes represent a default pathway.

Export of basolateral cargoes has been thought to occur in common transport carriers, though it is possible that either multiple carriers exist, or that protein sorting into these carriers is differentially regulated. Rustom et al. [157] found that a soluble marker chromogranin B-YFP was sorted into basolateral carriers containing VSVG-FP, though notably many CrB-YFP carriers lacked VSVG-CFP and *vice-versa*. Apical carriers completely lacked CrB-YFP however, and deletion of the CrB-YFP sorting motif caused the soluble protein to enter both types of carriers. This suggests that some basolateral cargo may share common compartments, and therefore common requirements for TGN exocytosis. Lastly, Rustom et al. emphasized the

morphological differences in apical (GPI-CFP) and basolateral carriers (VSVG-YFP), with apical carriers being spherical and basolateral carriers being tubular. This differs from what some other groups have found [16], and may reflect differences in cell types.

An indirect biosynthetic pathway to the cell surface:

Although it has been long thought that proteins are transported directly from the TGN to the plasma membrane, recent evidence suggests that some proteins are delivered to endosomes prior to surface delivery. The basolateral cargoes transferrin-receptor [158], VSV G [159], and asialoglycoprotein receptor [160] were all found to transiently localize to endosomes prior to delivery at the plasma membrane. In contrast, secreted horseradish peroxidase took a direct route to the surface rather than trafficking through endosomes, indicating a requirement for sorting into the endosomal pathway [161]. In fact, Connolly and colleagues suggest that more than 50% of the newly synthesized transferrin receptor could be trafficked through this route, emphasizing the need for a distinct sorting signal for both TGN to endosome and endosome to plasma membrane trafficking. This latter signal could be the same adaptor complex binding motif required for export from endosomes, and which has been implicated in the surface delivery of newly synthesized basolateral proteins. Interestingly, adaptor protein (AP)-1b and rab8, a GTPase involved in basolateral sorting, are localized to endosomal compartments, not to the TGN [87].

Although AP-1b has been implicated in basolateral trafficking, it is unclear how or if cargo is sorted at the TGN before being targeted to the plasma membrane from endosomes. Orzech et al. [94] found that the polymeric immunoglobulin receptor (pIgR) was targeted to endosomes from the TGN by phosphorylation-dependent interaction with AP-1. This indicates

that TGN to endosome trafficking may require protein kinase-mediated phosphorylation to generate a sorting motif. It would be interesting to examine the dependence of other proteins', such as VSV G and transferrin-receptor, endosomal-targeting on phosphorylation.

The particular types of endosomes serving as sorting stations may represent multiple compartments. Lock and Stow [162] have recently shown that E-cadherin enters Rab11-positive recycling endosomes *en route* to the basolateral membrane in polarized cells, as well as to the plasma membrane of non-polarized cells. This study defines the endosomal compartment as Rab11-positive recycling endosomes. Another study found that the basolateral cargo VSV G traverses transferrin-labeled endosomes before reaching the plasma membrane [159]. Interestingly, Rab11 is not associated with transferrin-positive compartments in polarized MDCK cells [163], suggesting multiple sorting stations may exist in the endosomal pathway with distinct cargo.

Observation of another cargo molecule may suggest an interesting stage in protein trafficking from the TGN. Turner and Arvan [164] found that two trafficking pathways, one from the TGN and the other from endosomes, directed secretion of procathepsin B. The researchers proposed that TGN export of procathepsin B by AP-1 and clathrin is inefficient, while export from endosomes overcomes this deficiency. This hypothesis should be further tested by expressing increasing amounts of cargo and determining the extent to which the cargo intersects the endosomal compartment.

The existence of an indirect pathway to the basolateral surface is well supported by current data, however it is unclear whether apical proteins also take this indirect route to the cell surface. The study described here used an apical version of the basolateral marker VSV G, though evidence that other apical markers follow this pathway is presently lacking. This

pathway appears to depend on AP-1b [87, 159] which is not involved in apical biosynthetic trafficking, and thus is unlikely to regulate biosynthetic delivery of apical cargo. This hypothesis could be tested using an endosome-crosslinking approach described by Ang et al [159] in which endocytosed peroxidase-conjugated ligand is chemically crosslinked in endosomes to inactivate this compartment. TGN staged cargo is then released from a temperature block and the surface delivery is observed over a time course. Comparing treated and untreated samples, apical surface delivery of cargo can be determined to follow or bypass the endosomal compartment.

Aims of My Project

Though the understanding of protein trafficking through the biosynthetic pathway is expanding rapidly, many questions remain unanswered. Are apical and basolateral proteins sorted into discrete carriers from the TGN of non-polarized cells? What represents the molecular requirement for GTP hydrolysis in apical export from the TGN? Does a similar requirement exist for basolateral export? What other effectors regulate apical export from the TGN? These questions will be addressed by generating an assay that can accurately recapitulate export from the TGN, testing the requirements for export and the potential role of two GTPases, and ultimately identifying novel effectors of apical export by fractionating cytosolic proteins and isolating export activity. Together, these findings will expand the present understanding of apical cargo exit from the TGN, and potentially shed light on some of the differences between apical and basolateral cargo trafficking in non-polarized cells.

Specific aim 1: To develop an assay that measures apical carrier formation from the TGN.

Though a variety of *in vitro* assays are available for studying protein export from the TGN, few have been analyzed for the ability to recapitulate apical export events. To test the

ability of two assays for recapitulating this process, I exploited the pH-dependence of apical export. Adding bafilomycin A (a pharmacological reagent which blocks acidification of the TGN) or expressing influenza M2 proton pore (which generates an acid-activated proton leak in organelles of the biosynthetic pathway) allowed me to determine whether apical export in these assays was sensitive to pH perturbation. I found that a perforated cell based assay was sensitive to pH disruption while a Golgi membrane based assay was incapable of discerning this effect.

Specific aim 2: To characterize the selective requirements for TGN export of HA compared with a basolateral marker.

Using the perforated cell assay tested in aim 1, I next analyzed the requirements for export from the TGN of an apical cargo (influenza hemagglutinin [HA]) and a basolateral cargo (TGN46). Initially, I characterized the *in vitro* assay and the exported cargo, including the regulation of export by GTP hydrolysis. As mentioned in earlier sections of this chapter, the small GTPase ARF1 has been associated with the regulation of protein export from the TGN. Specifically, one group had shown that a compound regulating ARF1 activity (brefeldin A) selectively inhibited HA surface delivery [116]. I removed ARF1 from the reconstitution reaction and characterized the effect on apical and basolateral export.

Specific aim 3: To identify novel proteins that regulate HA export from the TGN.

As very few effectors of apical export from the TGN have been described, I next used the perforated cell assay to identify novel effectors of HA export from the TGN. Biochemical fractionation using column chromatography provides a fraction enriched in HA export activity. The proteins in this fraction are identified and their potential role in HA export are described. I further examined the role of dynamin 2 in HA export and found that this GTPase is required for HA export but not export of a basolateral cargo. This provides a role for GTP hydrolysis in HA export and supports the hypothesis that dynamin 2 regulates apical but not basolateral export from the TGN [103].

The goal of these studies was to identify proteins that regulate apical protein export from the TGN. These data will help us to understand how proteins are selectively packaged into distinct containers and identify mechanisms by which these are released from the TGN. Additionally, this work will provide novel effectors of membrane trafficking from the TGN, which could fill some missing information in the process of apical-cargo containing vesicle formation during biosynthetic sorting.

2. ***In vitro* assays differentially recapitulate protein export from the *trans*-Golgi network.**

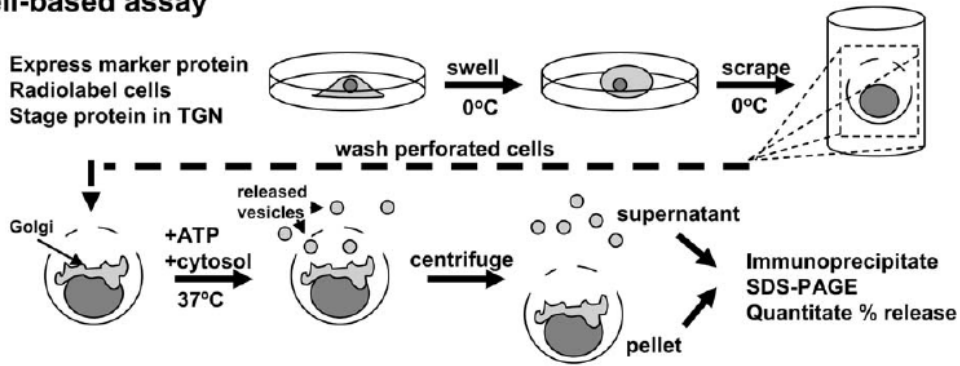
In vitro assays have been broadly applied to reconstitute trafficking events along the biosynthetic and endocytic pathways of eukaryotic cells [165]. Cell-based assays employ mild detergents or mechanical means to perforate the plasma membrane and release cytosolic components while maintaining the integrity of intracellular membrane compartments (Fig. 1). In contrast, cell-free assays are performed using isolated membrane fractions enriched in a particular organelle. Cell-based assays can allow analysis of multiple steps along a trafficking pathway, while cell-free assays are generally designed to reconstitute an individual membrane fission or fusion step. Both cell-based and cell-free assays have proven useful for dissecting the role of various components in intracellular trafficking events. In many instances, these assays have been utilized to dissect the requirements for polarized biosynthetic sorting of cargo molecules from the *trans*-Golgi network (TGN; [86, 166-168]. Interestingly, segregation of apical and basolateral marker proteins into distinct transport carriers that bud from the TGN appears to occur even in non-polarized cells, enabling the use of non-differentiated cell types for such assays [16, 45, 81]. However, the extent to which these assays recapitulate *in vivo* sorting and regulation of membrane traffic has not been systematically examined.

Here we have compared cell-based and a cell-free *in vitro* assays for their ability to reconstitute polarized protein sorting from the TGN. We previously found that efficient apical delivery of the marker protein influenza hemagglutinin (HA) in polarized Madin-Darby canine kidney (MDCK) cells requires TGN acidification [169]. In particular, expression of the acid-activated proton channel influenza M2 selectively inhibited TGN-to apical surface delivery of HA but had no effect on delivery of a basolaterally-destined protein [169]. Moreover, expression of a dominant-negative inhibitor of the GTPase dynamin has been shown to inhibit TGN export of apical proteins [74], suggesting a requirement for GTP hydrolysis in apical membrane delivery. Therefore, we asked whether cell-based and cell-free assays accurately reconstitute GTP- and acid pH-dependent export of HA from the TGN. Surprisingly, only the cell-based assay accurately recapitulated both of these *in vivo* requirements for HA sorting.

In the cell-based assay, HeLa cells grown to 70% confluence on 10cm dishes were infected with replication-defective recombinant adenovirus encoding influenza HA. Cells were

starved for 30 min in methionine-free medium, pulsed for 15 min in medium supplemented with 150 $\mu\text{Ci/ml}$ tran- ^{35}S -label (MP biochemicals), and chased for 2-3 h at 19°C to stage newly-synthesized HA in the TGN. Cells were incubated on ice with swell buffer (10mM HEPES pH 7.2, 15mM KCl), scraped into break buffer (50mM HEPES pH 7.2, 110mM KCl), and washed with break buffer by centrifugation at 800xg for 5 min at 4°C. Cells were then brought to volume in GGA buffer (25mM HEPES, pH 7.4, 38mM K-aspartate, 38mM K-glutamate, 38mM K-gluconate, 2mM EGTA, 1mM DTT, and 2.5mM MgCl_2). Release was reconstituted at 37°C for 1 h in the presence of 1mM ATP, 8mM phosphocreatine, 5g/ml creatine phosphokinase, and 100 μg rat brain cytosol in a total volume of 50 μl . Released vesicles were separated from cells by centrifugation for 5 min at 12,500 rpm in an Eppendorf microcentrifuge. Supernatants and pellets were solubilized and HA immunoprecipitated using monoclonal anti-HA antibody. Samples were analyzed by SDS-PAGE and the efficiency of HA release was quantitated upon phosphorimager analysis as previously described [115].

Cell-based assay



Cell-free assay

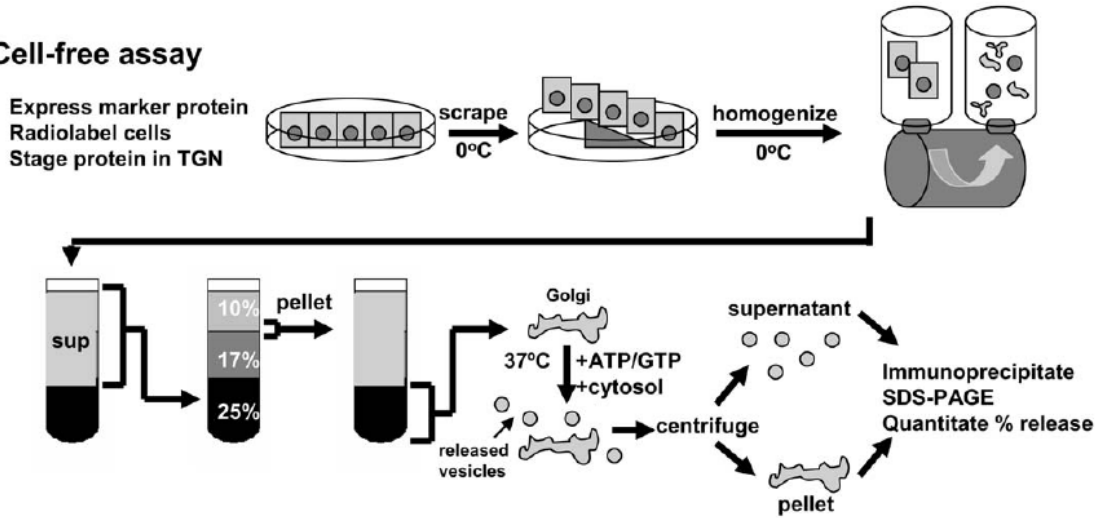


Figure 2.1: Schematic description of in vitro cell-based and cell-free assays.

We also used a cell-free assay to reconstitute the export of radiolabeled, TGN-staged HA from isolated Golgi membranes. Ten 15-cm plastic dishes containing confluent MDCK cells infected with replication-defective recombinant adenovirus were incubated with calcium-free PBS containing 1mM magnesium chloride for 10 min at 37°C to disrupt tight junctions and facilitate subsequent access of methionine to basolateral transporters, then radiolabeled and chased as described above. The cells were then scraped from the dish in PBS, pelleted, and resuspended in 2.5 ml homogenization buffer (20mM Tris HCl pH 7.8, 1mM EDTA, 0.25% sucrose, 1x protease inhibitor cocktail [Calbiochem]). The resuspended cells were passed through a ball-bearing homogenizer with a 0.001 inch clearance fifteen times, and then centrifuged at 1000xg at 4°C to obtain a post-nuclear supernatant. This was mixed with an equal volume of 50% Nycodenz (final volume 6 ml) and overlaid sequentially with 4ml 17.5%, 2ml 10%, and balanced with TE buffer (20mM Tris pH 7.8, 1mM EDTA). The gradient was centrifuged at 56,000xg in a Sorvall TH641 rotor for 3 h to float Golgi membranes to the 17.5%/10% interface. The 10%/17.5% interface and much of the 10% fraction were collected (visible as a solid white band), diluted 3-fold with homogenization buffer, and centrifuged for 1 h at 100Kxg to pellet the membranes. Aliquots were flash frozen and stored at -80°C. To reconstitute export, 50 µg of membranes were thawed rapidly then placed on ice. The Golgi membranes were mixed with 2-fold concentrated ATP regenerating system, 1 mM GTP, and 2 mg/ml cytosol in a final volume of 100 µl. Tubes were mixed gently by tapping and placed at 37°C for 1 h. Golgi membranes were separated from released vesicles by centrifugation for 10 min at 12,500 rpm in a microcentrifuge, and HA was immunoprecipitated and analyzed as described above to quantitate release.

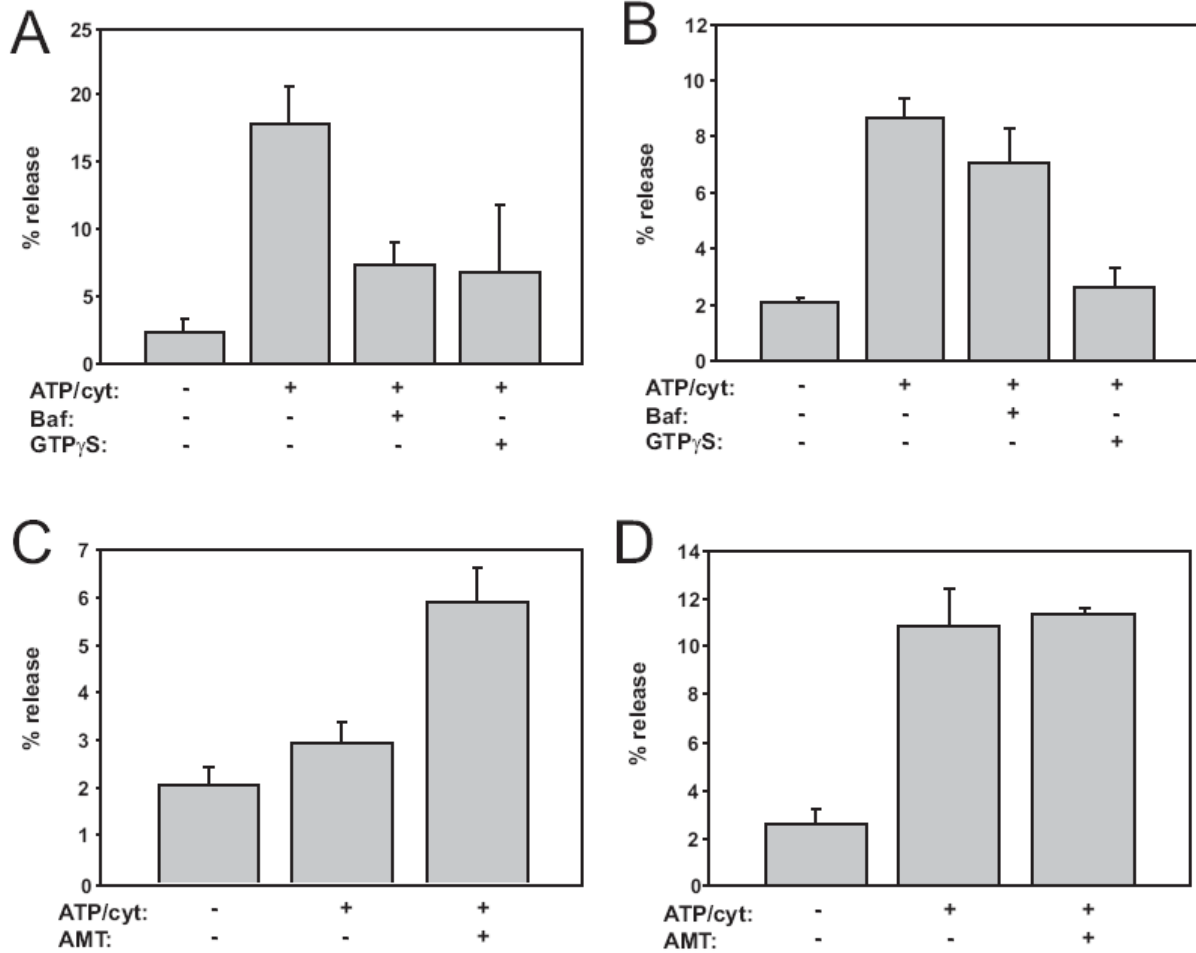


Figure 2.2. Comparison of GTP and pH requirements in cell-based versus cell-free assays.

Cells expressing HA were radiolabeled, chased at 19°C and either perforated (panel A) or used as a source for Golgi membrane isolation (panel B). The effect of bafilomycin A₁ (5 μM) and GTP γ S (10-100 μM) on TGN export was evaluated as described in the text. The mean \pm S.D. of triplicate samples is plotted, P<0.05 comparing untreated in A to +Baf and +GTP γ S, or untreated in B compared to +GTP γ S. Export of TGN-staged HA in the cell-based assay is inhibited in cells expressing influenza M2 but restored by addition of the proton channel blocker amantadine (AMT, panel C), whereas export from Golgi membranes prepared from influenza M2-expressing cells is robust and unaffected by inclusion of amantadine (panel D) The mean \pm range of duplicate samples is plotted, statistics were not performed due to the low sample size.

We routinely observed cytosol- and ATP-dependent release from both assays (Fig. 2). The release of TGN-staged HA in either assay typically ranged between 5-20% of total and represented a 2-10-fold increase over background release measured in the absence of ATP and cytosol. To examine whether this release was sensitive to physiologically-relevant regulators of apical membrane traffic, we tested the effect on these assays of including the non-hydrolyzable nucleotide GTP γ S as well as the vacuolar ATPase inhibitor bafilomycin A₁ (Baf). Both of these treatments disrupt cell surface delivery of HA *in vivo* in both HeLa and MDCK cells (unpublished results, [113]). Surprisingly, both GTP γ S and Baf inhibited HA release from the cell-based assay (Fig. 2A) whereas only GTP γ S inhibited HA release from isolated Golgi membranes (Fig. 2B). Interestingly, HA and VSV G (a basolateral marker) released from Golgi fractions were shown to be equally efficient at fusing with basolateral membranes [170]. One might imagine that HA may be missorted in the Golgi assay, though the sensitivity to GTP γ S suggests otherwise, as basolateral protein export from the TGN is fairly insensitive to this treatment (10-100 μ M) [115, 171].

To further examine the requirement for TGN acidification in these assays, we evaluated the effect of expressing influenza M2, an acid-activated proton channel that effectively neutralizes the pH of the TGN. We previously found that expression of M2 inhibits apical delivery of HA *in vivo*, and that the effect of M2 expression is completely rescued by addition of the M2 channel blocker amantadine to cells [169]. HA export in our *in vitro* cell-based assay is significantly inhibited in cells expressing M2, and restored to control levels by inclusion of amantadine in the reconstitution reaction ([115]and Fig. 2C). However, HA export from Golgi membranes prepared from M2-expressing cells was unaffected by amantadine (Fig. 2D), confirming that release from isolated Golgi fractions occurs via a pH-independent mechanism.

Recent studies have found that some biosynthetic cargo traverse endosomes *en route* to the plasma membrane (reviewed in [1]). One interpretation of the data shown here may be that pH-dependent release of HA occurs from endosomes rather than the TGN, as in the absence of endosomes (Golgi assay) HA release is pH-independent. It is not known whether HA travels through endosomes before reaching the plasma membrane, though this itinerary has only been observed for basolateral cargo to date. This will be an important question to address, and may explain the differences between these two assays.

In summary, comparison of a cell-based assay and a cell-free assay for pH-dependent export of the apical cargo molecule influenza hemagglutinin (HA) demonstrates that the former more closely reconstitutes regulation and sorting events that occur *in vivo*. While the cell-based assay maintained the physiological dependence of HA release from the TGN on luminal pH, export in the cell-free Golgi assay was not affected by Baf or by expression of active M2. Together, these data suggest that isolated Golgi membranes do not maintain physiological ion gradients that enable acidification of the TGN. Therefore, the observed release of HA from Golgi membranes would be comparable to the release from perforated cells in the presence of Baf (though the actual values from these two different assays can not be compared directly). Interestingly, whereas neutralization of TGN pH in permeabilized cells severely compromised the export of HA, we observed comparably efficient release of TGN-staged HA from Golgi membranes in the cell-free assay, even though the TGN is apparently not acidified under these assay conditions. Therefore, release of HA in the cell-free assay does not appear to accurately reconstitute physiological sorting of HA, and may reflect redirection of HA into alternative transport carriers that mediate pH-independent sorting pathways.

3. ARF1-Independent Protein Sorting and Export from the *trans*-Golgi Network.

INTRODUCTION

Newly-synthesized transmembrane and secretory proteins in eukaryotic cells traverse a complex route to their final destinations. The biosynthetic pathway begins when newly synthesized proteins are translocated into the endoplasmic reticulum and ends at the *trans*-Golgi network (TGN), a Golgi-associated tubular network where proteins are sorted into distinct membranous carriers. The TGN serves as a sorting station to segregate proteins destined for endosomes, lysosomes, and the plasma membrane. To add to this complexity, proteins destined for the cell surface can be sorted into distinct types of transport carriers. This additional level of sorting is most obvious in polarized epithelial cells, where the plasma membrane is differentiated into discrete apical and basolateral domains. In these cells, delivery of newly-synthesized apically- and basolaterally-destined proteins from the TGN to the cell surface is critical for the maintenance of the different protein and lipid compositions at either cell surface domain (reviewed in [172, 173]). Interestingly, the distinct sorting of “apical” and “basolateral” proteins into separate carriers that bud from the TGN is recapitulated in nonpolarized epithelial cells, as well as in several non-differentiated cell types including fibroblasts and Vero cells [16, 17, 45, 81, 157]. Nonpolarized cells thus provide a useful model in which to investigate the regulation of TGN sorting and export of different classes of proteins, including markers of the apical and basolateral biosynthetic pathways.

While considerable research has been directed toward dissecting the signals on cargo molecules that mediate their polarized delivery, the mechanisms by which these signals are interpreted and the machinery involved in sorting apical and basolateral proteins remains largely unknown. Basolateral targeting signals are generally localized to discrete amino acid sequences in the cytoplasmic domains of proteins. Cytosolic adaptor protein (AP) complexes recognize these motifs and link the cargo to a coat protein such as clathrin [174]. Various AP complexes have been implicated in targeting proteins to the basolateral but not the apical surface [95, 96, 108]. However, TGN-derived vesicles containing basolaterally-destined proteins are not clathrin-coated [72]. A role for coatomer in basolateral protein export has also been suggested [175];

however, a recent report has questioned the requirement for any coats in the formation of TGN-derived basolateral carriers enriched in basolateral proteins [176].

In contrast to basolateral proteins, sorting of apically-targeted proteins generally depends on motifs within the luminal or transmembrane domains, although some examples of cytoplasmically-disposed apical targeting signals have also been described [177, 178]. N- and O-linked carbohydrates are required for apical targeting of a subset of proteins [179-183]. The association of some proteins with sphingolipid-enriched microdomains or rafts in the TGN has also been proposed to direct their apical delivery [184].

Influenza hemagglutinin (HA) has been used extensively as a marker for the apical pathway in polarized cells. Sorting information resides within the transmembrane domain of HA, although no transferable amino acid sequence has been identified [65, 185]. HA is efficiently incorporated into lipid rafts, though the correlation between lipid raft association and polarity is unclear [65, 123, 185]. While little is known about how this protein is packaged into apically-destined vesicles at the TGN, cell surface delivery of HA is disrupted by expression of influenza M2, an acid-activated proton channel that elevates the pH of acidified intracellular compartments, including the TGN [143, 186-189].

In order to begin to identify the cytosolic requirements for the formation of apically-destined vesicles from the TGN, I have reconstituted ATP- and cytosol-dependent TGN export of pre-staged HA in perforated HeLa cells. My data suggest that this transport assay faithfully recapitulates *in vivo* requirements for efficient HA release from the TGN. Moreover, I find that ADP ribosylation factor 1 (ARF1), a small GTP-binding protein required for recruitment of adaptor and coat proteins to the Golgi complex and the TGN, is not required for efficient HA release. Additionally, HA release under ARF-depleted conditions remains sensitive to selective inhibitors that disrupt HA export in the presence of ARF1, suggesting that ARF depletion does not cause rerouting of HA into alternative transport carriers. Together, my data suggest that packaging and export of apical proteins does not require the assembly of known coat protein complexes.

RESULTS

Reconstitution of HA release from perforated cells-

As a prelude to identifying cellular factors that regulate the TGN sorting and export of apical proteins, I tested the ability of several previously described *in vitro* transport assays to reconstitute the release of TGN-staged HA in epithelial cells. My goal was to develop an assay that was reproducible, relatively robust, and recapitulated *in vivo* sorting in the TGN. Although I could reconstitute pH-sensitive HA release from mechanically-perforated polarized MDCK cells [143], vesicle release in this assay was inefficient and the degree of perforation obtained was inconsistent. Reconstitution of HA release from isolated Golgi preparations purified from polarized MDCK cells was both efficient and reproducible, but did not recapitulate physiological properties of sorting observed *in vivo* (see chapter 2). However, I found that release of TGN-staged HA from hypo-osmotically-swelled, perforated HeLa cells was relatively robust, reproducible, and sensitive to conditions that inhibit HA transport *in vivo*. HeLa cells expressing HA were metabolically-radiolabeled for 10 min and newly-synthesized HA was staged in the TGN by incubation for 2 h at 19°C. Subsequently, the cells were perforated by swelling and scraping, and vesicle release was reconstituted in the presence or absence of an ATP-regenerating system and cytosol. As shown in Fig. 3.1A, release of HA was robust only when both ATP and cytosol were present. The efficiency of HA release was dependent on the concentration of cytosol, with maximal release observed at 2 mg/ml (Fig. 3.2A). Moreover, using this assay, I observed similar kinetics of HA release when transport was reconstituted using either rat brain or rabbit liver cytosol (Fig. 3.2B).

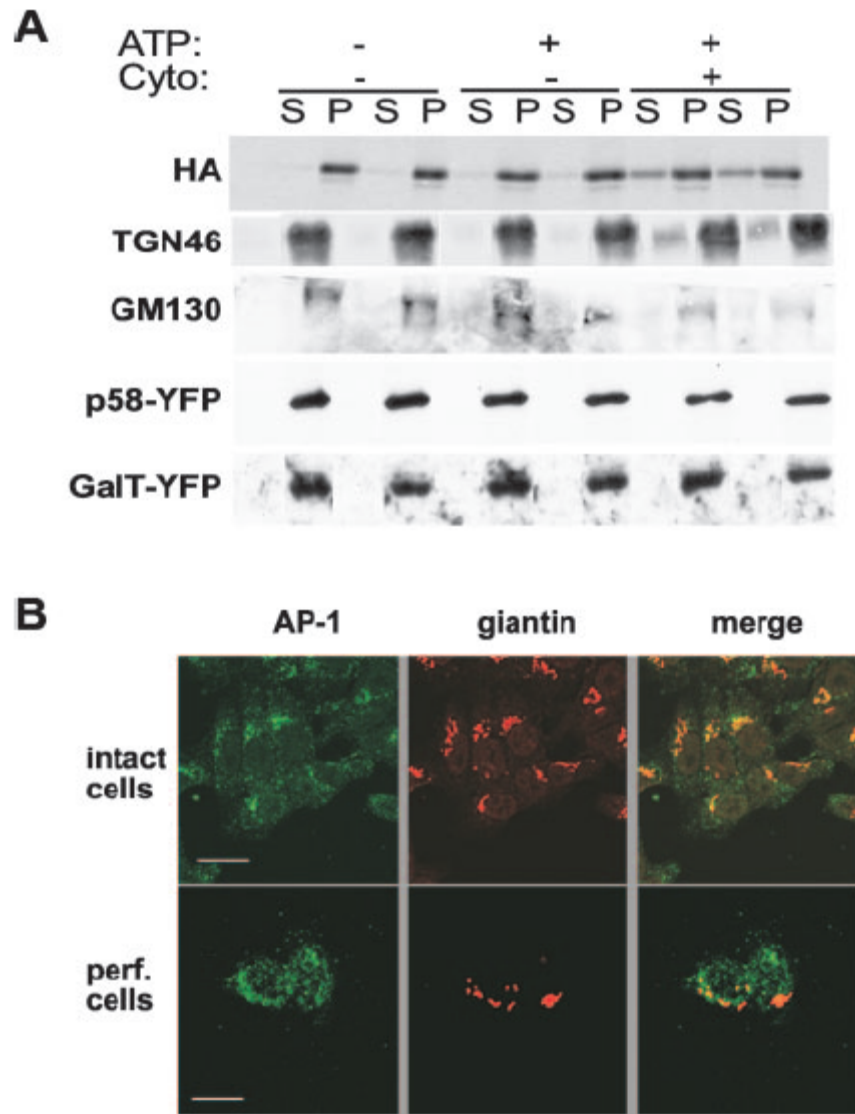


Figure 3.1. ATP- and cytosol-dependent release of TGN-staged HA from perforated cells.

(A) HeLa cells expressing radiolabeled, TGN-staged HA were perforated as described in Materials and Methods and vesicle release was reconstituted in the presence or absence of an ATP regenerating system (ATP) and cytosol (Cyto; 2 mg/ml). Released HA (top panel) was recovered in the supernatant (S) and compared to cell-associated HA in the pellet (P). The endogenous protein TGN46 was also released in an ATP- and cytosol-dependent manner as assessed by immunoblotting, however the peripheral Golgi protein GM130, the trans-Golgi marker GalT-YFP, and p58-YFP, which is localized to the intermediate compartment and Golgi complex at steady state, were not released under these conditions. (B) The cellular distribution of Golgi markers AP-1 and giantin were examined by indirect immunofluorescence labeling of intact cells and perforated HeLa cells after reconstitution of vesicle release. Scale bar: 15 μ m.

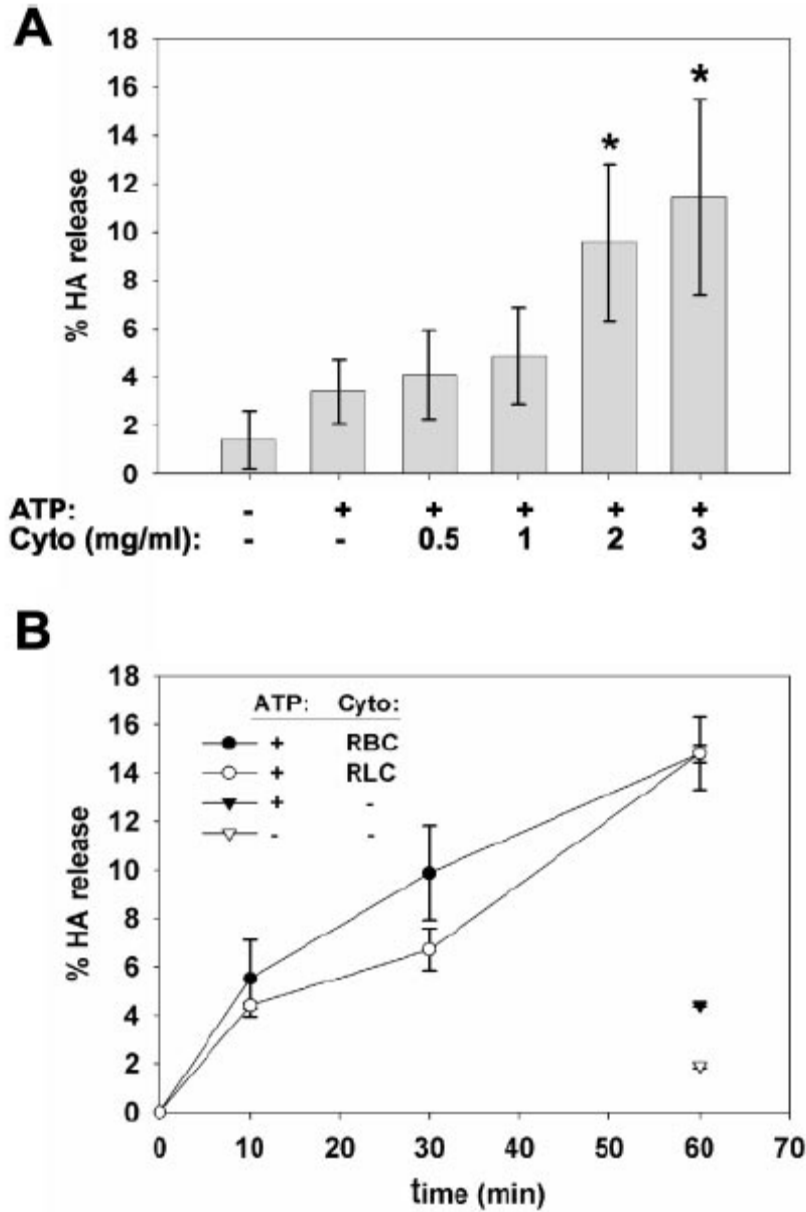


Figure 3. 2. Kinetics and cytosol dose-dependence of HA release.

(A) HA release from permeabilized HeLa cells was reconstituted for 1 h in the presence of increasing concentrations of rat brain cytosol (RBC). * $p=0.002$ compared with ATP alone; $n=9$. (B) The kinetics of HA release were monitored in perforated HeLa cells incubated with 2 mg/ml RBC or rabbit liver cytosol (RLC).

To confirm that HA release in this assay was not due to nonselective fragmentation of the Golgi/TGN upon reconstitution, I examined the release of Golgi resident proteins in this assay. Reconstitution of vesicle release did not dislodge the Golgi-associated peripheral membrane protein GM130 (Fig. 3.1A). In addition, I did not observe measurable release of p58-YFP or the *trans*-Golgi marker GalT-YFP. However, release of TGN46, a TGN protein that constitutively cycles via the TGN and the basolateral cell surface of polarized MDCK cells [190] was very efficiently reconstituted in the presence of ATP and cytosol (Fig. 3.1A). Efficient release of this protein from purified rat liver Golgi membranes has previously been reported by another group [139]. The release of TGN46 in my assay likely represents release of this protein from the TGN as opposed to the budding of endocytic vesicles from the cell surface because: 1. this protein localizes to the TGN in HeLa cells at steady state and after incubation at 19°C, and 2. the small population of TGN46 that can be biotinylated at the plasma membrane at steady state was not released into the medium upon cell perforation and reconstitution (unpublished observations).

I also used immunofluorescence microscopy to examine the effect of perforation and reconstitution on the morphology and localization of the Golgi complex/TGN. Staining with antibodies directed against the Golgi-resident protein giantin and the TGN-localized AP-1 complex demonstrated that these compartments remain concentrated in the perinuclear region of perforated cells after reconstitution, similar to their localization in intact cells (Fig. 3.1B).

TGN-staged HA should be released in intact membrane-bound carriers. To test this, I first combined immunoelectron microscopy with negative staining to visualize the membranes of released carriers containing HA. Released transport carriers were fixed and processed for visualization of HA positive structures. Anti-HA antibodies localized to membrane-limited, spherical vesicles with an average diameter of 86 +/-13 nm (mean +/- S.D.; n=47; Fig. 3.3A). To examine the topology of released HA, I examined whether the protease-sensitive luminal domain was protected from trypsin cleavage. Supernatants from transport reconstitution experiment were incubated with trypsin in the presence or absence of Triton X-100, then centrifuged at high speed to pellet membrane-bound vesicles (Fig. 3.3B). In the absence of detergent, cleavage of HA was virtually undetectable, and nearly all of the protein was recovered intact in the pelleted vesicle fraction. By contrast, when Triton X-100 was included, HA was efficiently cleaved and was recovered primarily in the supernatant.

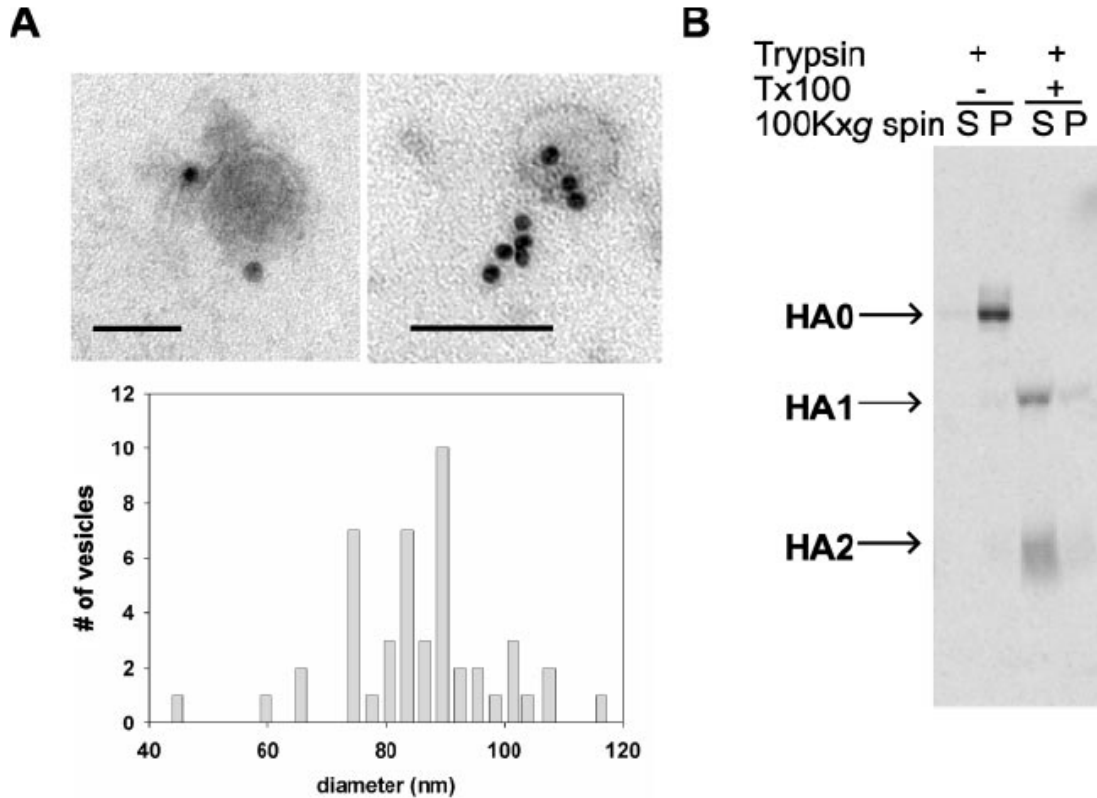


Figure 3. 3. Released HA is recovered in membrane-bound vesicles.

(A) Newly-synthesized HA was staged in the TGN of HeLa cells by incubation for 2 h at 19°C, and vesicle release was reconstituted after perforation. HA-containing vesicles released into the supernatant were visualized by immunogold labeling followed by negative staining. Two representative vesicles are shown. Scale bars: 100 nm. The lower panel shows the histogram of vesicle diameter (nm) measured from 47 vesicles (mean dia \pm S.D. = 86 nm \pm 13). (B) Released HA is protected from luminal proteolytic cleavage. Radiolabeled HA released from perforated, reconstituted cells was treated with trypsin in the absence or presence of detergent (Tx100). After addition of soybean trypsin inhibitor to quench the reaction, the sample was centrifuged at 100,000 x g and HA was immunoprecipitated from the resulting supernatant (S) and pellet (P). The mobilities of intact (HA0) and the two HA trypsin cleavage products (HA1 and HA2) on SDS-PAGE are marked.

Nucleotide dependence of HA release-

A number of GTPases have been implicated in the delivery of HA from the TGN to the plasma membrane, including ARF1 and G_{sa} [86, 113]. To determine whether there is a requirement for GTP or GTP hydrolysis in HA release, I tested the effect of poorly-hydrolyzable GTP analogs in my assay [191]. Inclusion of GTP γ S in the reconstitution reaction decreased HA release in a dose-dependent manner, with complete inhibition of ATP-dependent release observed at 100 μ M concentration (Fig. 3.4A). However, the more poorly hydrolyzable GTP analog guanosine 5'-[β , γ -imido]triphosphate (GMP-PNP) did not inhibit HA release, even at high concentration (Fig. 3.4C). Neither GTP γ S nor GMP-PNP affected TGN46 release at 100 μ M concentration indicating that GTP hydrolysis is not required for efficient release of TGN46 from the TGN (Figs. 3.4B and 3.4D).

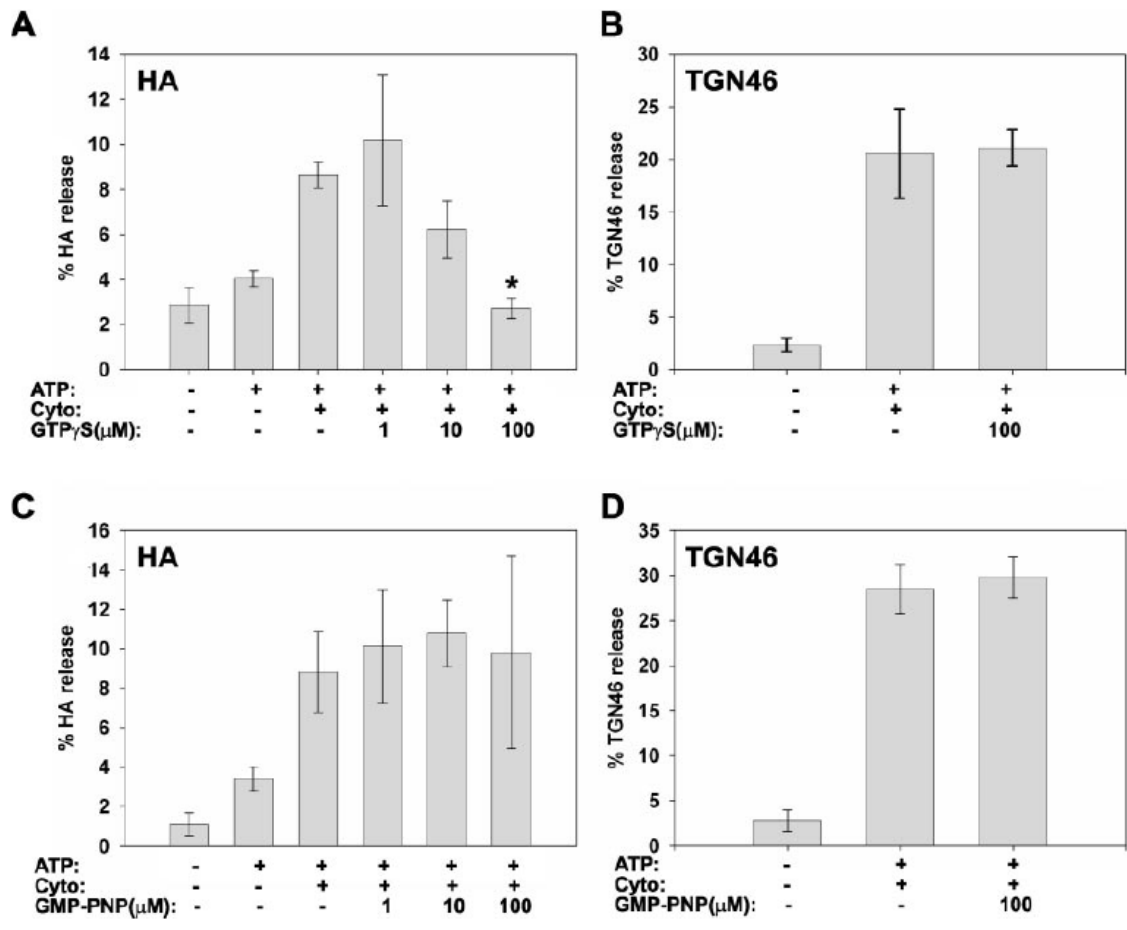


Figure 3. 4. Effect of GTP γ S and GMP-PNP on release of HA and TGN46 from the TGN.

The release of TGN-staged HA (panels A and C) and TGN46 (panels B and D) was quantitated in the presence of increasing concentrations of GTP γ S (A and B) or GMP-PNP (C and D). The mean \pm S.D. of triplicate samples is plotted in each case. Similar results were obtained in three independent experiments (* P<0.001 vs. 0 μ M GTP γ S).

HA release is sensitive to in vivo perturbants of biosynthetic traffic-

It has been shown that disruption of TGN pH by expression of the acid-activated ion channel influenza M2 selectively inhibits efficient release of apical proteins including HA from the TGN in intact MDCK and HeLa cells [143, 186]. To examine whether this requirement for acidic TGN luminal pH is preserved in the perforated cell assay, I examined HA release in HeLa cells co-infected with adenovirus encoding either M2 or as a control, M2 in the reverse orientation. After radiolabeling and incubation at 19°C, cells were perforated and transport was reconstituted. One set of M2-containing samples was reconstituted in the presence of the M2 channel blocker amantadine (AMT). HA release in perforated cells expressing active M2 was decreased by roughly 50% relative to HA release observed in control cells (Fig. 3.5A). Moreover, the effect of M2 on HA release was abrogated by inclusion of AMT in the reconstitution mixture. The effect of M2 on HA release was reproducible and statistically significant ($p < 0.001$ vs. control cells; $p = 0.04$ vs. M2-expressing cells reconstituted in the presence of AMT by paired t-test analysis of 9 independent experiments.) By contrast, release of the basolaterally-targeted protein TGN46 was unaffected by expression of active M2 expression (Fig. 3.5B). In the experiment shown, a slight inhibition was observed in the presence of AMT; however, this was neither statistically significant nor reproducible.

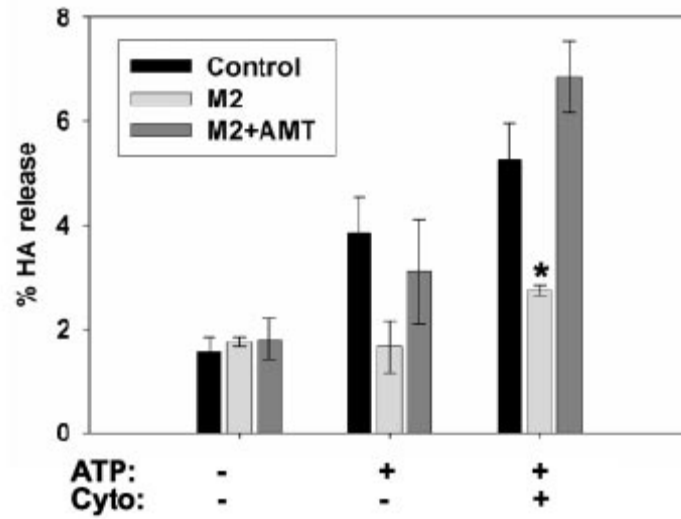
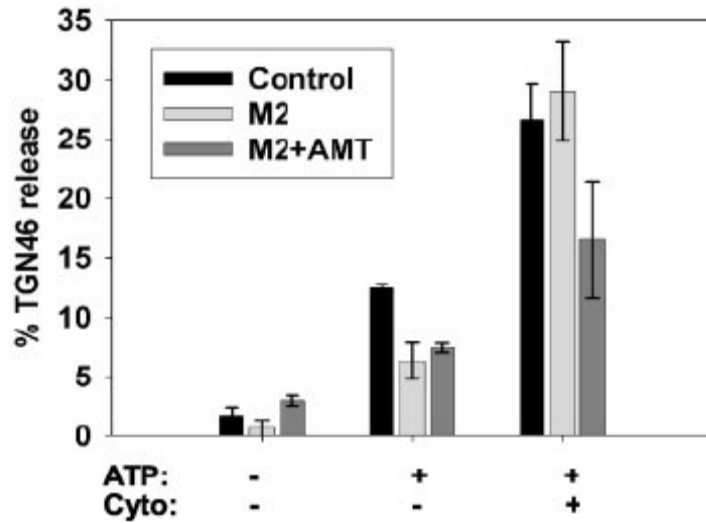
A**B**

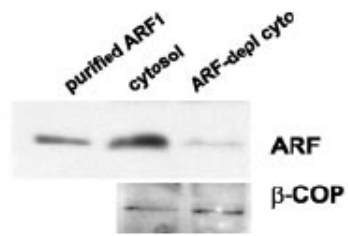
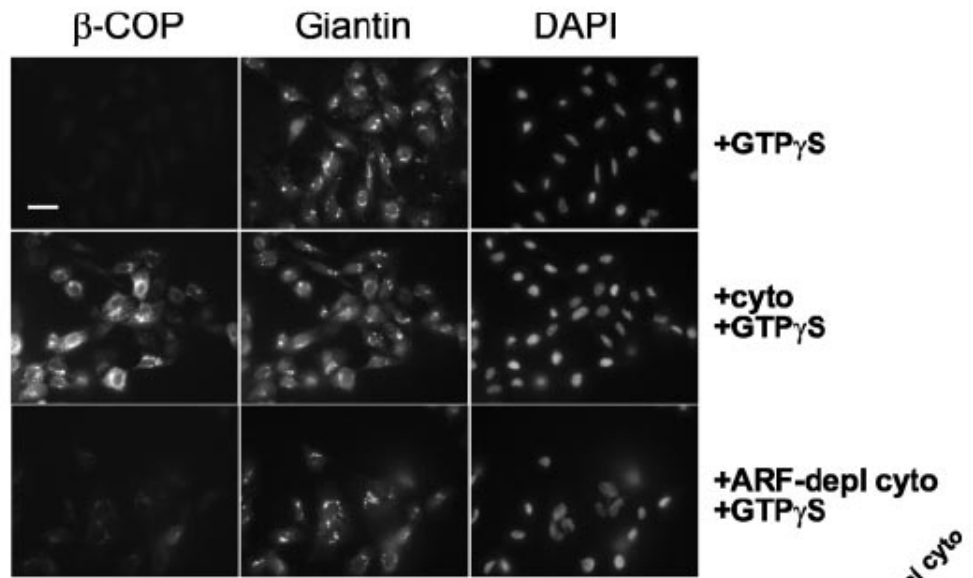
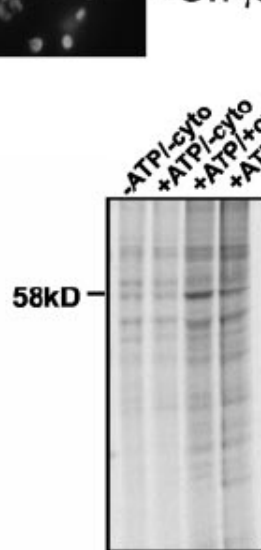
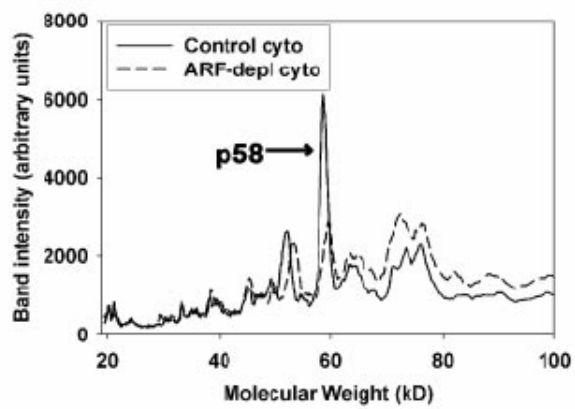
Figure 3. 5. Disruption of TGN luminal pH inhibits HA but not TGN46 release from perforated cells.

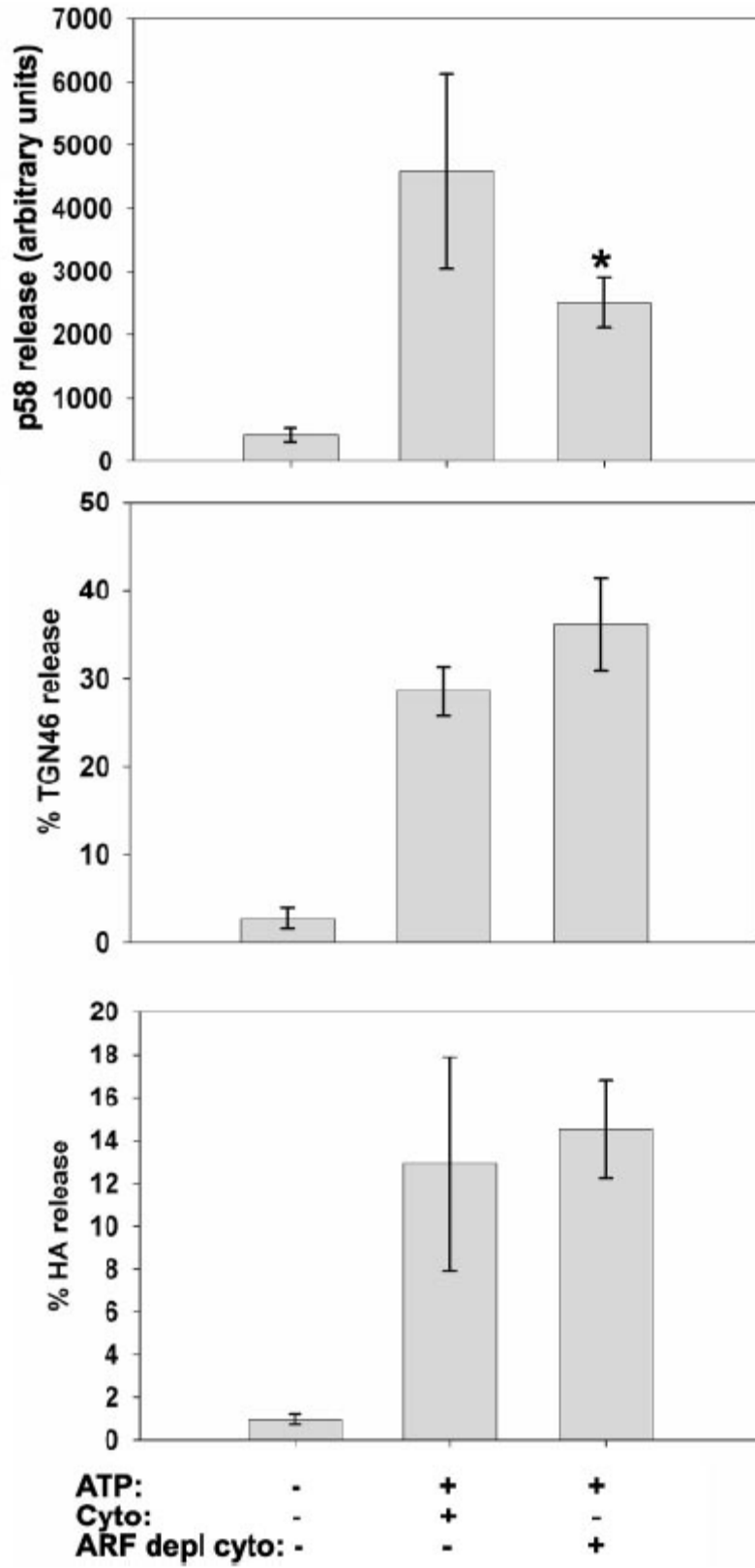
(A) HA release was measured from permeabilized cells co-infected with adenovirus encoding M2 or a control virus (encoding the M2 gene in the reverse orientation). Amantadine (AMT, 5 μ M) was included during reconstitution of the indicated M2-expressing samples to inhibit M2 activity. The mean release \pm range of duplicate samples is plotted. A representative experiment is shown; statistical significance was calculated by paired t-test of nine independent experiments (* $P < 0.001$ relative to control, ** $P = 0.04$ relative to AMT-treated samples). (B) TGN46 release from perforated M2-expressing or control cells was quantitated by immunoblotting. The mean release \pm range of duplicate samples is plotted. This experiment was performed 4 times with similar results. The slight inhibition observed in AMT-treated cells in this experiment is due to an aberrant point in this experiment and is not statistically significant.

ARF-independent release of HA-

A role for ARF1 has been suggested in numerous transport steps through and from the Golgi complex, but whether it functions in the release of apical proteins from the TGN is not known. Although ARF1 is dissociated from the TGN in intact MDCK cells by brefeldin A (BFA), this drug does not function the same *in vitro* as it does *in vivo* [192]. Therefore, to address the role of ARF1 in HA release *in vitro*, I used anion-exchange chromatography to deplete rat brain cytosol of ARF1. Immunoblotting of the resulting cytosol routinely demonstrated removal of >87% of ARF1 with no loss of β -COP (Fig. 3.6A).

β -COP is readily recruited to the Golgi complex of digitonin-permeabilized cells incubated with exogenous cytosol in the presence of ARF1 and GTP γ S. Whereas I observed robust binding of β -COP to the Golgi complex in permeabilized cells incubated with control cytosol, only background levels of binding were observed in cells incubated with ARF-depleted cytosol (Fig. 3.6B). Furthermore, recruitment of clathrin to the Golgi complex/TGN was also decreased by depletion of ARF1 from cytosol, confirming that recruitment of these coats in this system is still dependent on ARF1 function (unpublished observation).

A**D****B****C**



D

Figure 3. 6. HA release from the TGN is ARF-independent (previous two pages).

(A) Immunoblotting of ARF-depleted vs. control cytosol using antibodies against ARF (upper panel) and γ -COP (lower panel). Purified bovine ARF1 was included as a positive control. In this preparation, the resulting cytosol was depleted of ARF relative to control cytosol by 87% (B). Digitonin-permeabilized HeLa cells were incubated with 500 μ M GTP γ S and 2 mg/ml control or ARF-depleted cytosol for 10 min at 37°C prior to fixation and processing for indirect immunofluorescence to detect γ -COP or giantin. Cell nuclei were stained using DAPI. Scale bar: 25 μ m. (C) Uninfected HeLa cells were briefly radiolabeled, then incubated for 2 h at 19°C to stage newly-synthesized endogenous proteins in the TGN. Vesicle release was reconstituted after cell perforation in the presence or absence of an ATP-regenerating system (ATP) and with control or ARF-depleted cytosol. Released vesicles were centrifuged at 100,000 x g in the presence of 1M KCl to remove peripheral proteins, and the pelleted vesicles were solubilized and analyzed by SDS-PAGE. The release of a 58 kD protein (p58, arrow) was reduced upon reconstitution with ARF-depleted cytosol compared to control. The corresponding trace shows the intensity of bands in the gel (right two lanes); the band corresponding to p58 is marked. (D) The effect of ARF-depleted cytosol on the release of p58 (top panel; mean \pm S.D. of four experiments; *P=0.03 relative to control cytosol); TGN46 (middle panel; mean \pm S.D. of triplicate samples), and HA (lower panel; mean \pm S.D. of triplicate samples) is plotted.

I next examined the effect of ARF-depleted cytosol on the release of endogenous proteins in HeLa cells in my *in vitro* assay. Uninfected HeLa cells were radiolabeled for 15 min then incubated in chase medium at 20°C for 2 h to accumulate newly-synthesized proteins in the TGN. After perforation, vesicle release was reconstituted using ATP and control or ARF-depleted cytosol. Released vesicles were centrifuged in high salt-containing buffer to remove peripheral proteins whose association with membranes might be ARF-dependent, and the protein profile in the pelleted vesicles was analyzed by SDS-PAGE and densitometry (Fig. 3.6C). While the overall profile of proteins released in the presence of control and ARF-depleted cytosol was similar, I reproducibly observed a decrease in the release of a ~58 kDa protein (p58) when transport was reconstituted using ARF-depleted cytosol (Fig. 3.6C). Together, these data suggest that ARF depletion effectively inhibits ARF1 function in perforated cells.

I next examined the effect of ARF-depleted cytosol on release of HA and TGN46 from perforated cells. By contrast with p58, whose release was inhibited by ~50% (Fig. 3.6D, upper panel), depletion of ARF1 had no effect on the release of TGN46 (Fig. 3.6D, middle panel) or HA (Fig. 3.6D, bottom panel).

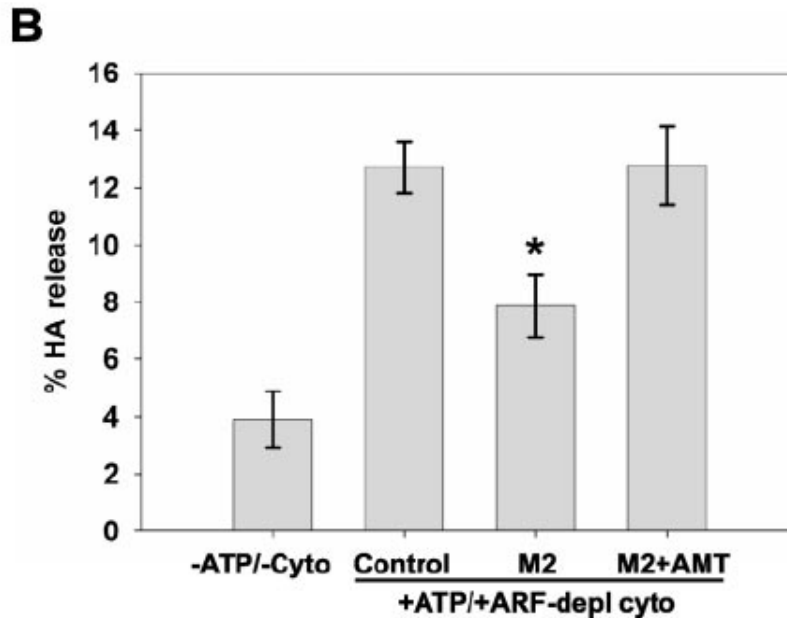
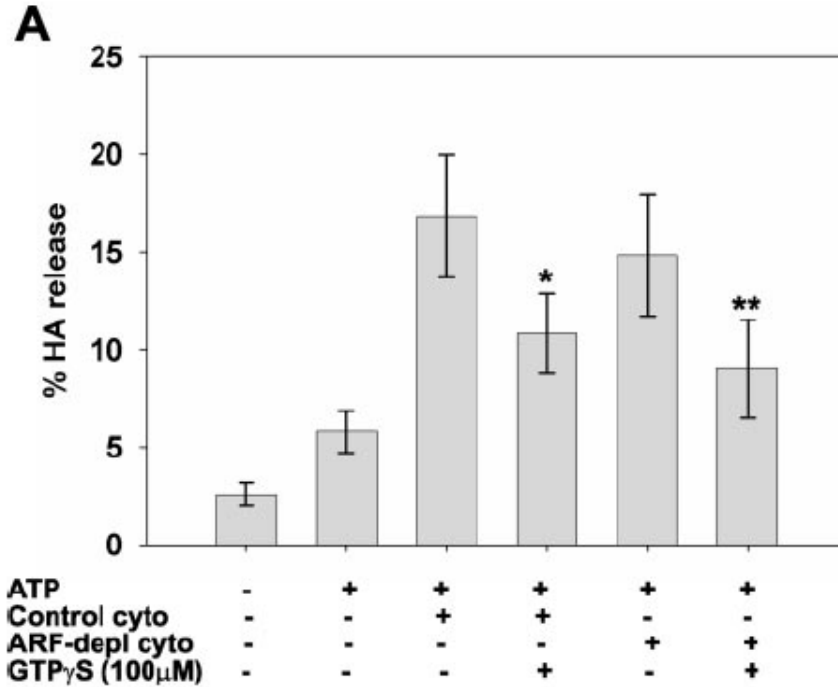


Figure 3. 7. ARF-independent HA release from the TGN is inhibited by GTP γ S and by expression of influenza M2.

(A) HA release from the TGN of cells reconstituted in the presence of ARF-depleted or control cytosol with or without 100 μ M GTP γ S. A representative experiment (mean \pm S.D. of triplicate samples) is shown; statistical significance was calculated by t-test analysis of four experiments (*P=0.013 vs. control; **P=0.015 vs. ARF-depleted cytosol). (B) HA release from the TGN of cells expressing M2 was reconstituted in the presence of ARF-depleted or control cytosol. Amantadine (AMT) was included in the indicated samples. The graph represents the mean \pm S.E. of nine samples (*P= 0.003 vs. control; 0.012 vs. M2+AMT).

Other laboratories have shown that when ARF is depleted from cytosol, release of proteins can still occur *in vitro* but is no longer sensitive to inhibition by poorly-hydrolyzable GTP analogs [192, 193]. I therefore tested whether HA release in the presence of ARF-depleted cytosol was affected by GTP γ S. Release of HA was inhibited under these conditions at the same concentrations of GTP γ S that blocked release in control cytosol (Fig. 3.7A). Moreover, expression of active M2 inhibited HA release reconstituted in the presence of ARF-depleted cytosol, suggesting that HA is not shunted into alternative transport carriers in the absence of ARF1 (Fig. 3.7B). Together, these results suggest that the release of TGN-derived transport carriers containing HA is not regulated by ARF1 and by inference, does not require the function of known adaptors and coat proteins.

DISCUSSION

Identifying the molecular requirements for specific steps in protein trafficking has proven difficult due to the numerous compartments within the biosynthetic pathway. To circumvent this issue, many studies have employed *in vitro* assays to reconstitute a specific step in membrane transport. Here I have used a perforated cell assay to examine the requirements for TGN export of influenza hemagglutinin, a raft-associated protein that has apical sorting information when expressed in polarized epithelial cells. Release of TGN-staged HA from perforated, salt-washed cells was dependent on addition of an ATP-regenerating system and cytosol and was not due to nonspecific fragmentation of the Golgi complex, as no release of peripheral or integral Golgi proteins was observed. HA was released in the correct topology in roughly spherical intact transport carriers with an average diameter of 86 ± 13 nm. Importantly, the assay allows rapid removal of cytosolic components prior to reconstitution, and appears to preserve physiological pH gradients within organelles, as expression of the acid-activated proton channel influenza M2 inhibited the release of HA in my assay. By contrast, while I was also able to efficiently reconstitute HA release from TGN-containing Golgi membranes isolated by subcellular fractionation, release in this assay was insensitive to M2 activity (chapter 2). Interestingly, HA release from perforated cells was profoundly inhibited by GTP γ S, but was unaffected by depletion of clathrin (unpublished observation) or ARF1, a GTPase that regulates the binding of

all known coats and adaptor proteins to the TGN. Thus, the formation of HA-containing transport carriers appears to proceed via novel regulatory mechanisms.

I also reconstituted ATP- and cytosol-dependent release of TGN46, a protein localized to the TGN at steady state but which cycles constitutively through the basolateral cell surface of polarized epithelial cells [190, 194]. The release of TGN46 in my assay system was remarkably robust (typically ~40% within 30 min), consistent with a previous report that also noted very efficient release of the rat homolog of TGN46 (TGN38) from isolated Golgi membranes [139]. TGN46 colocalizes with GFP-tagged vesicular stomatitis virus glycoprotein (VSV G) to transport carriers emanating from the TGN, suggesting that this protein is an appropriate marker for the basolateral biosynthetic pathway [72, 176]. However, release of TGN-staged VSV G in my assay system was consistently less efficient than release of TGN46 (unpublished observation). The difference in TGN export efficiency may reflect distribution of TGN46 into alternate export pathways; for example, previous studies have demonstrated rapid cycling of this protein between the TGN and endosomes [195, 196].

In contrast to the release of HA, export of TGN46 from the TGN was insensitive to expression of active influenza M2. TGN-staged VSV G release was also insensitive to M2 in my assay system (unpublished observation). These results are consistent with my previously published studies demonstrating a selective effect of M2 expression on the TGN export of apically-sorted proteins in polarized MDCK cells [143], and add further support to the hypothesis that segregation of apical and basolateral proteins into distinct transport carriers also occurs in non-polarized cells.

Cytosol prepared from a number of sources, including rat brain, rabbit liver, and MDCK cells, was able to support HA release with similar dose-dependence. The ability to use various cytosol sources allows the potential modification of cytosolic components by using either genetically altered animals or modified cells. The kinetics of HA release could be monitored in my assay, and similar rates of HA release were observed when TGN export was reconstituted using either rat brain or rabbit liver cytosol. Previous studies have implicated specific cytosolic proteins, including members of the annexin family [101, 102], a heterotrimeric G_s protein [86], dynamin [74], and cdc42 [92] in the TGN export of apical proteins. The ability to measure the rate of protein release from the TGN should prove useful in experiments designed to determine

the order in which different cytoplasmic components function in the formation of HA-containing transport carriers.

Guanine nucleotide analogs have been used extensively to mimic GTP in systems where the nucleotide would be rapidly hydrolyzed. I found that GTP γ S but not GMP-PNP inhibited HA release from the TGN, while TGN46 release was not affected by either GTP analog. My result is consistent with the previous demonstration that HA traffic from the TGN to the apical plasma membrane in streptolysin O-permeabilized MDCK cells was inhibited by GTP γ S [113]. GMP-PNP and GTP γ S are structurally very different, and binding of these nucleotides differentially alters the conformation of the small G protein H-Ras [197]. Differences between the effects of GTP analogs on membrane transport have been previously reported: for example, ARF1 recruitment to Golgi membranes is enhanced by GTP γ S but not by GMP-PNP [198].

Morphology of TGN-derived transport carriers.

Although numerous adaptor and coat proteins are known to bind TGN membranes, the requirement for these proteins in polarized biosynthetic transport remains unclear. Simon et al. demonstrated that release of sialylated VSV G from Golgi-enriched MDCK membranes requires ARF and occurs via COPI-coated vesicles [112, 175], whereas another group has suggested a requirement for AP-3 in the TGN export of VSV G [95]. Vesicular and tubular structures coated with p230, a peripheral protein of unknown function, have also been observed emanating from the TGN; however whether biosynthetic cargo molecules are enriched in these carriers is not known [98]. Galpha interacting protein (GAIP) has been reported to regulate the fission of VSV-G-containing TGN-derived tubules that are devoid of clathrin or coatamer [199], and a similar redistribution of VSV G and TGN46 was observed upon expression of a dominant-negative mutant of protein kinase D [72]. Finally, Polishchuk et al. [176] recently reported that export of VSV G from the TGN is independent of coat formation and occurs via the protrusion and detachment of large sections of TGN membrane that also contain TGN46. These differences in transport requirements may reflect a physiological redundancy in the routes that VSV G can use to reach the cell surface; alternatively, at high levels of expression or upon perturbation of the regulatory mechanisms that control cargo loading and export from the TGN, VSV G may be rerouted to alternative pathways that are not normally prominent.

How the sorting and TGN export of proteins that are targeted apically in polarized cells is regulated is no better understood. Apical targeting signals on many proteins, including HA, are localized to the transmembrane or luminal domains of these molecules, and are thus unavailable to bind directly to cytoplasmic adaptors [185, 200]. Thus, it is not surprising that the regulation of apically-destined protein export would be distinct from basolateral transport, as I observed. Indeed, the molecular requirements for *fusion* of TGN-derived carriers with the apical plasma membrane of MDCK cells are known to be distinct from those involved in basolateral delivery [201].

Several studies have used live-cell imaging to characterize Golgi export of fluorescent apical marker proteins in both nonpolarized and polarized cells. Kreitzer et al. [74] described a mixture of vesicular and very long tubular carriers enriched in a non-raft-associated apical cargo molecule that emanated from the TGN of MDCK cells and fused with the plasma membrane. Other groups have reported that a fluorescent apically-targeted GPI-anchored (raft-associated) protein is transported from the TGN primarily in “small” spherical carriers in both nonpolarized and polarized cells, compared with transport carriers enriched in basolateral cargo [16, 157]. In contrast, Jacob and Naim [17] described the release of large globular structures from the TGN that contained both raft-associated and raft-independent apically-targeted cargoes; these large structures resolved into distinct carriers later during transport. Most recently, Polishchuk et al. [202] reported that raft-associated GPI-anchored proteins are sorted from the TGN to the basolateral membrane of MDCK cells in the same carriers that contain VSV G, and then selectively transcytosed to the apical membrane.

In contrast to the wide variety of morphologies observed in live cells, the size and structure of transport carriers I isolated upon *in vitro* reconstitution of HA export was relatively uniform (86 ± 13 nm dia). My data are very consistent with a previous study by Wandinger-Ness et al. [203], who reported a diameter of 78 ± 15 nm for TGN-derived, HA-containing vesicles immuno-isolated from perforated MDCK cells. Although the vesicles I identified were devoid of a noticeable coat, they were comparable in size to COP I (50 ± 16 nm dia; [204]), COPII (70 ± 20 nm dia; [205]), and clathrin (95.9 ± 10.5 nm dia; [206]) coated vesicles. It is possible that tubule formation is inefficient in my *in vitro* reconstitution assay; alternatively, large globular or tubular transport carriers may not be efficiently released or separated from perforated cells.

HA export from the TGN is ARF1-independent.

ARF1 is required for the binding of all adaptor and coat proteins that have been localized to the TGN. As such, I were somewhat surprised to find no requirement for ARF1 in the release of either HA or TGN46. Depletion of ARF1 from the cytosol used to reconstitute TGN export inhibited the association of coatomer and clathrin with the Golgi complex, but an effect on the release of only a single protein could be detected. Happe and Weidman [193] have previously observed that intra-Golgi transport was also efficiently reconstituted in the absence of ARF1, but was no longer sensitive to inhibition by GTP γ S. However, I found that HA release in the absence of ARF1 was still inhibited by GTP γ S. I conclude that another GTP-binding protein(s) is required for the formation of HA-containing transport carriers.

Previous studies have suggested a role for ARF1 in apical biosynthetic transport. BFA, a drug that inhibits ARF1 function, has been reported to cause rerouting of apical proteins, including HA, to the basolateral cell surface of MDCK cells [116, 207, 208]. While the drug has no effect on the morphology of the Golgi complex of MDCK cells, BFA treatment resulted in the redistribution of both HA and a chimeric protein containing TGN38-derived sorting information into a network of tubules emanating from the TGN [116]. However, cell surface delivery of basolateral markers in MDCK cells was unaffected even at high concentrations of BFA [207, 208]. These results are most consistent with a role for ARF1 in sorting of apical cargo as opposed to the formation of apically-destined vesicles. To test this idea, I asked whether TGN export of HA upon reconstitution with ARF-depleted cytosol was sensitive to inhibition by influenza M2. I found that HA release in ARF-depleted cytosol was still inhibited by expression of active M2. This suggests that the fidelity of HA sorting into transport carriers devoid of basolaterally-destined proteins remained intact in the absence of ARF1 function

Although I found no evidence for a direct role for ARF1 in HA export from the TGN, it is possible that ARF1 is important for other steps in TGN-to-cell surface transport. For example, ARF1 could mediate retrograde trafficking of proteins whose function is required for sorting. It has been hypothesized that lectin-like sorting receptors may be responsible for recognition of glycan sorting signals on some apical proteins in the TGN [182]. An alternative hypothesis is that ARF1 mediates the recruitment of molecular motors that drive surface delivery of TGN-derived vesicles. ARF1 has been recently implicated in recruitment of the Arp2/3 complex to the Golgi complex [209, 210]. In conjunction with N-WASP, the Arp2/3 complex can drive actin

polymerization that propels HA-containing transport carriers from the Golgi region to the cell periphery [211]. Thus ARF1 may function in post-Golgi delivery of newly synthesized apical proteins to the plasma membrane *in vivo*, but this function may not be observed in my *in vitro* assay.

In summary, I have used an *in vitro* reconstitution assay that faithfully preserves *in vivo* requirements for polarized protein sorting to demonstrate that the formation of TGN-derived transport carriers enriched in a raft-associated apical protein requires cytosolic factors but occurs independently of ARF1 function. The existence of apical sorting mechanisms independent of ARF1 at the TGN is a novel finding. Future experiments will be directed towards identifying the cytosolic machinery involved in this transport step. In addition, it will be important to determine whether similar factors are involved in TGN release of raft-independent apical cargo molecules that contain different sorting information.

4. Identification of cytosolic proteins important for HA release from the *trans*-Golgi network.

Polarized cells possess two plasma membrane domains. The apical domain faces the lumen of organs, while the basolateral domain faces adjacent cells in a monolayer as well as the underlying extracellular matrix. These two domains are composed of different protein compositions, and this distribution is regulated at least in part by the biosynthetic segregation of apical and basolateral proteins upon leaving the TGN. Non-polarized cells, which possess a single continuous plasma membrane, recapitulate this sorting of apical and basolateral marker proteins, indicating that this pathway is relevant to all cells.

Because my previous studies demonstrated a requirement for cytosolic proteins for efficient TGN export of apical cargo (chapter 3), I undertook a fractionation approach to identify cytosolic proteins involved in this process. The perforated cell assay described in earlier chapters was used as a screen to identify those fractions that reconstituted efficient export of HA from the TGN; and 8 of 11 bands in an active fraction were subsequently identified by peptide mass fingerprinting. Future studies will address the contribution of these proteins to efficient apical protein export from the TGN.

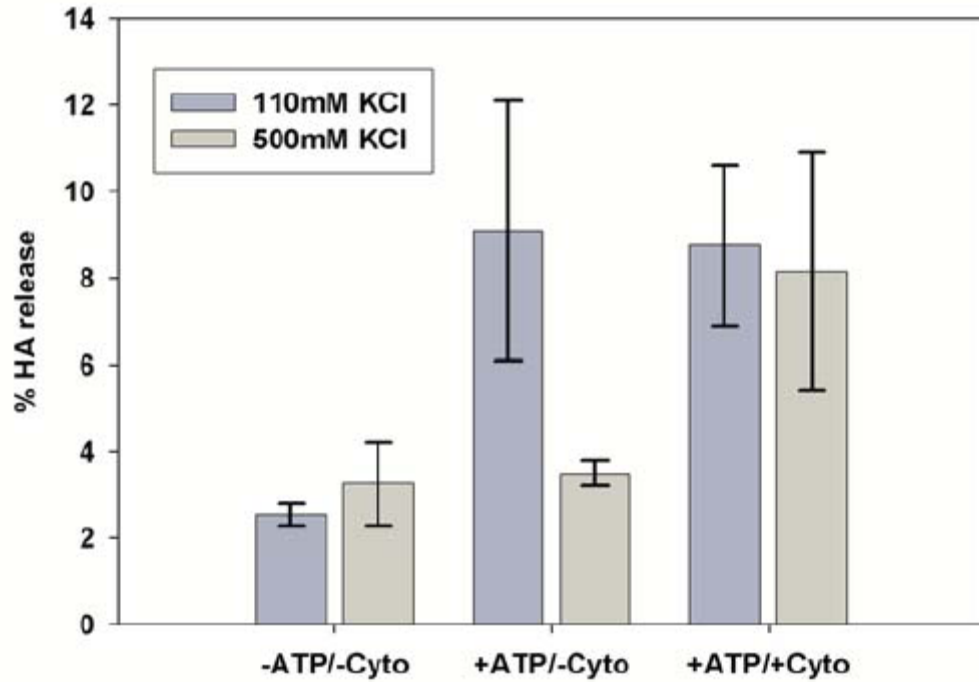


Figure 4. 1: 500mM KCl buffer increases cytosol dependent release of HA staged in the TGN.

HeLa cells expressing HA were radiolabeled and chased at 19°C. Cells were perforated and either washed with 100mM KCl solution (dark gray bars) or 500mM KCl solution (light gray bars). Reactions were then reconstituted with or without ATP and cytosol as described.

HA release from the TGN is dependent on exogenous cytosol:

To identify cytosolic proteins involved in HA export from the TGN I took advantage of the *in vitro* assay previously described in chapter 2 [115]. Influenza HA expressed in HeLa cells was radiolabeled and staged by temperature block in the TGN. The cells were perforated by hypotonic swelling and scraping in isotonic buffer. Initial experiments showed a significant amount of HA release in the absence of cytosol (fig 4.1). By washing the perforated cells with 500mM KCl, HA export from the TGN became more dependent on the addition of exogenous cytosol (fig 4.1). Thus, this assay is an appropriate method with which to identify cytosolic proteins important for HA export. In all of the experiments described in this chapter, cells were perforated and washed with high salt buffer prior to reconstitution of TGN export.

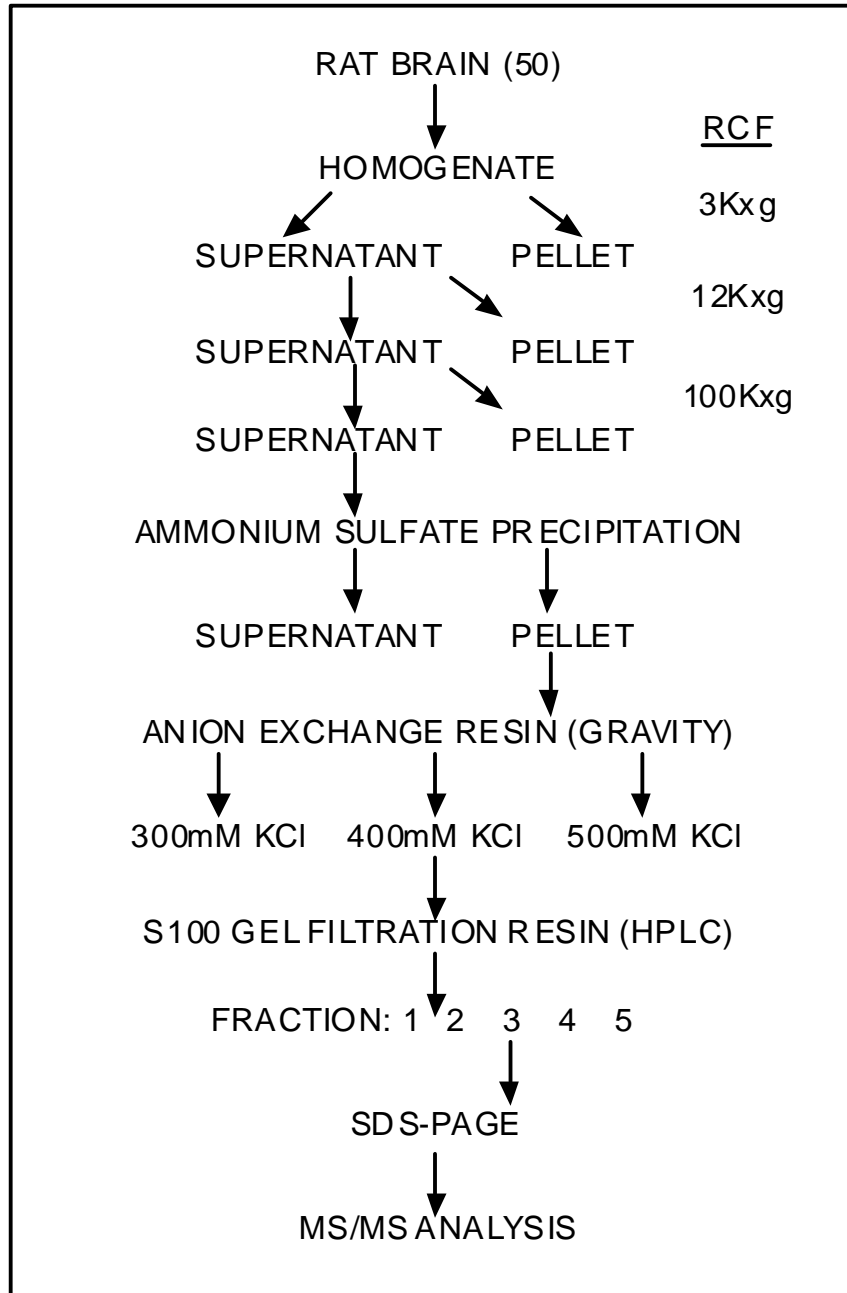


Figure 4. 2: Schematic describing the enrichment of HA release activity from rat brains.

50 rat brains were homogenized and a high speed supernatant was prepared. This high speed supernatant was mixed slowly with saturated ammonium sulfate in 50mM HEPES to 60% v/v. The precipitated proteins were pelleted, brought to volume in 100mM KCl 50mM HEPES pH 7.2, and desalted by gel-filtration exchanged into the same buffer. The sample was then applied to a fast flow Q anion exchange column in 100mM KCl. Proteins were eluted in batches of 100mM KCl increasing ionic concentration. Eluted proteins were concentrated and buffer exchanged using iCon centrifugal concentrators (Pierce). The fraction of proteins eluted at 400mM KCl (300-400mM fraction) was buffer exchanged into 25mM HEPES 7.2, 250mM sucrose, 2mM EDTA, 2mM EGTA and applied to a FPLC S100 gel filtration column equilibrated with the same buffer. Fractions were collected overnight in 3 ml volumes. 5 fractions were collected which contained detectable protein. These were concentrated 6-fold by iCon centrifugal concentrators and buffer exchanged with 50mM HEPES 7.4, 100mM KCl.

Table 2: Enrichment of HA release activity using standard chromatographic techniques.

(Total protein is determined as % starting material recovered in the fraction multiplied by 588mg. Specific activity represents the % of HA released per mg of protein added. Total activity is the specific activity multiplied by the total protein. Purification factor represents the specific activity divided by 6.43%/mg. Yield % represents the total activity divided by 3780.84).

<i>Purification step</i>	<i>total protein (mg)</i>	<i>specific activity (%/mg)</i>	<i>total activity</i>	<i>Purification factor (fold)</i>	<i>yield %</i>
Cytosol	588	6.43	3780.84	1	100
60% AS	217.7	14.08	3065.216	2.19	81.1
FFQ	24	45.8	1099.2	7.12	29.1
Gel filtration	1.96	99.9	195.804	15.5	5.18

HA release activity is enriched by ion-exchange fractionation:

HA export activity (% HA released from perforated cells per mg cytosol) was followed through a series of fractionation steps applied to rat brain cytosol. Initially, I used ammonium sulfate precipitation to enrich HA release activity two-fold (see table 2 and fig 4.2). I found that the HA release activity was precipitated by 60% ammonium sulfate (v/v) salt precipitation. In attempt to further purify the activity using this step, I performed a sequential precipitation by first removing proteins precipitated at lower concentrations of ammonium sulfate (25%, 35%, 45%), then increasing the concentration to 60% ammonium sulfate to precipitate this activity. Unfortunately, the activity could not be enriched through this approach (no significant increase was found comparing 60% ammonium sulfate precipitated material to any of the sequentially precipitated material; data not shown). This could suggest that the activity is more complex than a single protein, or that prolonged exposure to ammonium sulfate destroys this activity.

Next, I followed HA release activity after step-wise elution of cytosolic proteins from an anion exchange column that separates proteins on the basis of their electrostatic charge. Eluted material was then concentrated and tested at various concentrations individually and in combinations for HA release from perforated cells. A portion of the activity was eluted in the 300-400mM KCl step (fraction c in fig 4.8). As little as 25 µg of this fraction was capable of reconstituting HA release from the TGN. This fraction however was not sufficient for HA release, as release required the addition of other fractions. Though more than one fraction could reconstitute release in the presence of fraction c, the particular components in these fractions

were not identified. Finding release activity in more than one fraction was not very surprising, as ion exchange chromatography could remove proteins with different charges from the column in different fractions, possibly disrupting a complex. Since fraction c was common to both reactions with increased activities (fig 4.8 asterisks), I continued to characterize this fraction.

Are known effectors of membrane trafficking enriched in the 400mM fraction?

I next analyzed the enrichment of various trafficking effectors in this 400mM fraction to determine whether the levels of known proteins that have been previously implicated in regulating export from the TGN could be correlated with the increase in HA release activity in this fraction relative to the starting cytosol.

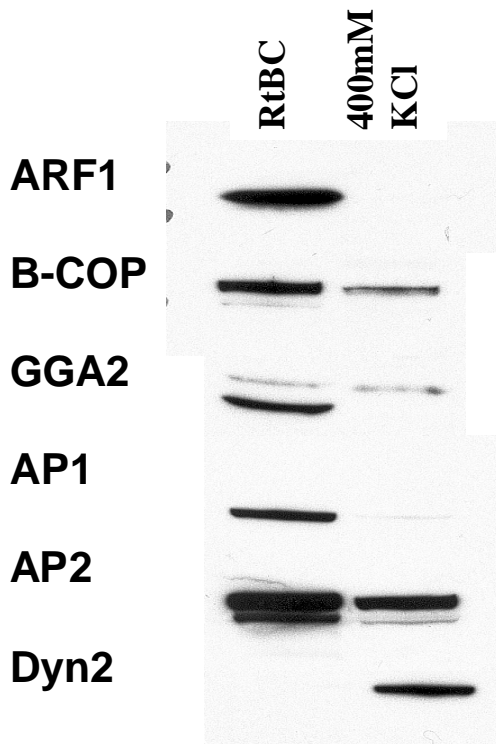


Figure 4.3: Dynamin 2 is enriched in the 400mM fraction compared to an equal concentration of cytosol.

Western blotting was performed for six known regulators of protein trafficking from the TGN. Although most are depleted compared to control (RtBC), dynamin 2 is highly enriched in the 400mM fraction.

To determine the enrichment or depletion of these effectors, I compared the concentration of each in equivalent amounts of rat brain cytosol and the 400mM ion-exchange fraction by western blotting. ARF-1, AP1?, GGA2, AP2a, and β -COP were all depleted in the 400mM fraction

compared to cytosol, while dynamin 2 was highly enriched in this fraction (fig 4.3). This was intriguing, as dynamin 2 could represent the GTP γ S-sensitive factor described in chapter 3.

Dynamin 1 was initially identified as a pinchase (an effector of vesicle fission) important for the recycling of synaptic vesicles[212, 213]. Since that finding, dynamin isoforms have been implicated in both biosynthetic and endocytic vesicle formation, specifically at the stage of vesicle fission from the source membrane (e.g., Golgi or plasma membrane)[73]. The antibody used for western blotting recognizes only type 2 dynamin (BD biosciences). Dynamin 2 is expressed in all cell types, while dynamin 1 is expressed only in neuronal cells. In HeLa cells, endogenous dynamin 2 was found both in the cytoplasm and in a perinuclear region (fig 4.4a), that was later shown to colocalize with the Golgi marker giantin (fig 4.4b).

Acute removal of dynamin 2 from cytosol would provide strong evidence that this protein was directly regulating the trafficking events being observed. Therefore, I initially attempted to immunodeplete dynamin from cytosol and observe the effect on HA release from perforated cells. For this assay to accurately report the effects of dynamin, it is important that perforated cells do not retain endogenous dynamin. To test whether salt washed cells were depleted of dynamin 2, I digitonin-permeabilized cells grown on glass coverslips, washed them with 500mM KCl buffer, then fixed the cells and incubated with anti-dynamin antibody to detect any residual dynamin 2. Dynamin 2 was found to associate with giantin-positive Golgi membranes (fig 4.4b), regardless of salt wash. The salt wash did remove cytosolic dynamin (comparing fig 4.4.b to 4.4.a), though the amount of dynamin present on the Golgi may be enough to promote HA release.

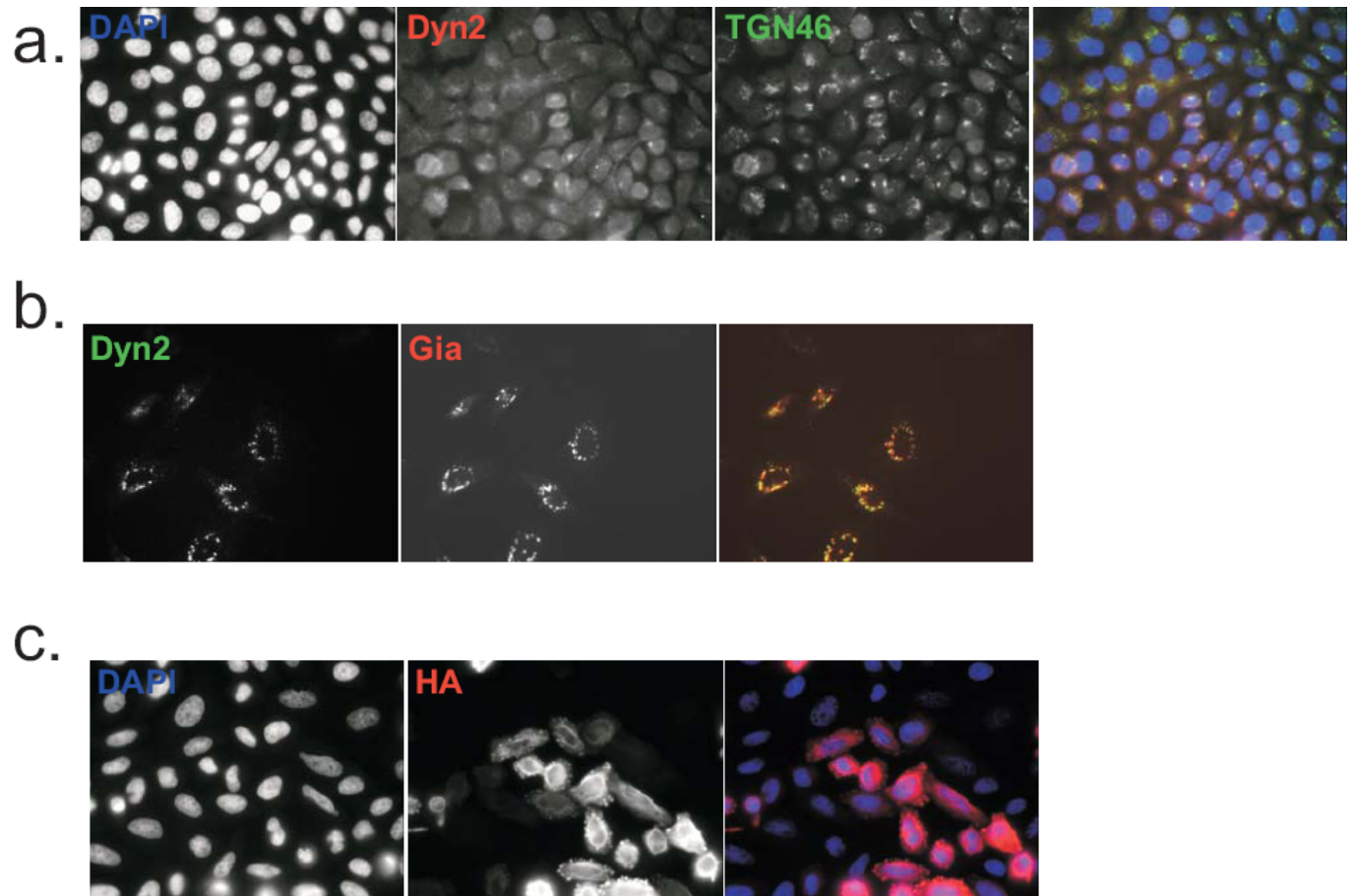


Figure 4. 4: Dynamin 2 localization in HeLa cells.

A. Dynamin 2 colocalizes with TGN46 in HeLa cells. HeLa cells were labeled for dynamin 2 (red), TGN46 (green), and DAPI (blue). B. In perforated cells, dynamin 2 colocalizes with giantin. HeLa cells grown on glass coverslips were perforated with digitonin and washed with 500mM KCl solution. Dynamin 2 (green) remains associated with the Golgi (red). C. Dynamin 2 K44A mutant stains a perinuclear compartment when expressed in HeLa cells.

As I could not remove dynamin 2 from perforated cells to study its effect on TGN export, I took the alternative approach, of overexpressing a well-characterized dominant-negative GTPase-deficient mutant of dynamin 2 (K44A) [214]. This mutation prevents GTP hydrolysis which is thought to regulate the membrane scission activity of dynamin [135]. Indirect immunofluorescence staining of HeLa cells infected with an adenovirus encoding dynamin 2 K44A revealed both perinuclear and cytoplasmic staining (figure 4.4.c.) indicating that the mutant protein is able to associate with membranes. Furthermore, I found upon perforation of HeLa cells expressing this mutant and pelleting the cells, dynamin 2 K44A remained associated with the membrane pellet as opposed to the cytosol (data not shown).

Effect of dynamin 2 K44A expression on HA and G surface delivery:

Dynamin 2 has been implicated in VSV G trafficking [77], therefore I asked whether expression of the dynamin 2 K44A mutant affected HA surface delivery. HeLa cells coexpressing dynamin 2 K44A and either HA or VSV G were radiolabeled, the membrane proteins staged in the TGN by a temperature block, and the cells warmed to 37°C for the indicated times. Surface delivery was determined by trypsinization (HA) or cell surface biotinylation (VSV G). Both HA and VSV G possess glycans that are sialylated in the *trans*-Golgi/TGN. HA sialylation was mildly impaired (quantitation not shown, see figure 4.6 gel) while VSV-G sialylation was not obviously affected (quantitation not shown, see figure 4.7.a. gel) by expression of K44A, suggesting that intra-Golgi traffic is not significantly impaired in these cells. The kinetics of cell surface delivery of TGN-staged HA were significantly impaired by dynamin 2 K44A expression (figure 4.6), while the initial rate of VSV G surface delivery was unaffected (figure 4.7.a.). However, at later chase times (90 min; figure 4.7.b.), I found that

VSV G surface delivery was affected in dynamin 2 K44A-expressing cells compared with control. A similar result, namely effects of dynamin 2 K44A at late times of delivery but not at early ones, was previously observed by another group [77]. The late effect of dynamin 2 K44A on G surface delivery may represent a role for dynamin 2 in recycling of endocytosed VSV G [215], or could reflect the lower sensitivity of the VSV G trafficking assay compared with our assay for HA delivery.

Control	+	+	-	-	+	+	-	-	+	+	-	-
Dyn2K44A	-	-	+	+	-	-	+	+	-	-	+	+
Time	0	0	0	0	20	20	20	20	40	40	40	40

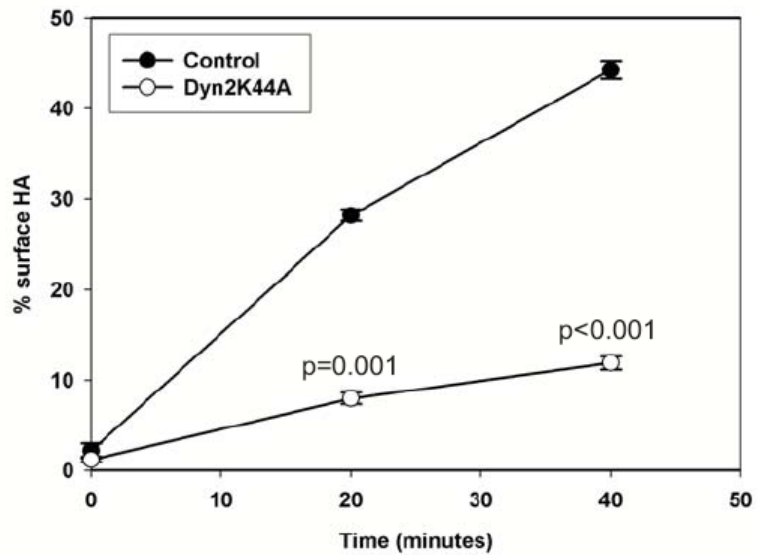
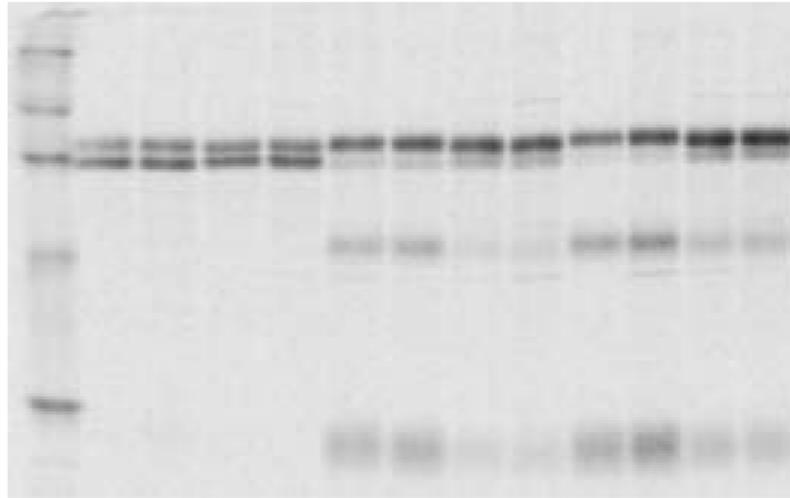
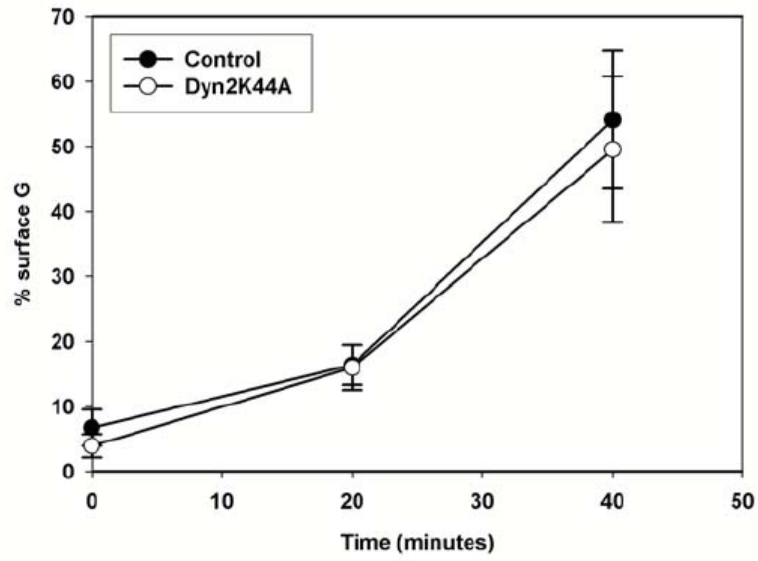
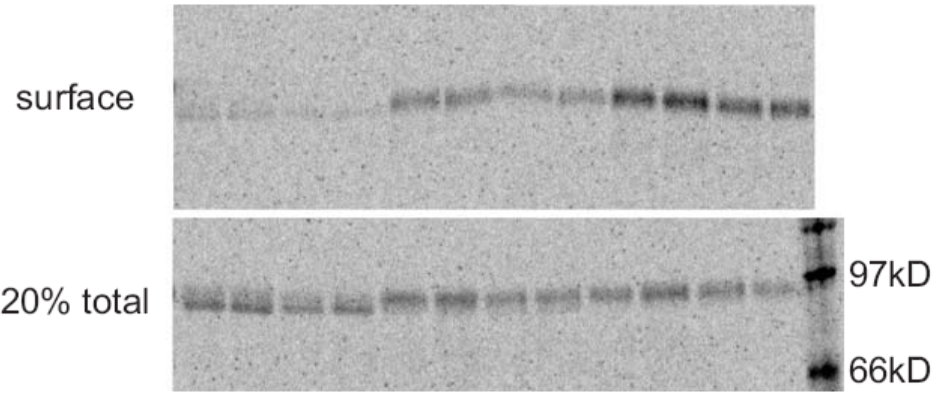


Figure 4. 5: Dynamin 2 K44A expression inhibits HA trafficking through the biosynthetic pathway.

HeLa cells expressing HA and either Dynamin 2 K44A or control were radiolabeled and chased at 19°C to stage cargo in the TGN. After release of the temperature block, cells were warmed to 37°C for indicated times. At each timepoint, cells were placed on ice and surface trypsinized. Cells were then solubilized and HA was immunoprecipitated. A. Top- SDS-PAGE showing HA cleavage as it arrives at the surface. Bottom- graphical representation of above gel. Values represent mean +/- standard deviation, p-values are based on Students T-test.

a.

Control	+	+	-	-	+	+	-	-	+	+	-	-
Dyn2K44A	-	-	+	+	-	-	+	+	-	-	+	+
Time	0	0	0	0	20	20	20	20	40	40	40	40



b.

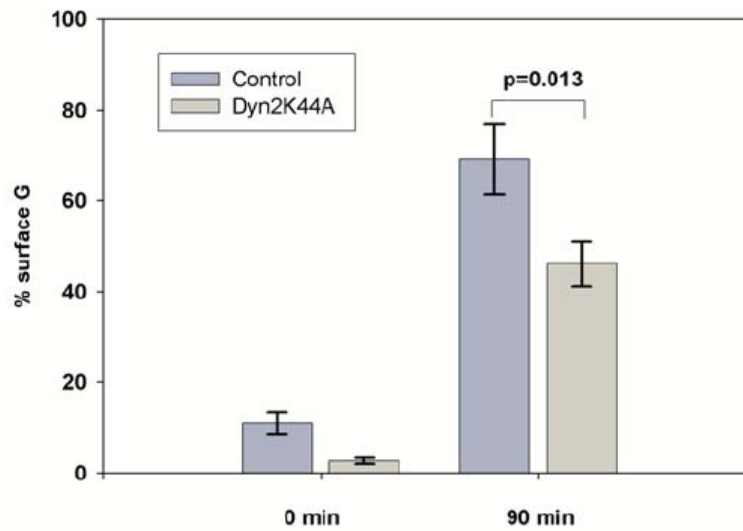


Figure 4. 6: Dynamin 2 K44A expression inhibits VSV G trafficking only at late time points (previous page).

HeLa cells expressing VSV G and either Dynamin 2 K44A or control were radiolabeled and chased at 19°C to stage cargo in the TGN. After release of the temperature block, cells were warmed to 37°C for indicated times. At each timepoint, cells were placed on ice and biotinylated. Cells were solubilized, immunoprecipitated for VSV G, and finally precipitated with streptavidin-sepharose. A. Top- SDS-PAGE showing 80% of the biotinylated VSV G versus 20% of the total. Bottom- graphical representation of the above gel. B. HeLa cells expressing VSV G were labeled as described and warmed for 90 min before biotinylation on ice. Values represent mean +/- standard deviation of % surface VSV G, (n=5) p-values are based on Students t-test.

Effect of dynamin 2 K44A expression on HA and VSV G export from the TGN:

To examine the effect of dynamin 2 K44A expression on HA and VSV G export from the TGN, I used the perforated cell assay [115]. HeLa cells were infected with adenoviruses expressing HA or VSV G and either a control virus or dynamin 2 K44A. The next day cells were starved, radiolabeled with radioactive methionine, and proteins staged by a temperature block in the TGN. Cells were perforated as described previously and release of cargo was reconstituted for 1 h at 37°C. HA release from cells expressing dynamin 2 K44A was decreased by ~50% compared to control cells, consistent with a role for dynamin 2 in export of HA from the TGN (figure 4.7). In contrast, VSV G export was not inhibited under these conditions but appeared to be stimulated by dynamin 2 K44A expression (figure 4.7) suggesting that dynamin 2 does not regulate VSV G export from the TGN, and consistent with my *in vivo* kinetic studies. These data suggest that dynamin 2 regulates HA but not VSV G export from the TGN.

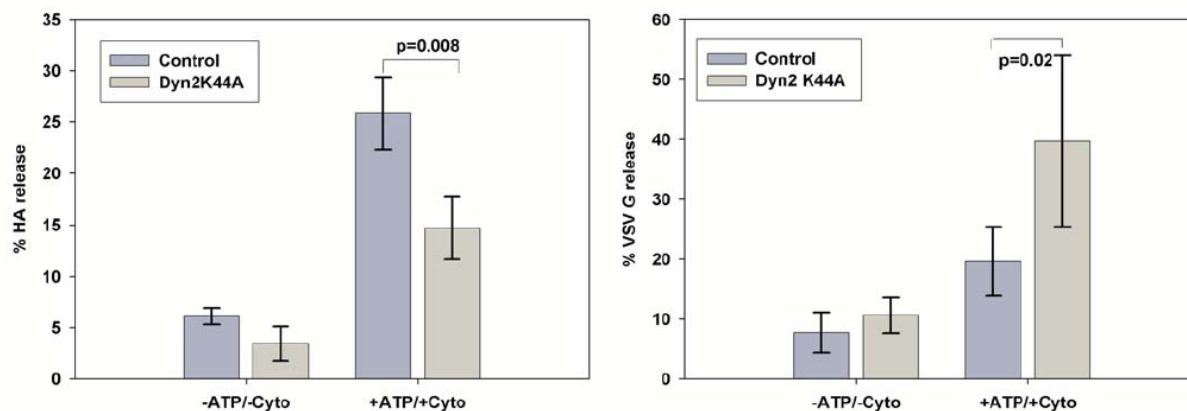


Figure 4. 7: Dynamin 2 K44A differentially regulates HA and VSV G export from the TGN.

HeLa cells expressing HA or VSV G and either control or Dynamin 2 K44A were radiolabeled and chased as described in the methods section. Cells were perforated and TGN export was reconstituted in vitro. After 1 h at 37°C, the supernatant was separated from the pellet, solubilized, and immunoprecipitated for the appropriate marker (HA or G). Left- HA export is inhibited significantly by Dynamin 2 K44A expression. Right- VSV G export is stimulated by Dynamin 2 K44A expression.

Further isolation of HA release activity from rat brain cytosol

I proceeded to further fractionate the 400mM fraction using gel filtration chromatography in order to narrow down possible candidate proteins involved in TGN export of HA. Rather than screen the resulting fractions by testing them with combinations of the other fractions as I did previously, in these experiments I added a suboptimal amount of complete cytosol to each reaction. In chapter 3, I showed that 2 mg/mL was the optimal concentration of cytosol for efficient HA release from perforated cells (refer to fig). In this assay, 0.5 mg/mL (25 ug in a 50 ul reaction) was not sufficient for HA release (fig 4.8). Thus, I added this amount of cytosol to each of my fractions to see whether I could now reconstitute HA export.

The 400mM FFQ fraction was loaded on an S100 high performance liquid chromatography column and eluted at a rate of 0.1 mL/min. 5 mL fractions were collected, concentrated ten-fold, and tested for HA release activity. The activity eluted in a bell-shaped distribution with significant increases above background in fractions 2, 3, and 4 (fig. 4.8). Interestingly, fractions 2, 3, and 4 contained a discrete number of bands in common (fig. 4.8, gels). The peak fraction (fraction 3) was therefore used for mass spec analysis to identify proteins that are potentially important for HA export.

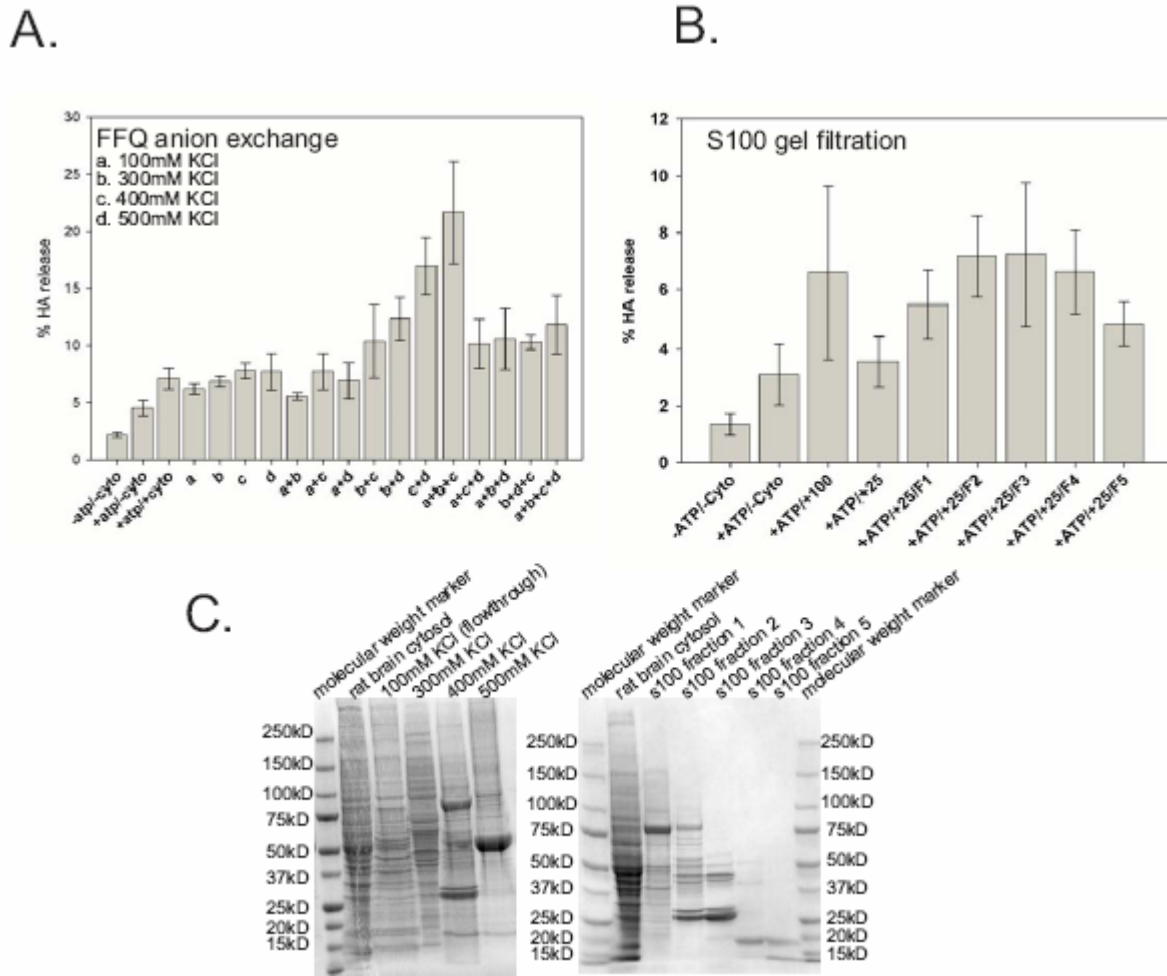


Figure 4. 8: Fractionation of rat brain cytosol for enrichment of HA release activity.

A. Fractions eluted from the ion exchange column are enriched for HA release activity. HeLa cells expressing HA were radiolabeled and chased at 19°C for 3 h. Cells were perforated as described and release from the TGN was reconstituted with various mixtures of the fractions collected compared to release in the absence or presence of ATP and cytosol. Fraction C (400mM KCl) addition correlated with increased HA release. B. Fractions collected from the S100 gel filtration of the 400mM FFQ fraction show a Poisson distribution of HA release activity. Release was measured as described in A in the presence of suboptimal rat brain cytosol concentration (25µg). The distribution of release may represent two peaks or one broad peak. C. Coomassie stained SDS-PAGE (4-20%) shows the protein profile of enrichment.

Proteins identified in the fraction enriched for HA release activity:

By peptide mass fingerprinting, Manimalha Balasubramani of the proteomics core facility determined the most probable identity of the proteins in the gel filtration fraction containing HA release activity. Six highly probable hits and two weaker but significant hits identified the proteins listed in table 3. At least 4 other bands did not generate hits, indicating that either these bands were not high enough quality for analysis or that these bands represent

unidentified proteins. Analysis of greater amounts of these proteins might alleviate the problem by increasing the true data compared to noise (random peaks by mass spec).

Figure 4.9 shows the coverage of peptides from mass spec analysis for the most probable hits. High coverage increases the probability that these are real hits and can be used to rule out highly homologous proteins. Amazingly, all eight proteins that were identified have been implicated in biosynthetic trafficking, specifically from the Golgi complex (Table 2). Diacylglycerol kinase regulates the generation of secretory vesicles from the TGN [104]. Creatine kinase and gamma enolase are metabolic enzymes important for the generation of ATP, which is required for vesicle formation from the TGN. Protein phosphatase 2A has been suggested to regulate the interaction of adaptor protein complexes with cargo molecules [105]. Rho GDI alpha has been suggested to regulate trafficking of basolateral cargo, but not apical cargo in polarized epithelia [201]. 14-3-3 proteins may compete with COP-I for certain cargo to promote anterograde trafficking [216]. 14-3-3 proteins have also been shown to regulate the plasma membrane ATPase in plants [217], and thus could potentially regulate the vacuolar ATPase activity required for HA export from the TGN, though proteomic analysis of 14-3-3 interacting partners has not shown this association [218]. Lastly, Secernin 1 was identified in mast cells as a protein important for regulated secretion [219]. Each of these proteins could potentially play a role in HA export,

As a preliminary test for the roles of DAGK and PP2A, I examined the effects of pharmacological inhibitors of these proteins on HA release in the presence of rat brain cytosol. In initial studies, I found no effect of the PP2A inhibitor okadaic acid or of a chemical inhibitor of diacylglycerol kinase on HA export from the TGN. Interestingly, addition of a polyclonal antibody against 14-3-3 epsilon (but not an antibody against 14-3-3 zeta) inhibited HA release in a single experiment, suggesting that this isoform may be a potential candidate to analyze in the future.

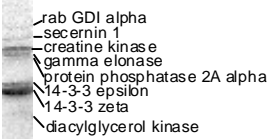
Table 1: Proteins identified by mass spec analysis.

Protein	Role in trafficking
DAG kinase alpha	Formation of secretory vesicles from TGN [104]
Rab GDI alpha	TGN export of VSV G [201]
Secernin 1	Secretion of hexosaminidase [219]
Creatine kinase	Indirect (metabolic)
Gamma enolase	Indirect (metabolic)
PP2A alpha	Regulation of Adaptor complexes [105]
14-3-3 zeta	ER export of Kir6.2 [216]
14-3-3 epsilon	???

Figure 4. 9: Proteins identified by peptide mass fingerprinting.

A. The Coomassie stained acrylamide gel with bands labeled for predicted protein ID. B. Sequences of proteins identified with high probability values. Amino acids in red represent peptides identified by mass spec and therefore coverage of sequence matching mass spec data.

3



14-3-3 zeta

1 MDK**NELVQKA** **KLAEQAERYD** **DMAACMKSVT** **EQGAELSNEE** **RNLLSVAYK**
 51 VVGARRSSWR **VVSSIEQKTE** **GAEKKQQMAR** **EYREKIEEMEL** **RDICNDVLSL**
 101 LEK**FLIPNAS** **QPESKVFYFK** **MKGDYRYLA** **EVAAGDDKKG** **IVDQSQQAYQ**
 151 **EAFETSKKEM** **QPTHPIRLGL** **ALNFSVFYFE** **ILNSPEK_{ACS}** **LAKTAFDEAI**
 201 **AELDTLSEES** **YKDSTLIMQL** **LRDNLTLWTS** **DTQGDEAEAG** **EGGEN**

gamma enolase

1 SIQKIWAREI LDSR**GNPTVE** **VDLHTAKGLF** **RAAVPSGAST** **GIYEAELELRD**
 51 GDKQRYLGKG VLKAVDHINS TIAPALISSG LSVVEQEK**LD** **NLMLELDGTE**
 101 **NKSKFGANAI** LGVSLAVCK**A** **GAAEKDLPLY** **RHIAQLAGNS** **DLILPVPAPFN**
 151 **VINGGSHAGN** **KLAMQEFMIL** **PVGAESFRDA** **MRLGAEVYHT** **LKGVIKDKYG**
 201 **KDATNVGDEG** **GFAPNILENS** **EAELELVKEAI** **DKAGYTEKMV** **IGMDVAASEF**
 251 **YRDGKYDLDF** **KSPADPSRCI** **TGDQLGALYQ** **DFVRNYPVVS** **IEDPFDQDDW**
 301 **AAWSKFTANV** **GIQIVGDDLT** **VTNPKRIERA** **VEEKACNCLL** **LKVNQIGSVT**
 351 EAIQACK**LAQ** **ENGWGMVSH** **RSGETEDTFI** **ADLVVGLCTG** **QIKTGAPCRS**
 401 ERLAK**YNQLM** **RIEELGEEA** **RFAGHNFRNP** **SVL**

protein phosphatase 2A alpha

1 MAAADGDDSL YPIAVLIDEL **RNEDVQLRLN** **SIK**KLSTIAL**** **ALGVERTRSE**
 51 LLPFLTDTIY DEDEVLLALA EQLGTFITLV GGPEYVHCLL PPLESLATVE
 101 ETVVRDKAVE SLR**AISHEHS** **PSDLEAHFVP** **LVKR**LAGGDW**** **FTSR**TSACGL****
 151 FSVCYPRVSS AVKAE LRQYF RNLCSDDTPM VRRAAASKLG EFAKVLELDN
 201 VK**SEIIPMFS** **NLASDEQDSV** **RLLAVEACVN** **IAQLLPQEDL** **EALVMPTLRQ**
 251 AAEDK**SWRVR** **YMVADKFTEL** **QKAVGPEITK** **TDLVPAFQNL** **MK**DCEAEVRA****
 301 **AASHKVK**EFC**** ENLSADCREN VIMTQILPCI KELVSDANQH VK**SALASVIM**
 351 **GLSPILGKDN** TIEHLLPLFL AQLKDECPEV RLNIISNLDC VNEVIGIR**QL**
 401 **SQSLLPAIVE** **LAEDAKWRVR** LAIIIEYMPLL AGQLGVEFFD EKLNSLCMAW
 451 LVDHVYAIRE AATSNLKKLV EKFGK**EWAHA** **TIIPKVLAMS** **GDPNYLHRMT**
 501 TLFICINVLSE VCGQDIT**KH** **MLPTVLRMAG** DPVANVRFNV AKSLQK**IGPI**
 551 **LDNSTLQSEV** **KPILEKLTQD** QDVDVKYFAQ EALTVLSLA

rab GDI alpha

1 MDEEYDIVVL GTGLTECILS GIMSVNGKKV LHMDR**NPYYG** **GESSITPLE**
 51 **ELYKRFQLE** **GPPEMGRGR** **DWNVDLIPKF** **LMANGQLVKM** **LLYTEVTRYL**
 101 DFK**VVEGSFV** **YKGGKIYKVP** STETEALASN LMGMEKRRF RK**FLVVFANF**
 151 **DENDPKTFEG** **VDPQTSMRD** VYRKFDLGQD VIDFTGHALA LYR**TDDYLVO**
 201 **PCLETINRIK** **LYSESLARYG** **KSPYLYPLYG** **LGELPQGFAR** **LSAIYGGTYM**
 251 LNKPVHDIIM ENKVVGVKS EGEVAR**CKQL** **ICDPSYIPER** VRKAGQVIRI
 301 ICILSHPIKN TNDANSCQII IPQNQVNRKS DIYVCMISYA HNVAAQ**GKYI**
 351 **AIASITVETA** **EPEKEVEPAL** **ELLEPIDQKF** VAISDLYEPI DDGSESQVFC
 401 SCSYDATTHF ETTNCNDIKDI YKR**MAGSAFD** **FENMKR**KQND**** VFGADQ

Discussion:

Here I have identified a number of interesting candidates responsible for HA export from the TGN, which I will discuss individually. In addition, I found that one of these proteins, dynamin 2, appears to regulate HA export from the TGN. Further purification of the HA release activity from cytosol has limited the number of proteins which may represent this activity. The potential role of each of these proteins is discussed.

Dynamin 2

I found that dynamin 2 was highly enriched in a cytosolic fraction that efficiently reconstituted HA release, and that expression of a dominant-negative mutant of dynamin selectively inhibited *in vitro*-reconstituted TGN export of HA but not VSV G. Consistent with this, TGN to surface delivery of HA in intact cells was compromised by expression of K44A, whereas the initial rate of VSV G delivery was unaffected. Together, the data presented in this chapter suggest that dynamin 2 plays an important role in HA but not VSV G export from the TGN. This is potentially interesting, though additional experiments are required to better characterize the role of dynamin 2 in this process. For example, it will be important to determine the effect of acute dynamin 2 depletion on HA export. I found that washing perforated cells with a sodium based salt wash (rather than a potassium based buffer) resulted in loss of dynamin 2 staining coincident with giantin-labeled Golgi membranes (data not shown) though the reason for this observation is unclear. This could potentially provide a method to deplete dynamin 2 from perforated cells, though the effect of this salt-wash regimen would also have to be determined on efficient export from the TGN (comparing export of a variety of cargo and resident Golgi proteins similar to fig 3.1). It would also be very interesting to determine the proteins that interact with dynamin 2 and how these proteins may regulate HA export. Some candidates may include cortactin, profilin I, and other actin-regulating proteins, as these proteins have been implicated in vesicle formation from the TGN [77]. This could be determined by generating a library of dynamin 2 mutants incapable of interacting with proteins like cortactin, or other actin-modifying binding-partners.

Although phosphatidylinositol 4,5 bis-phosphate is often considered the signal required for dynamin recruitment to membranes, the proline-rich domain (PRD) of dynamin 2 associates with

the Golgi complex [122]. Interestingly, this same domain interacts with G β ? proteins which are thought to regulate cargo export from the TGN [122]. This may be the signal which targets dynamin 2 to the Golgi complex, which can be determined by testing the effect of dynamin 2 K44A with or without the PRD. If the PRD is the sole Golgi-recruitment signal, the PRD-mutant should not affect HA export as it would not compete with Golgi associated endogenous dynamin. Furthermore, overexpressing the PRD should inhibit HA export from the TGN. These data would link dynamin 2 localization and function at the Golgi complex.

Diacylglycerol kinase

Diacylglycerol kinase has been implicated in vesicle formation from the TGN in polarized epithelial cells (unpublished observation, JR Henkel and OA Weisz)[220]. Though I did not observe an effect of a diacylglycerol kinase inhibitor on HA export from perforated cells, this does not rule out a role for diacylglycerol kinase in HA release from the TGN. Diacylglycerol kinase phosphorylates diacylglycerol to generate phosphatidic acid, a substrate for the generation of phosphatidylinositol (reviewed in [221]). Phosphatidylinositol species have been implicated in HA export from the TGN [84, 97, 99], though the particular role of these lipids in TGN export is not clear. It is possible that this kinase regulates the sorting of HA, as trafficking in streptolysin-O perforated polarized cells followed apical delivery of HA (not TGN export) as an endpoint. Therefore, if diacylglycerol kinase inhibition causes HA to be mis-sorted into other trafficking pathways such as TGN to endosome (as discussed in chapter 3 concerning ARF1's role in TGN export), one would not expect an inhibition of export, but a change in the requirements for export. This can be determined by using the same criteria applied to HA export in chapter 3, analyzing the effect of GTP γ S and M2 expression on HA export in the presence or absence of the diacylglycerol kinase inhibitor.

Secernin 1

Secernin 1 is not well characterized, but appears to participate in regulated secretion in mast cells. Its function in other cell types is completely unknown. It will be important to understand not just if this protein plays a role in constitutive trafficking from the TGN, but exactly how it functions to regulate secretion. Analysis for discrete motifs does not provide an obvious answer. Initially, I would suggest using immunodepletion of secernin 1 from cytosol to

observe an effect on TGN export of HA or VSV G from perforated cells. To then identify a potential function of secernin 1, one could use tandem affinity purification to isolate secernin 1 from cells along with proteins interacting with secernin 1. I would also suggest correlative light-electron microscopy and immunolocalization of HA to identify the stage at which RNAi knockdown of secernin 1 affects HA trafficking (vesicle formation, scission, or sorting). Together, this type of approach should determine a mechanism by which secernin 1 regulates HA export, if one exists.

14-3-3 epsilon/zeta

The preliminary observation that anti-14-3-3epsilon antibody inhibits HA export from the TGN suggests potential mechanisms for control of apical trafficking. Based on published work, there are two mechanisms by which 14-3-3epsilon may direct HA export, either direct or indirect. 14-3-3epsilon could interact directly with the cytoplasmic tail of HA, driving export from the TGN by serving as a coat protein or as an adaptor to a coat [222]. Alternatively 14-3-3 could indirectly affect trafficking via regulation of the actin cytoskeleton through modulation of Rho GTPase effectors [218].

14-3-3epsilon has been shown to directly interact with many transmembrane proteins and direct their export through the biosynthetic pathway. Moreover, a group identified 14-3-3 proteins as components enriched in apical transport carriers derived from the TGN [223]. It is not clear how specific the requirements are for individual isoforms, as many 14-3-3 proteins interact with similar proteins through phosphorylated amino-acid residues. ER export of some potassium channels requires the interaction of these tetrameric channels with 14-3-3 epsilon dimers [224]. This association appears to prevent interaction of the channel with coatamer complex I (COPI), thus promoting anterograde trafficking rather than retrograde trafficking [222]. However, HA possesses neither a COPI interaction motif nor a clear 14-3-3 epsilon interaction motif. Moreover, by western blotting, I did not find 14-3-3 epsilon co-immunoprecipitating with HA (data not shown), thus arguing against this direct hypothesis. This was done at steady state in the absence or presence of okadaic acid to block dephosphorylation. Orthovanadate and other phosphatase inhibitors may better preserve HA phosphorylation, and could be tested for preservation of HA-14-3-3 interaction. This could also be tested by

mutagenesis screening of the HA cytoplasmic tail, specifically at positions which could be phosphorylated.

The indirect hypothesis seems a more feasible explanation for the effect of 14-3-3 on HA export from the TGN. 14-3-3 interacts directly with regulators of Rho GTPases [218]. Furthermore, HA trafficking is regulated by actin polymerization and a number of actin interacting proteins (WASP, Arp2/3, dynamin). 14-3-3 interaction with A kinase anchoring protein-Lbc (AKAP) negatively regulates Rho activity by activating its guanine nucleotide exchange factor [218]. Rho activation results in actin depolymerization, and therefore could negatively regulate HA export. As the effect of 14-3-3 binding to AKAP requires protein kinase A [225], this hypothesis can be tested by using inhibitors of PKA. PKA inhibition should decrease HA export from the TGN, while a dominant active PKA should promote HA export. This would provide a starting point to understand the molecular differences between apical and basolateral trafficking.

In summary, these studies suggest potential candidates for the regulation of apical protein export from the TGN. The role of these proteins in polarized traffic awaits confirmation using the approaches discussed above.

5. Conclusion and Future Directions

Differential surface expression of plasma membrane proteins in polarized epithelial cells is required for the proper function of many organs including the gastrointestinal system, the renal system, and glands. The polarity of these proteins is regulated by both the biosynthetic addition of new membrane to the plasma membrane as well as removal of proteins and lipids from this membrane. Polarized epithelial cells, composed of an apical domain and a basolateral domain, sort newly synthesized apical proteins in the TGN into discrete carriers compared to basolateral proteins. Although the fidelity of this sorting process is critical for the proper function of nearly all organs, there is little known regarding how these proteins are segregated from each other in the TGN. In this work, I have developed a method to analyze TGN export of cargo biochemically, and have identified two proteins important in the trafficking of an apical cargo, influenza HA.

Little is known regarding the regulation and mechanics of HA export from the TGN. A model for HA export from the TGN is described in figure 5.1. Cholesterol depletion inhibits HA export, which is expected of a raft-dependent sorting mechanism [123]. Although a direct role has not yet been described, the phosphatidylinositol binding protein annexin XIII may link cholesterol organization to HA export from the TGN [101]. As annexin XIII binds both cholesterol and phosphatidylinositol, it may also link raft-dependent sorting to phosphatidylinositol metabolism. Phosphatidylinositol-4,5-bisphosphate would then provide the signal for dynamin II recruitment as well as FAPP2 recruitment to the site of raft-dependent cargo accumulation [97, 226]. 14-3-3 proteins may regulate the activity of phosphatidylinositol kinases to increase phosphatidylinositol species in the local membrane. Alternatively, diacylglycerol-kinase may regulate HA export by increasing the local concentration of phosphatidic acid and generating the precursor for phosphatidylinositol. The role of secernin is unknown, and may introduce an additional regulatory mechanism. ARF-1 does not appear to regulate HA export from the TGN, but another ARF-family GTPase is likely involved in HA export, as brefeldin A (BFA), an inhibitor of some ARF-GTPases, abrogates HA surface delivery. This effect may be at the TGN or may occur in endosomes. It is unclear whether HA

traverses an indirect route to the apical surface, though it has been shown that an apical protein is capable of such a pathway. Last, a pH-dependent component, which may sense membrane potential or local pH has yet to be characterized. Thus, a large number of questions and potential effectors remain.

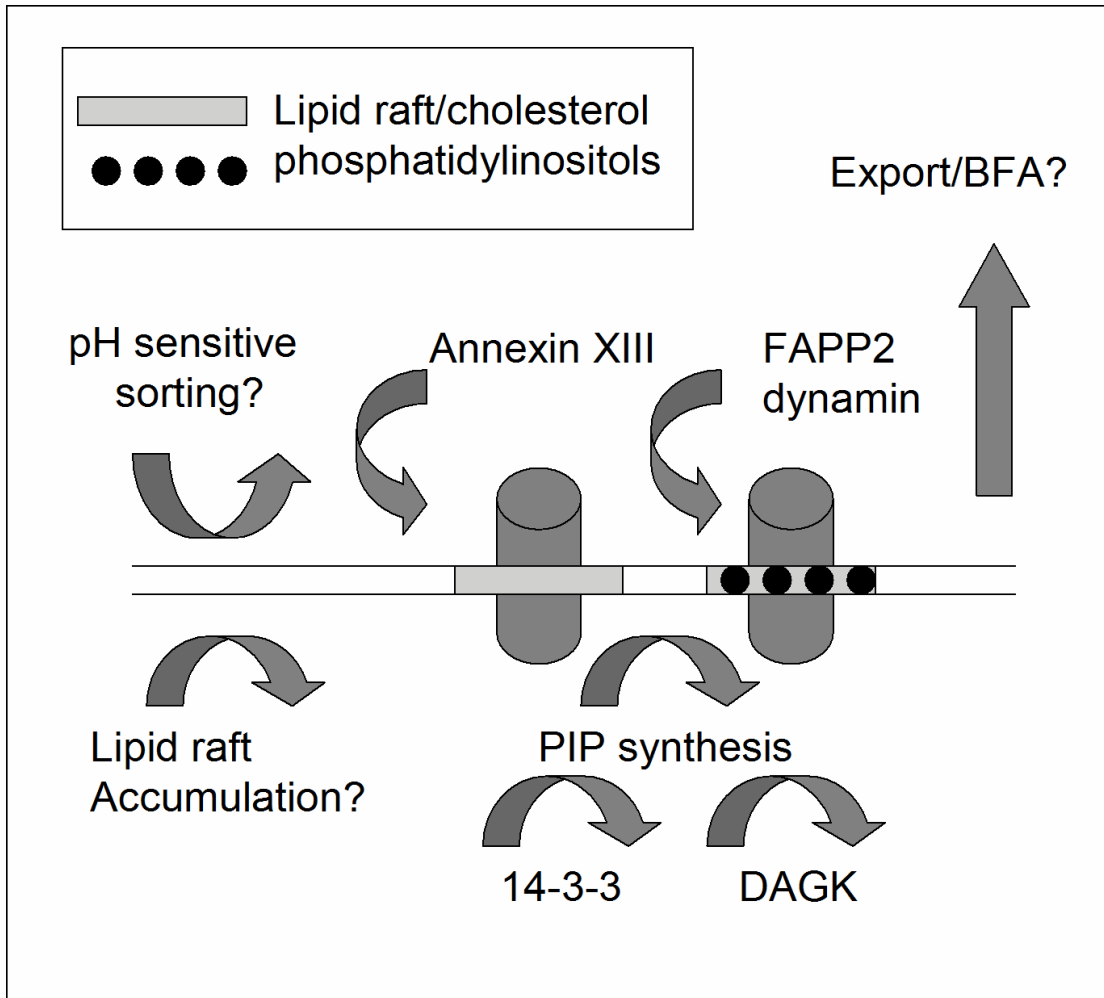


Figure 5.1. Model describing HA export from the TGN.

HA is incorporated into lipid rafts, which provides the sorting information. A pH-sensitive packaging of HA into vesicles occurs. Annexin XIII is recruited to the rafts and binds phosphatidylinositol (PI). Phosphatidylinositol-kinases are activated by 14-3-3 proteins or diacylglycerol-kinase (DAGK), generating increasing levels of PI lipids which recruit FAPP2, and subsequently dynamin II. Export is then potentially regulated by a brefeldin A (BFA) sensitive GTPase, or this factor regulates post-Golgi trafficking.

The future endeavors to characterize TGN export regulators will likely take advantage of new and novel methods. Genetic and chemical screens will be invaluable in generating a list of potential candidates. Presently, genetic screens are most feasible in either yeast or drosophila,

though some research groups are beginning to attempt such methods in animal cells. Chemical screens, though applicable to any cell type that can be grown in culture, require expensive equipment and reagents. Until recently, this method has been exclusively employed by pharmaceutical companies, though with the advent of high throughput systems and advanced robotics, chemical libraries and the robots needed to sift through them are now available to many academic researchers. Making use of these two methods and applying them to screening for polarized export will provide a plethora of information and a more extensive list of effectors.

Applications for the scraped cell assay:

In chapter 2, I described an assay to study export of TGN staged apical cargo. In the following chapters I characterize the roles of a handful of cytosolic proteins in cargo export. This assay, however, will prove useful to answer additional questions regarding apical cargo export. It is unclear whether all apical cargo share a common transport carrier from the TGN to the cell surface. This assay can be applied, with properly designed proteins, to study this process. Different cargo molecules, such as HA and p75, can be epitope-tagged on their cytoplasmic domains allowing for the immunoisolation of transport carriers from the supernatant. Asking whether HA can be coimmunoprecipitated with p75 and vice versa will reveal whether these two proteins are present in the same transport carrier. I would expect that the two apical cargo are trafficked in discrete carriers, as Jacob and Naim found segregation of two apical cargo at the level of the TGN [17]. Isolation of HA containing vesicles would also allow for the characterization of the vesicular protein content. This may reveal the endogenous cargo that normally takes this pathway to the cell surface. I would expect to find proteins such as annexins, similar to what Kai Simons' group found [223]. Furthermore, these immunoprecipitated vesicles can be analyzed for their ability to fuse with isolated plasma membrane domains. This would help characterize the missorting of cargo, and may describe mechanisms for polarized targeting.

How does brefeldin A affect HA surface delivery?

In chapter 3, I show that the brefeldin A-sensitive ARF1 GTPase is not involved in export of either apical or basolateral cargo from the TGN. Wagner et al have described HA surface delivery in polarized cells as being brefeldin A sensitive [116]. I also found that brefeldin A inhibits

both apical and basolateral surface delivery in intact HeLa cells. This suggests two hypotheses: Either ARF1 is critical for a post-TGN step in surface delivery (eg. sorting of SNARE proteins), or that ARF1 is not the brefeldin A-sensitive protein involved in TGN export. The first hypothesis can be tested by western blot of immunisolated vesicles for the detection of specific syntaxins or vesicular associated membrane proteins (VAMPs). The second hypothesis has become intriguing due to recent discovery of additional brefeldin A sensitive proteins. Interestingly, the ARF-related protein ARL1 is both localized to the TGN and sensitive to brefeldin A [117]. This GTPase recruits a number of proteins to the TGN including the putative-coat proteins golgin-97 and golgin-245 [227], though this mechanism has been only implicated in basolateral trafficking pathways [90, 228]. It will be interesting to see if these proteins regulate trafficking of apical cargo.

Does dynamin 2 regulate HA containing vesicle fission from the TGN?

In chapter 4, I describe a role for dynamin 2 in HA export from the TGN. Interestingly, dynamin 2 has also been implicated in p75 export from the TGN [74, 103], even though it has been suggested that these two types of cargo take different routes to the cell surface [17]. This brings up the possibility that dynamin 2 regulates an early step in TGN export of apical cargo, prior to the segregation of raft-dependent and raft-independent cargo. It would be interesting to perform correlative light-electron microscopy to characterize the role of dynamin 2 K44A in vesicle or tubule formation from the TGN. I would expect that dynamin 2 is involved in the fission of transport carriers, though it may also play a role in the generation of large pleomorphic transport intermediates. It would also be exciting to colocalize p75 and HA using immuno-gold labeling and electron microscopy on cells expressing dynamin 2 K44A. Are these two proteins stalled in a common compartment, or is it at a stage where they are already segregated? Last, a large number of dynamin mutants have been characterized recently associated with Charcot-Marie Tooth disease [229]. It would be exciting to characterize the effects of these mutants on protein trafficking from the TGN versus trafficking from endosomes. Can these two events be differentiated? This would allow analysis of dynamin's role in one process without complications of the other.

Isolation of cytosolic proteins involved in HA export from the TGN: the fun has just begun!

It is clear that many more cytosolic proteins are involved in HA export than the few I have discussed here. Many of the fractions that were discarded can be further fractionated to isolate HA release activities. Furthermore, the fractions from the FFQ column can be analyzed using suboptimal cytosol to truly determine which fractions contained HA release activity. This could take many years to complete, but the reagents are all available.

Identifying 14-3-3 epsilon as a mediator of HA export from the TGN is only the tip of the iceberg. As evident from the discussion of chapter 4, there are many potential roles for 14-3-3 epsilon in this process. Characterizing this will require empirical reasoning to address the many possible regulatory mechanisms. Initially, they can be tested very easily. Does 14-3-3 epsilon coprecipitate with immunoprecipitated HA? Does dominant negative 14-3-3 epsilon affect HA export from the TGN? How about hGH or ghGH? Does it affect trafficking of pH-sensitive cargo? Last, does 14-3-3 regulate PI5K or actin polymerization? Can 14-3-3 stimulate HA export in the presence of actin depolymerizing drugs, such as latrunculin? These questions, if answered, will begin to shed light on the role of 14-3-3 epsilon in HA export from the TGN.

6. Reference list:

1. Perret, E., et al., *Evolving endosomes: how many varieties and why?* Curr Opin Cell Biol, 2005. **17**(4): p. 423-34.
2. Rodriguez-Boulau, E., G. Kreitzer, and A. Musch, *Organization of vesicular trafficking in epithelia.* Nat Rev Mol Cell Biol, 2005. **6**(3): p. 233-47.
3. Ponnambalam, S. and S.A. Baldwin, *Constitutive protein secretion from the trans-Golgi network to the plasma membrane.* Mol Membr Biol, 2003. **20**(2): p. 129-39.
4. Kohler, K. and A. Zahraoui, *Tight junction: a co-ordinator of cell signalling and membrane trafficking.* Biol Cell, 2005. **97**(8): p. 659-65.
5. Turksen, K. and T.C. Troy, *Barriers built on claudins.* J Cell Sci, 2004. **117**(Pt 12): p. 2435-47.
6. Cohen, D., et al., *Mammalian PAR-1 determines epithelial lumen polarity by organizing the microtubule cytoskeleton.* J Cell Biol, 2004. **164**(5): p. 717-27.
7. Cohen, D., E. Rodriguez-Boulau, and A. Musch, *Par-1 promotes a hepatic mode of apical protein trafficking in MDCK cells.* Proc Natl Acad Sci U S A, 2004. **101**(38): p. 13792-7.
8. Schuck, S. and K. Simons, *Polarized sorting in epithelial cells: raft clustering and the biogenesis of the apical membrane.* J Cell Sci, 2004. **117**(Pt 25): p. 5955-64.
9. Wang, L. and J.L. Boyer, *The maintenance and generation of membrane polarity in hepatocytes.* Hepatology, 2004. **39**(4): p. 892-9.
10. Ojakian, G.K. and R. Schwimmer, *Antimicrotubule drugs inhibit the polarized insertion of an intracellular glycoprotein pool into the apical membrane of Madin-Darby canine kidney (MDCK) cells.* J Cell Sci, 1992. **103** (Pt 3): p. 677-87.
11. Matenia, D., et al., *PAK5 kinase is an inhibitor of MARK/Par-1, which leads to stable microtubules and dynamic actin.* Mol Biol Cell, 2005. **16**(9): p. 4410-22.
12. Paladino, S., et al., *Protein oligomerization modulates raft partitioning and apical sorting of GPI-anchored proteins.* J Cell Biol, 2004. **167**(4): p. 699-709.
13. Caplan, M.J., et al., *Dependence on pH of polarized sorting of secreted proteins.* Nature, 1987. **329**(6140): p. 632-5.
14. Rodriguez-Boulau, E. and A. Musch, *Protein sorting in the Golgi complex: shifting paradigms.* Biochim Biophys Acta, 2005. **1744**(3): p. 455-64.
15. Folsch, H., *The building blocks for basolateral vesicles in polarized epithelial cells.* Trends Cell Biol, 2005. **15**(4): p. 222-8.
16. Keller, P., et al., *Multicolour imaging of post-Golgi sorting and trafficking in live cells.* Nat Cell Biol, 2001. **3**(2): p. 140-9.
17. Jacob, R. and H.Y. Naim, *Apical membrane proteins are transported in distinct vesicular carriers.* Curr Biol, 2001. **11**(18): p. 1444-50.
18. Casanova, J.E., G. Apodaca, and K.E. Mostov, *An autonomous signal for basolateral sorting in the cytoplasmic domain of the polymeric immunoglobulin receptor.* Cell, 1991. **66**(1): p. 65-75.
19. Sarnataro, D., et al., *Detergent insoluble microdomains are not involved in transcytosis of polymeric Ig receptor in FRT and MDCK cells.* Traffic, 2000. **1**(10): p. 794-802.

20. Lisanti, M.P., et al., *Preferred apical distribution of glycosyl-phosphatidylinositol (GPI) anchored proteins: a highly conserved feature of the polarized epithelial cell phenotype.* J Membr Biol, 1990. **113**(2): p. 155-67.
21. Zurzolo, C., et al., *Glycosylphosphatidylinositol-anchored proteins are preferentially targeted to the basolateral surface in Fischer rat thyroid epithelial cells.* J Cell Biol, 1993. **121**(5): p. 1031-9.
22. Lipardi, C., L. Nitsch, and C. Zurzolo, *Detergent-insoluble GPI-anchored proteins are apically sorted in fischer rat thyroid cells, but interference with cholesterol or sphingolipids differentially affects detergent insolubility and apical sorting.* Mol Biol Cell, 2000. **11**(2): p. 531-42.
23. Benting, J., et al., *Acyl and alkyl chain length of GPI-anchors is critical for raft association in vitro.* FEBS Lett, 1999. **462**(1-2): p. 47-50.
24. Slimane, T.A., et al., *Raft-mediated trafficking of apical resident proteins occurs in both direct and transcytotic pathways in polarized hepatic cells: role of distinct lipid microdomains.* Mol Biol Cell, 2003. **14**(2): p. 611-24.
25. Bastaki, M., et al., *Absence of direct delivery for single transmembrane apical proteins or their "Secretory" forms in polarized hepatic cells.* Mol Biol Cell, 2002. **13**(1): p. 225-37.
26. Tuma, P.L. and A.L. Hubbard, *Transcytosis: crossing cellular barriers.* Physiol Rev, 2003. **83**(3): p. 871-932.
27. Brandli, A.W., R.G. Parton, and K. Simons, *Transcytosis in MDCK cells: identification of glycoproteins transported bidirectionally between both plasma membrane domains.* J Cell Biol, 1990. **111**(6 Pt 2): p. 2909-21.
28. Monlauzeur, L., L. Breuza, and A. Le Bivic, *Putative O-glycosylation sites and a membrane anchor are necessary for apical delivery of the human neurotrophin receptor in Caco-2 cells.* J Biol Chem, 1998. **273**(46): p. 30263-70.
29. Matter, K., K. Bucher, and H.P. Hauri, *Microtubule perturbation retards both the direct and the indirect apical pathway but does not affect sorting of plasma membrane proteins in intestinal epithelial cells (Caco-2).* Embo J, 1990. **9**(10): p. 3163-70.
30. Casanova, J.E., et al., *Direct apical sorting of rat liver dipeptidylpeptidase IV expressed in Madin-Darby canine kidney cells.* J Biol Chem, 1991. **266**(36): p. 24428-32.
31. Apodaca, G., et al., *The polymeric immunoglobulin receptor. A model protein to study transcytosis.* J Clin Invest, 1991. **87**(6): p. 1877-82.
32. Hunziker, W., P. Male, and I. Mellman, *Differential microtubule requirements for transcytosis in MDCK cells.* Embo J, 1990. **9**(11): p. 3515-25.
33. Wiggin, G.R., J.P. Fawcett, and T. Pawson, *Polarity proteins in axon specification and synaptogenesis.* Dev Cell, 2005. **8**(6): p. 803-16.
34. Dotti, C.G. and K. Simons, *Polarized sorting of viral glycoproteins to the axon and dendrites of hippocampal neurons in culture.* Cell, 1990. **62**(1): p. 63-72.
35. Kobayashi, T., et al., *A functional barrier to movement of lipids in polarized neurons.* Nature, 1992. **359**(6396): p. 647-50.
36. Nakada, C., et al., *Accumulation of anchored proteins forms membrane diffusion barriers during neuronal polarization.* Nat Cell Biol, 2003. **5**(7): p. 626-32.
37. Winckler, B., P. Forscher, and I. Mellman, *A diffusion barrier maintains distribution of membrane proteins in polarized neurons.* Nature, 1999. **397**(6721): p. 698-701.
38. Sytnyk, V., et al., *Trans-Golgi network delivery of synaptic proteins in synaptogenesis.* J Cell Sci, 2004. **117**(Pt 3): p. 381-8.

39. Lopez de Heredia, M. and R.P. Jansen, *mRNA localization and the cytoskeleton*. Curr Opin Cell Biol, 2004. **16**(1): p. 80-5.
40. Horton, A.C. and M.D. Ehlers, *Dual modes of endoplasmic reticulum-to-Golgi transport in dendrites revealed by live-cell imaging*. J Neurosci, 2003. **23**(15): p. 6188-99.
41. Weiner, O.D., *Regulation of cell polarity during eukaryotic chemotaxis: the chemotactic compass*. Curr Opin Cell Biol, 2002. **14**(2): p. 196-202.
42. Munevar, S., Y.L. Wang, and M. Dembo, *Distinct roles of frontal and rear cell-substrate adhesions in fibroblast migration*. Mol Biol Cell, 2001. **12**(12): p. 3947-54.
43. Schmoranzler, J., G. Kreitzer, and S.M. Simon, *Migrating fibroblasts perform polarized, microtubule-dependent exocytosis towards the leading edge*. J Cell Sci, 2003. **116**(Pt 22): p. 4513-9.
44. Prigozhina, N.L. and C.M. Waterman-Storer, *Protein kinase D-mediated anterograde membrane trafficking is required for fibroblast motility*. Curr Biol, 2004. **14**(2): p. 88-98.
45. Yoshimori, T., et al., *Different biosynthetic transport routes to the plasma membrane in BHK and CHO cells*. J Cell Biol, 1996. **133**(2): p. 247-56.
46. Rapoport, T.A., et al., *Membrane-protein integration and the role of the translocation channel*. Trends Cell Biol, 2004. **14**(10): p. 568-75.
47. Helenius, A. and M. Aebi, *Roles of N-linked glycans in the endoplasmic reticulum*. Annu Rev Biochem, 2004. **73**: p. 1019-49.
48. Udenfriend, S. and K. Kodukula, *How glycosylphosphatidylinositol-anchored membrane proteins are made*. Annu Rev Biochem, 1995. **64**: p. 563-91.
49. Ahner, A. and J.L. Brodsky, *Checkpoints in ER-associated degradation: excuse me, which way to the proteasome?* Trends Cell Biol, 2004. **14**(9): p. 474-8.
50. Sato, K., *COPII coat assembly and selective export from the endoplasmic reticulum*. J Biochem (Tokyo), 2004. **136**(6): p. 755-60.
51. Murshid, A. and J.F. Presley, *ER-to-Golgi transport and cytoskeletal interactions in animal cells*. Cell Mol Life Sci, 2004. **61**(2): p. 133-45.
52. Moussalli, M., et al., *Mannose-dependent endoplasmic reticulum (ER)-Golgi intermediate compartment-53-mediated ER to Golgi trafficking of coagulation factors V and VIII*. J Biol Chem, 1999. **274**(46): p. 32539-42.
53. Fullekrug, J., P. Scheiffele, and K. Simons, *VIP36 localisation to the early secretory pathway*. J Cell Sci, 1999. **112** (Pt 17): p. 2813-21.
54. Antonny, B. and R. Schekman, *ER export: public transportation by the COPII coach*. Curr Opin Cell Biol, 2001. **13**(4): p. 438-43.
55. Mironov, A.A., et al., *Intra-Golgi transport: a way to a new paradigm?* Biochim Biophys Acta, 2005. **1744**(3): p. 340-50.
56. Love, H.D., et al., *Isolation of functional Golgi-derived vesicles with a possible role in retrograde transport*. J Cell Biol, 1998. **140**(3): p. 541-51.
57. Lanoix, J., et al., *GTP hydrolysis by arf-1 mediates sorting and concentration of Golgi resident enzymes into functional COP I vesicles*. Embo J, 1999. **18**(18): p. 4935-48.
58. Orci, L., et al., *Exclusion of golgi residents from transport vesicles budding from Golgi cisternae in intact cells*. J Cell Biol, 2000. **150**(6): p. 1263-70.
59. Mironov, A.A., et al., *Small cargo proteins and large aggregates can traverse the Golgi by a common mechanism without leaving the lumen of cisternae*. J Cell Biol, 2001. **155**(7): p. 1225-38.

60. Trucco, A., et al., *Secretory traffic triggers the formation of tubular continuities across Golgi sub-compartments*. Nat Cell Biol, 2004. **6**(11): p. 1071-81.
61. Potter, B.A., R.P. Hughey, and O.A. Weisz, *Role of N- and O-glycans in polarized biosynthetic sorting*. Am J Physiol Cell Physiol, 2006. **290**(1): p. C1-C10.
62. Rodriguez-Boulan, E. and A. Gonzalez, *Glycans in post-Golgi apical targeting: sorting signals or structural props?* Trends Cell Biol, 1999. **9**(8): p. 291-4.
63. Potter, B.A., et al., *N-glycans mediate apical recycling of the sialomucin endolyn in polarized MDCK cells*. Traffic, 2006. **7**(2): p. 146-54.
64. Tooze, S.A., G.J. Martens, and W.B. Huttner, *Secretory granule biogenesis: rafting to the SNARE*. Trends Cell Biol, 2001. **11**(3): p. 116-22.
65. Tall, R.D., M.A. Alonso, and M.G. Roth, *Features of influenza HA required for apical sorting differ from those required for association with DRMs or MAL*. Traffic, 2003. **4**(12): p. 838-49.
66. Sun, A.Q., et al., *A 14-amino acid sequence with a beta-turn structure is required for apical membrane sorting of the rat ileal bile acid transporter*. J Biol Chem, 2003. **278**(6): p. 4000-9.
67. Nies, A.T., et al., *Structural requirements for the apical sorting of human multidrug resistance protein 2 (ABCC2)*. Eur J Biochem, 2002. **269**(7): p. 1866-76.
68. Aridor, M. and L.M. Traub, *Cargo selection in vesicular transport: the making and breaking of a coat*. Traffic, 2002. **3**(8): p. 537-46.
69. Traub, L.M., *Common principles in clathrin-mediated sorting at the Golgi and the plasma membrane*. Biochim Biophys Acta, 2005. **1744**(3): p. 415-37.
70. Kinuta, M., et al., *Phosphatidylinositol 4,5-bisphosphate stimulates vesicle formation from liposomes by brain cytosol*. Proc Natl Acad Sci U S A, 2002. **99**(5): p. 2842-7.
71. Marks, B., et al., *GTPase activity of dynamin and resulting conformation change are essential for endocytosis*. Nature, 2001. **410**(6825): p. 231-5.
72. Liljedahl, M., et al., *Protein kinase D regulates the fission of cell surface destined transport carriers from the trans-Golgi network*. Cell, 2001. **104**(3): p. 409-20.
73. Cao, H., et al., *Disruption of Golgi structure and function in mammalian cells expressing a mutant dynamin*. J Cell Sci, 2000. **113** (Pt 11): p. 1993-2002.
74. Kreitzer, G., et al., *Kinesin and dynamin are required for post-Golgi transport of a plasma-membrane protein*. Nat Cell Biol, 2000. **2**(2): p. 125-7.
75. Noda, Y., et al., *KIFC3, a microtubule minus end-directed motor for the apical transport of annexin XIIIb-associated Triton-insoluble membranes*. J Cell Biol, 2001. **155**(1): p. 77-88.
76. Musch, A., *Microtubule organization and function in epithelial cells*. Traffic, 2004. **5**(1): p. 1-9.
77. Cao, H., et al., *Actin and Arp1-dependent recruitment of a cortactin-dynamin complex to the Golgi regulates post-Golgi transport*. Nat Cell Biol, 2005. **7**(5): p. 483-92.
78. Shemesh, T., et al., *Prefission constriction of Golgi tubular carriers driven by local lipid metabolism: a theoretical model*. Biophys J, 2003. **85**(6): p. 3813-27.
79. Yeaman, C., et al., *Protein kinase D regulates basolateral membrane protein exit from trans-Golgi network*. Nat Cell Biol, 2004. **6**(2): p. 106-12.
80. Matlin, K.S. and K. Simons, *Reduced temperature prevents transfer of a membrane glycoprotein to the cell surface but does not prevent terminal glycosylation*. Cell, 1983. **34**(1): p. 233-43.

81. Musch, A., et al., *Transport of vesicular stomatitis virus G protein to the cell surface is signal mediated in polarized and nonpolarized cells.* J Cell Biol, 1996. **133**(3): p. 543-58.
82. Martinez, O., et al., *The small GTP-binding protein rab6 functions in intra-Golgi transport.* J Cell Biol, 1994. **127**(6 Pt 1): p. 1575-88.
83. Young, J., et al., *Regulation of microtubule-dependent recycling at the trans-Golgi network by Rab6A and Rab6A'.* Mol Biol Cell, 2005. **16**(1): p. 162-77.
84. Godi, A., et al., *FAPPs control Golgi-to-cell-surface membrane traffic by binding to ARF and PtdIns(4)P.* Nat Cell Biol, 2004. **6**(5): p. 393-404.
85. Godi, A., et al., *ARF mediates recruitment of PtdIns-4-OH kinase-beta and stimulates synthesis of PtdIns(4,5)P2 on the Golgi complex.* Nat Cell Biol, 1999. **1**(5): p. 280-7.
86. Pimplikar, S.W. and K. Simons, *Regulation of apical transport in epithelial cells by a Gs class of heterotrimeric G protein.* Nature, 1993. **362**(6419): p. 456-8.
87. Ang, A.L., et al., *The Rab8 GTPase selectively regulates AP-1B-dependent basolateral transport in polarized Madin-Darby canine kidney cells.* J Cell Biol, 2003. **163**(2): p. 339-50.
88. Chen, W., et al., *Rab11 is required for trans-golgi network-to-plasma membrane transport and a preferential target for GDP dissociation inhibitor.* Mol Biol Cell, 1998. **9**(11): p. 3241-57.
89. de Graaf, P., et al., *Phosphatidylinositol 4-kinasebeta is critical for functional association of rab11 with the Golgi complex.* Mol Biol Cell, 2004. **15**(4): p. 2038-47.
90. Shin, H.W., et al., *Roles of ARFRP1 (ADP-ribosylation factor-related protein 1) in post-Golgi membrane trafficking.* J Cell Sci, 2005. **118**(Pt 17): p. 4039-48.
91. Cohen, D., A. Musch, and E. Rodriguez-Boulant, *Selective control of basolateral membrane protein polarity by cdc42.* Traffic, 2001. **2**(8): p. 556-64.
92. Musch, A., et al., *cdc42 regulates the exit of apical and basolateral proteins from the trans-Golgi network.* Embo J, 2001. **20**(9): p. 2171-9.
93. Diaz Anel, A.M. and V. Malhotra, *PKCeta is required for beta1gamma2/beta3gamma2- and PKD-mediated transport to the cell surface and the organization of the Golgi apparatus.* J Cell Biol, 2005. **169**(1): p. 83-91.
94. Orzech, E., et al., *Interactions of the AP-1 Golgi adaptor with the polymeric immunoglobulin receptor and their possible role in mediating brefeldin A-sensitive basolateral targeting from the trans-Golgi network.* J Biol Chem, 1999. **274**(4): p. 2201-15.
95. Nishimura, N., et al., *The delta subunit of AP-3 is required for efficient transport of VSV-G from the trans-Golgi network to the cell surface.* Proc Natl Acad Sci U S A, 2002. **99**(10): p. 6755-60.
96. Simmen, T., et al., *AP-4 binds basolateral signals and participates in basolateral sorting in epithelial MDCK cells.* Nat Cell Biol, 2002. **4**(2): p. 154-9.
97. Vieira, O.V., et al., *FAPP2 is involved in the transport of apical cargo in polarized MDCK cells.* J Cell Biol, 2005. **170**(4): p. 521-6.
98. Gleeson, P.A., et al., *p230 is associated with vesicles budding from the trans-Golgi network.* J Cell Sci, 1996. **109** (Pt 12): p. 2811-21.
99. Bruns, J.R., et al., *Multiple roles for phosphatidylinositol 4-kinase in biosynthetic transport in polarized Madin-Darby canine kidney cells.* J Biol Chem, 2002. **277**(3): p. 2012-8.

100. Jones, S.M., et al., *Role of dynamin in the formation of transport vesicles from the trans-Golgi network*. Science, 1998. **279**(5350): p. 573-7.
101. Lafont, F., et al., *Annexin XIIIb associates with lipid microdomains to function in apical delivery*. J Cell Biol, 1998. **142**(6): p. 1413-27.
102. Jacob, R., et al., *Annexin II is required for apical transport in polarized epithelial cells*. J Biol Chem, 2004. **279**(5): p. 3680-4.
103. Bonazzi, M., et al., *CtBP3/BARS drives membrane fission in dynamin-independent transport pathways*. Nat Cell Biol, 2005. **7**(6): p. 570-80.
104. Baron, C.L. and V. Malhotra, *Role of diacylglycerol in PKD recruitment to the TGN and protein transport to the plasma membrane*. Science, 2002. **295**(5553): p. 325-8.
105. Ghosh, P. and S. Kornfeld, *AP-1 binding to sorting signals and release from clathrin-coated vesicles is regulated by phosphorylation*. J Cell Biol, 2003. **160**(5): p. 699-708.
106. Folsch, H., et al., *A novel clathrin adaptor complex mediates basolateral targeting in polarized epithelial cells*. Cell, 1999. **99**(2): p. 189-98.
107. Eskelinen, E.L., et al., *The polarized epithelia-specific mu 1B-adaptin complements mu 1A-deficiency in fibroblasts*. EMBO Rep, 2002. **3**(5): p. 471-7.
108. Folsch, H., et al., *The AP-1A and AP-1B clathrin adaptor complexes define biochemically and functionally distinct membrane domains*. J Cell Biol, 2003. **163**(2): p. 351-62.
109. Rous, B.A., et al., *Role of adaptor complex AP-3 in targeting wild-type and mutated CD63 to lysosomes*. Mol Biol Cell, 2002. **13**(3): p. 1071-82.
110. Faundez, V., J.T. Horng, and R.B. Kelly, *A function for the AP3 coat complex in synaptic vesicle formation from endosomes*. Cell, 1998. **93**(3): p. 423-32.
111. Bonifacino, J.S., *The GGA proteins: adaptors on the move*. Nat Rev Mol Cell Biol, 2004. **5**(1): p. 23-32.
112. Simon, J.P., et al., *The in vitro generation of post-Golgi vesicles carrying viral envelope glycoproteins requires an ARF-like GTP-binding protein and a protein kinase C associated with the Golgi apparatus*. J Biol Chem, 1996. **271**(28): p. 16952-61.
113. Gravotta, D., M. Adesnik, and D.D. Sabatini, *Transport of influenza HA from the trans-Golgi network to the apical surface of MDCK cells permeabilized in their basolateral plasma membranes: energy dependence and involvement of GTP-binding proteins*. J Cell Biol, 1990. **111**(6 Pt 2): p. 2893-908.
114. Miller, S.G., L. Carnell, and H.H. Moore, *Post-Golgi membrane traffic: brefeldin A inhibits export from distal Golgi compartments to the cell surface but not recycling*. J Cell Biol, 1992. **118**(2): p. 267-83.
115. Ellis, M.A., et al., *ADP-ribosylation factor 1-independent protein sorting and export from the trans-Golgi network*. J Biol Chem, 2004. **279**(50): p. 52735-43.
116. Wagner, M., et al., *Brefeldin A causes structural and functional alterations of the trans-Golgi network of MDCK cells*. J Cell Sci, 1994. **107** (Pt 4): p. 933-43.
117. Van Valkenburgh, H., et al., *ADP-ribosylation factors (ARFs) and ARF-like 1 (ARL1) have both specific and shared effectors: characterizing ARL1-binding proteins*. J Biol Chem, 2001. **276**(25): p. 22826-37.
118. Cobbold, C., et al., *Novel membrane traffic steps regulate the exocytosis of the Menkes disease ATPase*. Hum Mol Genet, 2002. **11**(23): p. 2855-66.
119. Huber, L.A., et al., *Protein transport to the dendritic plasma membrane of cultured neurons is regulated by rab8p*. J Cell Biol, 1993. **123**(1): p. 47-55.

120. Choudhury, A., et al., *Rab proteins mediate Golgi transport of caveola-internalized glycosphingolipids and correct lipid trafficking in Niemann-Pick C cells.* J Clin Invest, 2002. **109**(12): p. 1541-50.
121. Ullrich, O., et al., *Rab11 regulates recycling through the pericentriolar recycling endosome.* J Cell Biol, 1996. **135**(4): p. 913-24.
122. Yang, Z., et al., *Dynamin II regulates hormone secretion in neuroendocrine cells.* J Biol Chem, 2001. **276**(6): p. 4251-60.
123. Keller, P. and K. Simons, *Cholesterol is required for surface transport of influenza virus hemagglutinin.* J Cell Biol, 1998. **140**(6): p. 1357-67.
124. Ying, M., et al., *Cholesterol loading induces a block in the exit of VSVG from the TGN.* Traffic, 2003. **4**(11): p. 772-84.
125. De Matteis, M.A. and A. Godi, *PI-loting membrane traffic.* Nat Cell Biol, 2004. **6**(6): p. 487-92.
126. Roth, M.G., *Phosphoinositides in constitutive membrane traffic.* Physiol Rev, 2004. **84**(3): p. 699-730.
127. Cozier, G.E., et al., *Membrane targeting by pleckstrin homology domains.* Curr Top Microbiol Immunol, 2004. **282**: p. 49-88.
128. Wang, Y.J., et al., *Phosphatidylinositol 4 phosphate regulates targeting of clathrin adaptor AP-1 complexes to the Golgi.* Cell, 2003. **114**(3): p. 299-310.
129. Burger, K.N., et al., *Dynamin is membrane-active: lipid insertion is induced by phosphoinositides and phosphatidic acid.* Biochemistry, 2000. **39**(40): p. 12485-93.
130. Hausser, A., et al., *Protein kinase D regulates vesicular transport by phosphorylating and activating phosphatidylinositol-4 kinase IIIbeta at the Golgi complex.* Nat Cell Biol, 2005. **7**(9): p. 880-6.
131. Lecat, S., et al., *Different properties of two isoforms of annexin XIII in MDCK cells.* J Cell Sci, 2000. **113** (Pt 14): p. 2607-18.
132. Proszynski, T.J., et al., *A genome-wide visual screen reveals a role for sphingolipids and ergosterol in cell surface delivery in yeast.* Proc Natl Acad Sci U S A, 2005. **102**(50): p. 17981-6.
133. Bard, F., et al., *Functional genomics reveals genes involved in protein secretion and Golgi organization.* Nature, 2006. **439**(7076): p. 604-7.
134. Pelkmans, L., et al., *Genome-wide analysis of human kinases in clathrin- and caveolae/raft-mediated endocytosis.* Nature, 2005. **436**(7047): p. 78-86.
135. Altschuler, Y., et al., *Redundant and distinct functions for dynamin-1 and dynamin-2 isoforms.* J Cell Biol, 1998. **143**(7): p. 1871-81.
136. Luvrak, S.U., M.L. Torgersen, and K. Sandvig, *Efficient endosome-to-Golgi transport of Shiga toxin is dependent on dynamin and clathrin.* J Cell Sci, 2004. **117**(Pt 11): p. 2321-31.
137. Hathaway, N.A. and R.W. King, *Dissecting cell biology with chemical scalpels.* Curr Opin Cell Biol, 2005. **17**(1): p. 12-9.
138. Daub, H., et al., *Evaluation of kinase inhibitor selectivity by chemical proteomics.* Assay Drug Dev Technol, 2004. **2**(2): p. 215-24.
139. McLauchlan, H.J., et al., *Characterization and regulation of constitutive transport intermediates involved in trafficking from the trans-Golgi network.* Cell Biol Int, 2001. **25**(8): p. 705-13.

140. Brewer, C.B. and M.G. Roth, *Polarized exocytosis in MDCK cells is regulated by phosphorylation*. J Cell Sci, 1995. **108 (Pt 2)**: p. 789-96.
141. Brignoni, M., et al., *Cyclic AMP modulates the rate of 'constitutive' exocytosis of apical membrane proteins in Madin-Darby canine kidney cells*. J Cell Sci, 1995. **108 (Pt 5)**: p. 1931-43.
142. Espejo, A., et al., *A protein-domain microarray identifies novel protein-protein interactions*. Biochem J, 2002. **367(Pt 3)**: p. 697-702.
143. Henkel, J.R., et al., *Influenza M2 proton channel activity selectively inhibits trans-Golgi network release of apical membrane and secreted proteins in polarized Madin-Darby canine kidney cells*. J Cell Biol, 2000. **148(3)**: p. 495-504.
144. Demaurex, N., et al., *Mechanism of acidification of the trans-Golgi network (TGN). In situ measurements of pH using retrieval of TGN38 and furin from the cell surface*. J Biol Chem, 1998. **273(4)**: p. 2044-51.
145. Wu, M.M., et al., *Mechanisms of pH regulation in the regulated secretory pathway*. J Biol Chem, 2001. **276(35)**: p. 33027-35.
146. Paroutis, P., N. Touret, and S. Grinstein, *The pH of the secretory pathway: measurement, determinants, and regulation*. Physiology (Bethesda), 2004. **19**: p. 207-15.
147. Gu, F., et al., *Functional dissection of COP-I subunits in the biogenesis of multivesicular endosomes*. J Cell Biol, 1997. **139(5)**: p. 1183-95.
148. Aniento, F., et al., *An endosomal beta COP is involved in the pH-dependent formation of transport vesicles destined for late endosomes*. J Cell Biol, 1996. **133(1)**: p. 29-41.
149. Hurtado-Lorenzo, A., et al., *V-ATPase interacts with ARNO and Arf6 in early endosomes and regulates the protein degradative pathway*. Nat Cell Biol, 2006. **8(2)**: p. 124-36.
150. Roth, M., *New candidates for vesicle coat proteins*. Nat Cell Biol, 2004. **6(5)**: p. 384-5.
151. Hirschberg, K., et al., *Kinetic analysis of secretory protein traffic and characterization of golgi to plasma membrane transport intermediates in living cells*. J Cell Biol, 1998. **143(6)**: p. 1485-503.
152. Toomre, D., et al., *Dual-color visualization of trans-Golgi network to plasma membrane traffic along microtubules in living cells*. J Cell Sci, 1999. **112 (Pt 1)**: p. 21-33.
153. Fehrenbacher, K.L., I.R. Boldogh, and L.A. Pon, *Taking the A-train: actin-based force generators and organelle targeting*. Trends Cell Biol, 2003. **13(9)**: p. 472-7.
154. Jacob, R., et al., *Distinct cytoskeletal tracks direct individual vesicle populations to the apical membrane of epithelial cells*. Curr Biol, 2003. **13(7)**: p. 607-12.
155. Heine, M., et al., *Alpha-kinase 1, a new component in apical protein transport*. J Biol Chem, 2005. **280(27)**: p. 25637-43.
156. Delacour, D., et al., *Requirement for galectin-3 in apical protein sorting*. Curr Biol, 2006. **16(4)**: p. 408-14.
157. Rustom, A., et al., *Selective delivery of secretory cargo in Golgi-derived carriers of nonepithelial cells*. Traffic, 2002. **3(4)**: p. 279-88.
158. Futter, C.E., et al., *Newly synthesized transferrin receptors can be detected in the endosome before they appear on the cell surface*. J Biol Chem, 1995. **270(18)**: p. 10999-1003.
159. Ang, A.L., et al., *Recycling endosomes can serve as intermediates during transport from the Golgi to the plasma membrane of MDCK cells*. J Cell Biol, 2004. **167(3)**: p. 531-43.
160. Laird, V. and M. Spiess, *A novel assay to demonstrate an intersection of the exocytic and endocytic pathways at early endosomes*. Exp Cell Res, 2000. **260(2)**: p. 340-5.

161. Connolly, C.N., et al., *Transport into and out of the Golgi complex studied by transfecting cells with cDNAs encoding horseradish peroxidase*. J Cell Biol, 1994. **127**(3): p. 641-52.
162. Lock, J.G. and J.L. Stow, *Rab11 in recycling endosomes regulates the sorting and basolateral transport of E-cadherin*. Mol Biol Cell, 2005. **16**(4): p. 1744-55.
163. Brown, P.S., et al., *Definition of distinct compartments in polarized Madin-Darby canine kidney (MDCK) cells for membrane-volume sorting, polarized sorting and apical recycling*. Traffic, 2000. **1**(2): p. 124-40.
164. Turner, M.D. and P. Arvan, *Protein traffic from the secretory pathway to the endosomal system in pancreatic beta-cells*. J Biol Chem, 2000. **275**(19): p. 14025-30.
165. Cook, N.R. and H.W. Davidson, *In vitro assays of vesicular transport*. Traffic, 2001. **2**(1): p. 19-25.
166. Fiedler, K., et al., *Annexin XIIIb: a novel epithelial specific annexin is implicated in vesicular traffic to the apical plasma membrane*. J Cell Biol, 1995. **128**(6): p. 1043-53.
167. Simon, J.P., et al., *In vitro generation from the trans-Golgi network of coatomer-coated vesicles containing sialylated vesicular stomatitis virus-G protein*. Methods, 2000. **20**(4): p. 437-54.
168. Musch, A., D. Cohen, and E. Rodriguez-Boulant, *Myosin II is involved in the production of constitutive transport vesicles from the TGN*. J Cell Biol, 1997. **138**(2): p. 291-306.
169. Henkel, J.R., et al., *Selective perturbation of apical membrane traffic by expression of influenza M2, an acid-activated ion channel, in polarized madin-darby canine kidney cells*. Mol Biol Cell, 1998. **9**(9): p. 2477-90.
170. Mayer, A., et al., *Cell-free reconstitution of the transport of viral glycoproteins from the TGN to the basolateral plasma membrane of MDCK cells*. J Cell Sci, 1996. **109** (Pt 7): p. 1667-76.
171. Pepperkok, R., et al., *Three distinct steps in transport of vesicular stomatitis virus glycoprotein from the ER to the cell surface in vivo with differential sensitivities to GTP gamma S*. J Cell Sci, 1998. **111** (Pt 13): p. 1877-88.
172. Nelson, W.J. and C. Yeaman, *Protein trafficking in the exocytic pathway of polarized epithelial cells*. Trends Cell Biol, 2001. **11**(12): p. 483-6.
173. Rodriguez-Boulant, E., A. Musch, and A. Le Bivic, *Epithelial trafficking: new routes to familiar places*. Curr Opin Cell Biol, 2004. **16**(4): p. 436-42.
174. Bonifacino, J.S. and L.M. Traub, *Signals for sorting of transmembrane proteins to endosomes and lysosomes*. Annu Rev Biochem, 2003. **72**: p. 395-447.
175. Simon, J.P., et al., *Coatomer, but not P200/myosin II, is required for the in vitro formation of trans-Golgi network-derived vesicles containing the envelope glycoprotein of vesicular stomatitis virus*. Proc Natl Acad Sci U S A, 1998. **95**(3): p. 1073-8.
176. Polishchuk, E.V., et al., *Mechanism of constitutive export from the golgi: bulk flow via the formation, protrusion, and en bloc cleavage of large trans-golgi network tubular domains*. Mol Biol Cell, 2003. **14**(11): p. 4470-85.
177. Chuang, J.Z. and C.H. Sung, *The cytoplasmic tail of rhodopsin acts as a novel apical sorting signal in polarized MDCK cells*. J Cell Biol, 1998. **142**(5): p. 1245-56.
178. Takeda, T., H. Yamazaki, and M.G. Farquhar, *Identification of an apical sorting determinant in the cytoplasmic tail of megalin*. Am J Physiol Cell Physiol, 2003. **284**(5): p. C1105-13.

179. Potter, B.A., et al., *Specific N-glycans direct apical delivery of transmembrane, but not soluble or glycosylphosphatidylinositol-anchored forms of endolyn in Madin-Darby canine kidney cells*. *Mol Biol Cell*, 2004. **15**(3): p. 1407-16.
180. Yeaman, C., et al., *The O-glycosylated stalk domain is required for apical sorting of neurotrophin receptors in polarized MDCK cells*. *J Cell Biol*, 1997. **139**(4): p. 929-40.
181. Gut, A., et al., *Carbohydrate-mediated Golgi to cell surface transport and apical targeting of membrane proteins*. *Embo J*, 1998. **17**(7): p. 1919-29.
182. Scheiffele, P. and J. Fullekrug, *Glycosylation and protein transport*. *Essays Biochem*, 2000. **36**: p. 27-35.
183. Alfalah, M., et al., *O-linked glycans mediate apical sorting of human intestinal sucrase-isomaltase through association with lipid rafts*. *Curr Biol*, 1999. **9**(11): p. 593-6.
184. Simons, K. and E. Ikonen, *Functional rafts in cell membranes*. *Nature*, 1997. **387**(6633): p. 569-72.
185. Lin, S., et al., *Mutations in the middle of the transmembrane domain reverse the polarity of transport of the influenza virus hemagglutinin in MDCK epithelial cells*. *J Cell Biol*, 1998. **142**(1): p. 51-7.
186. Henkel, J.R. and O.A. Weisz, *Influenza virus M2 protein slows traffic along the secretory pathway. pH perturbation of acidified compartments affects early Golgi transport steps*. *J Biol Chem*, 1998. **273**(11): p. 6518-24.
187. Pinto, L.H., L.J. Holsinger, and R.A. Lamb, *Influenza virus M2 protein has ion channel activity*. *Cell*, 1992. **69**(3): p. 517-28.
188. Ciampor, F., et al., *Evidence that the amantadine-induced, M2-mediated conversion of influenza A virus hemagglutinin to the low pH conformation occurs in an acidic trans Golgi compartment*. *Virology*, 1992. **188**(1): p. 14-24.
189. Grambas, S. and A.J. Hay, *Maturation of influenza A virus hemagglutinin--estimates of the pH encountered during transport and its regulation by the M2 protein*. *Virology*, 1992. **190**(1): p. 11-8.
190. Rajasekaran, A.K., et al., *TGN38 recycles basolaterally in polarized Madin-Darby canine kidney cells*. *Mol Biol Cell*, 1994. **5**(10): p. 1093-103.
191. Stumber, M., et al., *Synthesis, characterization and application of two nucleoside triphosphate analogues, GTPgammaNH(2) and GTPgammaF*. *Eur J Biochem*, 2002. **269**(13): p. 3270-8.
192. Spiro, D.J., et al., *Cytosolic ADP-ribosylation factors are not required for endosome-endosome fusion but are necessary for GTP gamma S inhibition of fusion*. *J Biol Chem*, 1995. **270**(23): p. 13693-7.
193. Happe, S. and P. Weidman, *Cell-free transport to distinct Golgi cisternae is compartment specific and ARF independent*. *J Cell Biol*, 1998. **140**(3): p. 511-23.
194. Reaves, B.J., G. Banting, and J.P. Luzio, *Luminal and transmembrane domains play a role in sorting type I membrane proteins on endocytic pathways*. *Mol Biol Cell*, 1998. **9**(5): p. 1107-22.
195. Reaves, B. and G. Banting, *Vacuolar ATPase inactivation blocks recycling to the trans-Golgi network from the plasma membrane*. *FEBS Lett*, 1994. **345**(1): p. 61-6.
196. Banting, G., R. Maile, and E.P. Roquemore, *The steady state distribution of humTGN46 is not significantly altered in cells defective in clathrin-mediated endocytosis*. *J Cell Sci*, 1998. **111** (Pt 23): p. 3451-8.

197. Hu, J.S. and A.G. Redfield, *Conformational and dynamic differences between N-ras P21 bound to GTPgammaS and to GMPPNP as studied by NMR*. *Biochemistry*, 1997. **36**(16): p. 5045-52.
198. Traub, L.M., J.A. Ostrom, and S. Kornfeld, *Biochemical dissection of AP-1 recruitment onto Golgi membranes*. *J Cell Biol*, 1993. **123**(3): p. 561-73.
199. Wylie, F.G., et al., *GAIP participates in budding of membrane carriers at the trans-Golgi network*. *Traffic*, 2003. **4**(3): p. 175-89.
200. Altschuler, Y., C. Hodson, and S.L. Milgram, *The apical compartment: trafficking pathways, regulators and scaffolding proteins*. *Curr Opin Cell Biol*, 2003. **15**(4): p. 423-9.
201. Ikonen, E., et al., *Different requirements for NSF, SNAP, and Rab proteins in apical and basolateral transport in MDCK cells*. *Cell*, 1995. **81**(4): p. 571-80.
202. Polishchuk, R., A. Di Pentima, and J. Lippincott-Schwartz, *Delivery of raft-associated, GPI-anchored proteins to the apical surface of polarized MDCK cells by a transcytotic pathway*. *Nat Cell Biol*, 2004. **6**(4): p. 297-307.
203. Wandinger-Ness, A., et al., *Distinct transport vesicles mediate the delivery of plasma membrane proteins to the apical and basolateral domains of MDCK cells*. *J Cell Biol*, 1990. **111**(3): p. 987-1000.
204. Spang, A., et al., *Coatamer, Arf1p, and nucleotide are required to bud coat protein complex I-coated vesicles from large synthetic liposomes*. *Proc Natl Acad Sci U S A*, 1998. **95**(19): p. 11199-204.
205. Matsuoka, K., et al., *COPII-coated vesicle formation reconstituted with purified coat proteins and chemically defined liposomes*. *Cell*, 1998. **93**(2): p. 263-75.
206. Pauloin, A., et al., *The majority of clathrin coated vesicles from lactating rabbit mammary gland arises from the secretory pathway*. *J Cell Sci*, 1999. **112** (Pt 22): p. 4089-100.
207. Low, S.H., et al., *Inhibition by brefeldin A of protein secretion from the apical cell surface of Madin-Darby canine kidney cells*. *J Biol Chem*, 1991. **266**(27): p. 17729-32.
208. Low, S.H., et al., *Selective inhibition of protein targeting to the apical domain of MDCK cells by brefeldin A*. *J Cell Biol*, 1992. **118**(1): p. 51-62.
209. Fucini, R.V., et al., *Golgi vesicle proteins are linked to the assembly of an actin complex defined by mAbp1*. *Mol Biol Cell*, 2002. **13**(2): p. 621-31.
210. Chen, J.L., et al., *Cytosol-derived proteins are sufficient for Arp2/3 recruitment and ARF/coatamer-dependent actin polymerization on Golgi membranes*. *FEBS Lett*, 2004. **566**(1-3): p. 281-6.
211. Rozelle, A.L., et al., *Phosphatidylinositol 4,5-bisphosphate induces actin-based movement of raft-enriched vesicles through WASP-Arp2/3*. *Curr Biol*, 2000. **10**(6): p. 311-20.
212. van der Blik, A.M. and E.M. Meyerowitz, *Dynamin-like protein encoded by the Drosophila shibire gene associated with vesicular traffic*. *Nature*, 1991. **351**(6325): p. 411-4.
213. Poodry, C.A., L. Hall, and D.T. Suzuki, *Developmental properties of Shibire: a pleiotropic mutation affecting larval and adult locomotion and development*. *Dev Biol*, 1973. **32**(2): p. 373-86.
214. Herskovits, J.S., et al., *Effects of mutant rat dynamin on endocytosis*. *J Cell Biol*, 1993. **122**(3): p. 565-78.

215. Thomas, D.C., C.B. Brewer, and M.G. Roth, *Vesicular stomatitis virus glycoprotein contains a dominant cytoplasmic basolateral sorting signal critically dependent upon a tyrosine*. J Biol Chem, 1993. **268**(5): p. 3313-20.
216. O'Kelly, I., et al., *Forward transport. 14-3-3 binding overcomes retention in endoplasmic reticulum by dibasic signals*. Cell, 2002. **111**(4): p. 577-88.
217. Camoni, L., et al., *Phosphorylation-dependent interaction between plant plasma membrane H(+)-ATPase and 14-3-3 proteins*. J Biol Chem, 2000. **275**(14): p. 9919-23.
218. Jin, J., et al., *Proteomic, functional, and domain-based analysis of in vivo 14-3-3 binding proteins involved in cytoskeletal regulation and cellular organization*. Curr Biol, 2004. **14**(16): p. 1436-50.
219. Way, G., et al., *Purification and identification of secernin, a novel cytosolic protein that regulates exocytosis in mast cells*. Mol Biol Cell, 2002. **13**(9): p. 3344-54.
220. Siddhanta, A. and D. Shields, *Secretory vesicle budding from the trans-Golgi network is mediated by phosphatidic acid levels*. J Biol Chem, 1998. **273**(29): p. 17995-8.
221. Luo, B., et al., *Diacylglycerol kinases*. Cell Signal, 2004. **16**(9): p. 983-9.
222. Yuan, H., K. Michelsen, and B. Schwappach, *14-3-3 dimers probe the assembly status of multimeric membrane proteins*. Curr Biol, 2003. **13**(8): p. 638-46.
223. Fiedler, K., R. Kellner, and K. Simons, *Mapping the protein composition of trans-Golgi network (TGN)-derived carrier vesicles from polarized MDCK cells*. Electrophoresis, 1997. **18**(14): p. 2613-9.
224. Nufer, O. and H.P. Hauri, *ER export: call 14-3-3*. Curr Biol, 2003. **13**(10): p. R391-3.
225. Gu, Y.M., et al., *Protein kinase A phosphorylates and regulates dimerization of 14-3-3zeta*. FEBS Lett, 2006. **580**(1): p. 305-310.
226. Salim, K., et al., *Distinct specificity in the recognition of phosphoinositides by the pleckstrin homology domains of dynamin and Bruton's tyrosine kinase*. Embo J, 1996. **15**(22): p. 6241-50.
227. Lu, L. and W. Hong, *Interaction of Arl1-GTP with GRIP domains recruits autoantigens Golgin-97 and Golgin-245/p230 onto the Golgi*. Mol Biol Cell, 2003. **14**(9): p. 3767-81.
228. Lock, J.G., et al., *E-cadherin transport from the trans-Golgi network in tubulovesicular carriers is selectively regulated by golgin-97*. Traffic, 2005. **6**(12): p. 1142-56.
229. McNiven, M.A., *Dynamin in disease*. Nat Genet, 2005. **37**(3): p. 215-6.
230. Apodaca, G., et al., *Reconstitution of transcytosis in SLO-permeabilized MDCK cells: existence of an NSF-dependent fusion mechanism with the apical surface of MDCK cells*. Embo J, 1996. **15**(7): p. 1471-81.
231. Ling, W.L., A. Siddhanta, and D. Shields, *The use of permeabilized cells to investigate secretory granule biogenesis*. Methods, 1998. **16**(2): p. 141-9.
232. Beckers, C.J., D.S. Keller, and W.E. Balch, *Semi-intact cells permeable to macromolecules: use in reconstitution of protein transport from the endoplasmic reticulum to the Golgi complex*. Cell, 1987. **50**(4): p. 523-34.
233. Acharya, U., et al., *Signaling via mitogen-activated protein kinase kinase (MEK1) is required for Golgi fragmentation during mitosis*. Cell, 1998. **92**(2): p. 183-92.
234. Stolz, D.B., et al., *Cationic colloidal silica membrane perturbation as a means of examining changes at the sinusoidal surface during liver regeneration*. Am J Pathol, 1999. **155**(5): p. 1487-98.
235. Altschuler, Y., et al., *Clathrin-mediated endocytosis of MUC1 is modulated by its glycosylation state*. Mol Biol Cell, 2000. **11**(3): p. 819-31.

Appendix A- Materials and Methods:

Section 1: Characterization of HA export from the TGN

Antibodies-

Monoclonal antibody Fc125 directed against influenza HA was a gift from Dr. T Braciale (University of Virginia, Charlottesville VA). Monoclonal antibody mAD against β -COP was from Sigma. Anti-ARF monoclonal antibody 1D9 was from AbCam. Polyclonal antibody against the AP-1 γ -subunit was a gift from Dr. Linton Traub (University of Pittsburgh, Pittsburgh PA). Anti-giantin and -GM130 were gifts from Dr. Adam Linstedt (Carnegie Mellon University, Pittsburgh PA). Anti-TGN46 antibody (AHP500) was obtained from Serotec. Anti-GFP polyclonal antibody was obtained from Molecular Probes. Anti-CD25 antibody was purchased from Serotec. Anti-HA-tag monoclonal antibody (HA.11) was from Covance. Anti-dynamin 2 was from BD biosciences.

Cell culture and virus infection-

Type II Madin Darby canine kidney (MDCK) cells were maintained in minimal essential medium (MEM) supplemented with 10% fetal bovine serum (FBS) and were infected with adenoviral vectors as described. HeLa cells were cultured in Dulbecco's Modified Eagle's medium (Gibco) supplemented with 10% fetal bovine serum. The generation and propagation of replication-defective recombinant adenoviruses encoding tetracycline-repressible influenza hemagglutinin Japan serotype (HA), influenza M2 Rostock serotype (M2), a control virus (encoding influenza M2 in the reverse orientation; M2rev), and constitutively-expressed tetracycline transactivator (TA) are described in [169]. The TGN marker TGG-expressing adenovirus was a gift from Juan Bonifacino (NIH). Adenovirus encoding HA tagged-Dynamin 2 K44A was a gift from Yorum Altschuler (The Hebrew University of Jerusalem-Ein Kerem Campus). Cells were infected using replication defective recombinant adenoviruses (m.o.i. 50 for HA, VSV G, or TGG; 200 for M2, dynamin 2 K44A, or M2rev; 100 for TA) as described previously [143, 169] and experiments were performed the following day. cDNA constructs encoding the amino terminus of human β 1-4 galactosyltransferase linked to yellow fluorescent protein (GalT-YFP) and the ER-Golgi-intermediated compartment cycling protein p58 linked to yellow fluorescent protein (p58-YFP) were provided by Dr. Jennifer Lippincott-Schwartz and transiently expressed in HeLa cells using Lipofectamine 2000 (Invitrogen).

Cytosol preparation-

Rabbit liver cytosol was prepared from one fresh rabbit liver using the protocol described for rat liver cytosol [230]. Fifty unstripped frozen rat brains (Pelfreeze) were thawed rapidly in rat brain homogenization buffer (RHB: 25mM HEPES pH 7.3, 250mM sucrose, 2mM EDTA, 2mM EGTA) supplemented with complete protease inhibitor tablets (Calbiochem). The brains were homogenized in ice cold RHB by three 15 second pulses in a Waring blender. The homogenate was centrifuged at 3,000xg for 10 min at 4°C. The supernatant was then centrifuged at 12,000xg for 20 min at 4°C. The supernatant was then centrifuged at 100,000xg for 60 min at 4°C. The resulting clear supernatant was aliquotted, flash frozen in liquid nitrogen, and stored at -80°C. ARF-depleted cytosol was prepared from rat brain cytosol using a previously-described

procedure [193]. The resultant cytosols ranged in concentration from ~36 mg/mL (rabbit liver cytosol) to ~12 mg/mL (rat brain cytosol) and were used in reconstitution assays at a concentration of 2 mg/mL unless otherwise stated.

Table 2: Rat Brain Cytosol preparation

	<i>mg/mL</i>	<i>volume mL</i>	<i>total g</i>	<i>% yield</i>	<i>removed solids g</i>
Homogenate	20.8	200	4.159	100	185.3
3,000xg Supernatant	24.2	160	3.865	92.926	28.7
12,000xg Supernatant	18.6	40	0.743	17.874	110.9
100,000xg Supernatant	14.5	25	0.363	8.726	3.9

Enriched Golgi assay-

Ten confluent 15cm dishes of MDCK cells were infected with appropriate adenoviruses. The next day, cells were starved in medium A for 20 min, starved in PBS supplemented with 1mM magnesium chloride (PBS+Mg) for 10 min, and pulsed for 15 min in methionine-free medium supplemented with tran³⁵S label (50 µCi/ml). The label was replaced with 19°C methionine-containing medium and proteins were staged in the TGN for 3 h at 19°C. Following the stage, cells were washed twice with PBS+Mg and scraped into 3ml PBS+Mg per dish. Cells were pelleted by centrifugation at 800 rpm in a Beckman GS-6R centrifuge for 15 min at 4°C. Pelleted cells (0.5ml volume) were resuspended in 2.5 ml Homogenization Buffer (20mM Tris HCl pH 7.8, 1mM EDTA, 0.25% sucrose, 1x protease inhibitor cocktail [Calbiochem]) and homogenized by passing through a 0.001 inch clearance ball-bearing homogenizer 15 times on ice. The homogenate was centrifuged at 2100 rpm in a Beckman GS-6R centrifuge for 15 min at 4°C. The supernatant was loaded at the base (25%) of a Nycodenz step gradient (10%, 17.5%, 25%) and centrifuged for 3 h at 56Kxg in a TH641 rotor. The 10%/17.5% interface was collected and diluted 3 fold with homogenization buffer. This Golgi fraction was collected by centrifugation at 100Kxg for 1 h and was resuspended in GGA buffer. Aliquots were stored at -80°C without significant loss in release. To reconstitute release, 1mM ATP, 8µM phosphocreatine, 5µg/ml creatine phosphokinase, 100 µg cytosol, and 50 µg membranes were mixed in GGA buffer for 1 h at 37°C. Golgi membranes were separated from released material by centrifugation at 12.5K rpm in an Eppendorf minicentrifuge for 10 minutes. Supernatants and pellets were solubilized in RIPA and Fc125 anti-HA antibody, immunoprecipitated, and separated by SDS-PAGE [115].

Protein staging in the TGN of HeLa cells-

HeLa cells infected with replication-defective recombinant adenoviruses were incubated for 30 min at 37°C (unless otherwise stated) in bicarbonate-free, cysteine-free, methionine-free Dulbecco's Modified Eagle Medium, then metabolically-radiolabeled for 10 min in the same medium supplemented with 50 µCi/ml tran³⁵S]-label (MP Biomedicals). The medium was then replaced with cold bicarbonate-free Minimal Essential Medium and the cells were incubated at 19°C for 2 h to stage newly-synthesized proteins in the TGN. The dishes were then transferred to an ice cold aluminum plate and the cells were perforated as described below prior to reconstitution of protein export.

Surface delivery assay-

Surface delivery of HA or VSV G was measured by cell surface trypsinization and biotinylation respectively as described previously [99]. Briefly, HeLa cells expressing HA or VSV G and dynamin K44A were labeled as described above. The cells were then warmed to 37°C for indicated times. At the given times, dishes were removed from 37°C and placed on a chilled aluminum plate on ice. Cells were washed twice with ice-cold PBS and either biotinylated with 1 mg/mL NHSS-biotin (Pearce) or trypsinized with TCPK-treated trypsin (Sigma) 200 µg/mL for 10 min. Biotinylation is quenched by washing 5 times with normal HeLa medium, while trypsinization is quenched by washing twice with excess (400 µg/mL) soy bean trypsin inhibitor (Sigma).

Reconstitution of vesicle release from perforated cells-

Protein export from the TGN was reconstituted using a modification of the assays described in [231, 232]. HeLa cells in 10 cm dishes expressing radiolabeled marker proteins (as described earlier) were incubated for 10 min on ice in 10 mM HEPES, pH 7.2, 15 mM KCl, and the cells were then scraped into break buffer (BB; 50 mM HEPES pH 7.2, 90 mM KCl) using a rubber policeman. The cells were then transferred to a 15 ml conical tube and the buffer adjusted to 500 mM KCl by addition of an equal volume of 50 mM HEPES pH 7.2, 1 M KCl. The suspension was centrifuged at 800 x g in a Beckman GS-6R centrifuge, the cell pellet was washed with BB, and then resuspended in GGA buffer (25 mM HEPES pH 7.4; 38 mM potassium glutamate; 38 mM potassium aspartate; 38 mM potassium gluconate; 2.5 mM MgCl₂; 2 mM EGTA free-acid; 1 mM DTT). During the perforation procedure, eppendorf tubes were preloaded with GGA buffer with or without an ATP regenerating system (1mM ATP, 8mM creatine phosphate, 50µg/ml creatine phosphokinase [all based on final concentrations in a total assay volume of 50µl]), cytosol (2 mg/ml final concentration), and other reagents as described in individual experiments in a final volume of 25 µl. Aliquots of the perforated cell suspension (25 µl) were distributed into these tubes, the samples were incubated at 37°C for 1 h unless otherwise specified, and then centrifuged in a tabletop microcentrifuge at 12,000 rpm for 2 min to pellet the cells. The supernatant (containing released vesicles) and pellet (cells) were collected separately. HA was immunoprecipitated from radioactive samples and quantitated by phosphorimager analysis. Export of endogenous proteins from non-radiolabeled cells was analyzed by immunoblotting. Western blots were quantitated after densitometric scanning using QuantityOne software. Data were analyzed by Student's t-test using SigmaStat software (Systat) unless otherwise indicated. P<0.05 was considered to be statistically significant.

Protease protection assay-

Supernatants from perforated cells reconstituted with an ATP regenerating system and cytosol were incubated with 100 µg/ml trypsin (bovine pancreas; treated with L-1-tosylamido-2-phenylethyl chloromethyl ketone; Sigma) in GGA buffer on ice, in the presence or absence of 0.05% Triton X-100. After 10 min, soybean trypsin inhibitor was added to a final concentration of 200 µg/ml. The samples were then centrifuged at 100,000 x g for 30 min in a Sorvall RC M120EX centrifuge. Pelleted vesicles were solubilized and HA was immunoprecipitated from the supernatants as described in [186]. The samples were run on 12% SDS-polyacrylamide gels, dried, and quantified as described above.

β-COP and ARF1 recruitment to permeabilized cells-

Coatomer and ARF recruitment were assayed to confirm depletion of functional ARF from rat brain cytosol using the method described in [233]. HeLa cells grown on coverslips were washed with GGA buffer, then permeabilized in GGA buffer with 40 μg/ml digitonin (Sigma) for 10 min at ambient temperature. The cells were then washed with 50mM HEPES pH 7.2, 500mM KCl for 15 min on ice, then washed again with GGA buffer and incubated with or without control or ARF-depleted cytosol and 500 μM guanosine 5'-O-(3-thiotriphosphate) (GTPγS) for 15 min at 37°C. Samples were fixed with 4% paraformaldehyde and processed for indirect immunofluorescence using antibodies against β-COP, ARF1, AP-1 and giantin.

Western blotting & Far-Western blotting-

Western blotting was performed as follows. Samples were separated on 10% SDS-PAGE and transferred to nitrocellulose in Transfer buffer for 1 h at 350mA. The membrane was washed in PBS and blocked overnight in 5% milk in PBS. The membrane was incubated for 1 h at room temperature with constant agitation in 5% milk-PBS supplemented with 1μg/ml antibody. The blot was washed 3 times in PBS, then incubated for 1 h at room temperature with constant agitation in 5% milk-PBS supplemented with 1 μg/ml secondary antibody conjugated to horseradish peroxidase (HRP). The blot was then washed 3 times with PBS, dried, and exposed to chemiluminescence substrate for development of signal. Far-Western blots were blocked in 3% Bovine Serum Albumin fraction V (BSA)-PBS overnight, and incubated for 1 h with 2 μg/ml avidin-HRP in 0.5% BSA-PBS under constant agitation. The blot was then washed 10 times with PBS, dried, and exposed to chemiluminescence substrate.

Electron microscopy-

This was performed as described previously [234], with minor modifications, except that the fixation time was changed to 1 h at room temperature.

Immunogold electron microscopy-

Immunogold electron microscopy was performed by centrifuging the supernatants from reconstituted reactions onto formvar coated nickel grids at 100,000 x g for 2 min in a Beckman Airfuge centrifuge. Samples were fixed in 8% paraformaldehyde, permeabilized for 2 min in 0.05% Triton X-100, then treated as described in [235]. Fc125 antibody was used as the primary antibody and 10nm-colloidal gold conjugated rabbit anti-mouse (Amersham Biosciences) was used as the secondary. Phosphotungstic acid (2%) or uranyl acetate (4%) were used as negative stains.

Indirect Immunofluorescence-

HeLa cells expressing the indicated proteins were fixed in 3.7% formaldehyde in PBS. The formaldehyde was quenched by washing extensively in PBS supplemented with 1mM glycine, then permeabilized with 0.1% tritonX-100 in PBS for 10 min at ambient temperature. Prior to incubation with primary antibody, cells were incubated with PBS supplemented with 2% bovine serum albumin (BSA) fraction V (Sigma). Primary antibodies were applied in PBS+BSA for 1 h at ambient temperature. The samples were washed extensively with PBS+BSA, and secondary antibody was applied in the same manner. Secondary antibodies used were goat anti-mouse alexa 647 and goat anti-rabbit alexa 488 (Molecular probes) at 1:500 dilution in PBS+BSA. The

cells were washed extensively in PBS+BSA followed by three rapid washes with PBS and mounting on glass slides using AquaPolymount (Polysciences Inc.). Images were acquired using a Nikon Optiphot microscope connected to a Hamamatsu C5985 chilled CCD camera (8 bit, 756 x 483 pixels) (for epifluorescence) or a Leica DMRXE microscope (for confocal sections). Digitonin permeabilization was performed as described previously [115].

Section 2: Biochemical fractionation of HA release activity from cytosol

Release Assay-

TGN-staged HA release was measured using the assay described in Ellis et al. 2004 [115]. In brief, infected cells were starved for 20 min in methionine- and cysteine-free medium (Medium A) at 37°C, pulsed with Medium A containing 100 µCi/ml of tran-S³⁵ label (ICN) for 15 min at 37°C, and chased for 2 h at 19°C in medium containing methionine (Medium B). Subsequently, cells were washed in Swell Buffer (10mM HEPES pH 7.2, 15mM KCl) for 10 min on ice, then covered with Break Buffer (50mM HEPES pH 7.2, 110mM KCl) and scraped with a rubber policeman. The cell suspension was washed in High Salt Buffer (50mM HEPES pH 7.2, 500mM KCl), followed by Break Buffer, and finally resuspended in GGA Buffer [115]. Aliquots of cells were dispensed into individual reactions containing 1mM ATP, 8mM phosphocreatine, 5 µg/ml creatine phosphokinase, and varying concentrations of rat brain cytosol or fractioned proteins. Reactions were placed at 37°C for 1h at which time the cells were pelleted from the released material by centrifugation at 12,000xg. Supernatant and pellet were individually immunoprecipitated in Detergent Solution (50mM Tris pH 8.0; 67mM EDTA; 1% NP-40; 0.4% deoxycholate), 0.2% SDS, and Fc125 monoclonal antibody against influenza HA japan strain. Immunoprecipitated proteins were separated on 10% SDS-polyacrylamide gels which were dried and exposed to a phosphor screen for quantification of radioactive signal.

Ammonium sulfate precipitation-

RtBC was mixed with saturated ammonium sulfate to 60% v/v ammonium sulfate on ice. Precipitate was isolated from soluble protein by centrifugation at 14,000 rpm in an Eppendorf microfuge at 4°C for 10 min. The supernatant was removed and the pellet resuspended in 50mM HEPES pH 7.4, 100mM KCl. The 60% AS fraction was then passed through a PD-10 desalting column (GE) as to manufacturer's instructions and buffer exchanged by elution from the column equilibrated with 50mM HEPES pH 7.4, 100mM KCl.

Anion exchange chromatography-

A 75ml Econocolumn (BioRad) was packed with a 10ml bed volume of fast flow Q matrix (GE) in FFQ equilibration buffer (50mM HEPES pH 7.4, 110mM KCl) according to manufacturer's instructions. Sample from the previous step was applied to the column and followed with 2.5 bed volumes of FFQ equilibration buffer. The fractions were collected in batches (after optimization as described in chapter 4) using 300mM KCl, 400mM KCl, and 500mM KCl HEPES solutions under the same conditions as described for FFQ equilibration buffer at 4°C with a flow-rate of 0.5 mL/min. Finally, eluted proteins were concentrated using iCon centrifugal concentrators according to the manufacturer's instructions (Pierce). Samples were flash-frozen in liquid nitrogen and stored at -80°C for future use.

Gel Filtration Chromatography-

The FFQ 400mM fraction was prepared as described above. The 2ml fraction (16mg protein) was applied to a sephacryl-100 HR FPLC column with a bed volume of 70ml and equilibrated with RHB (described above), at 4°C with a flow-rate of 0.1 mL/min. Fifty 3ml fractions were collected and assayed for protein concentration, and electrophoresed on 5-20% gradient polyacrylamide gels (BioRad) stained with Coomassie stain and dried for subsequent mass spec analysis. Collected fractions were screened for HA release activity as described above in the presence of 25µg RtBC.

Tryptic digest of isolated bands-

This was performed by the proteomics CORE facility. The gel plugs were removed from the Coomassie-stained gel using an automated spot picker. The gel plugs were washed with 100 mL of 1:1 (v/v) methanol / 50 mM NH₄HCO₃ two times, discarding the supernatant after each wash. CH₃CN (50µL) was added to the tube followed by complete drying of the gel plugs in a Speed-Vac. The dried gel plugs were incubated with 10 ml trypsin (2 mg/ml) for 4 h at 42°C. The digested peptides were extracted from the gel plugs using 60 ml of 1% CF₃CO₂H (TFA)/50% CH₃CN two times. The pooled extracted peptide supernatants were completely dried and stored at 4°C for subsequent MALDI analysis.

Peptide Mass Fingerprinting-

This was performed by the proteomics CORE facility. The mass spectrum for each tryptic digest was measured by MALDI-TOF mass spectrometry. The digest was dissolved in 3 ml of 0.3% CF₃CO₂H (TFA)/50% CH₃CN, then mixed with 3 µL of α-cyano-4-hydroxycinnamic acid (CHCA)-saturated with 0.3% TFA/ 50 % CH₃CN solution, and an aliquot (0.7 µL) was spotted onto a stainless steel MALDI target for analysis. The analysis was performed with an ABI 4700 MALDI TOF-TOF Mass spectrometer in reflectron mode. The resolution of the instrument, which has a 3.75 m ion flight path, at 2.5kDa is > 12,000, and mass accuracies of +/- 5 ppm with internal standardization and +/- 25 ppm with external standardization are routinely achieved. The Mass lists were then imported into a protein database search engine for putative protein identification. The licensed search engine software used was Mascot.